The effects of climate change and introduced species on tropical island streams

by

Therese Frauendorf
B.Sc., University of Notre Dame, 2007
M.Sc., Southern Illinois University Carbondale, 2012

A Dissertation Submitted in Partial Fulfillment
of the Requirements for the Degree of

DOCTOR OF PHILOSOPHY

in the Department of Biology

© Therese Frauendorf, 2019
University of Victoria

All rights reserved. This dissertation may not be reproduced in whole or in part, by photocopy or other means, without the permission of the author.

Supervisory Committee

The effects of climate change and introduced species on tropical island streams

by

Therese Frauendorf
B.Sc., University of Notre Dame, 2007
M.Sc., Southern Illinois University Carbondale, 2012

Supervisory Committee

Dr. Rana El-Sabaawi, Department of Biology
Supervisor

Dr. Francis Juanes, Department of Biology
Departmental Member

Dr. Brian Starzomski, Department of Environmental Studies
Outside Member

Dr. John Richardson, Department of Biology
Affiliate Member

Abstract

Climate change and introduced species are among the top five threats to freshwater systems face. Tropical regions are considered to be especially sensitive to the effects of climate change, while island systems are more susceptible to species introductions. Climate-driven changes in rainfall are predicted to decrease streamflow and increase flash flooding in many tropical streams. In addition, guppies (*Poecilia reticulata*), an invasive fish, have been introduced to many tropical freshwater ecosystems, either intentionally for mosquito population control, or accidentally because of the aquarium trade. This dissertation examines the effects of climate-driven change in rainfall and introduced guppies on stream structure (resource and invertebrate biomass and composition) and function (nutrient recycling) in Trinidad and Hawaii. In the first data chapter we used a time series to examine how nutrient recycling of guppies changes in the first 6 years after introduction to a new habitat and to examine drivers of these changes. We found that when guppy populations establish in a new environment, they show considerable variation in nutrient recycling through time. This resulted from changes in guppy density in the first two years of introductions, and changes in individual excretion in subsequent stages. In the following chapter we utilized a rainfall gradient that mimics forecasted, climate-driven changes in precipitation and resulting changes in streamflow to examine the effects of climate change on stream food resources and macroinvertebrates. We found that the drying of streams across the gradient was associated with a decrease in resource quality and a 35-fold decline in macroinvertebrate biomass. Invertebrate composition also switched to taxa with faster turnover rates. In the third data chapter we used this same space-for-time substitution approach to determine if climate-driven changes in stream

structure also affected stream function. We showed that population nutrient recycling rates declined at the drier end of our rainfall gradient as a result of drops in population densities. We also found that under the current climate scenario, community excretion supplied up to 70% of the nutrient demand, which was ten-fold lower with projected climate changes in streamflow. Lastly, since freshwater ecosystems often face multiple human impacts, including climate change and invasive species, we wanted to understand how climate-driven changes in flow might alter the impact of introduced guppies on stream ecosystems. We selected several streams with guppies and several without guppies along the Hawaii rainfall gradient to examine if the effect of guppies changed with differences in streamflow. We found that the two stressors had synergistic effects on macroinvertebrate biomass and nutrient recycling rates. We concluded that climate change appeared to enhance effects of guppies, through direct and indirect effects. Overall, this dissertation shows that both climate change and species invasion can affect stream ecosystems at multiple levels of organization. This dissertation demonstrates that the effects of anthropogenic stressors are not static through time, and emphasizes the need and utility of using several methodological approaches when measuring the temporal effects of stressors. We also underline the significance of assessing multiple stressor interactions, as more than one stressor often impacts ecosystems.

Table of Contents

List of Tables

List of Figures

Acknowledgments

I would like to start by expressing my most sincere gratitude to Rana El-Sabaawi, who has been the best Ph.D. advisor one could wish for. She has been very helpful and supportive at every step of the process for this dissertation. Without her advise, guidance, and insight, I would not be where I am today! She has taught me the importance of a balanced life and how to be a great mentor by leading as an example. I am especially grateful for her diligent, constructive, and patient feedback on any piece that I have written, which helped me become a much-improved scientific writer.

Next, I would like to thank Drs. John Richardson, Francis Juanes, and Brian Starzomski for the insightful committee meetings and feedback on my work throughout my Ph.D. I would also like to thank my collaborators. Dr. Dawn Phillips, who has been a big support in the field and lab and has given valuable advise for the Trinidad portion of my research. She has sadly passed away unexpected in October 2017. Dr. Richard MacKenzie, has been instrumental in the design and funding portion of the Hawaii led projects. Lastly, Drs. Andrés López-Sepulcre and Alex Lee, who contributed significantly to the development of PoPaM.

I would also like to express my gratitude towards the El-Sabaawi lab members, former and current, with shout outs to Dan Durston, Ainsley Fraser, Kim Kennedy, Laura Kennedy, and Emily May. Many thanks to my numerous lab and field assistants, without whom this work would not exist. Special thanks to James Akau, Maybeleen Apwong, Katie Harms, Elsabet Lapoint, La'akea Low, Patra Foulk, Tyrell Froese, Ralph Tingley, and Misha Warbanski. In addition, a big thank you to Paul Selmants for his insight on the

earlier space-for-time substitution work, Ralph Tingley for his help with the streamflow data, and Abby Frazier for her rainfall calculations on the Hawaii project.

Next, I would like to thank my funding sources that have supported me throughout the years of my research with support from the Dr. Arne H. Lane Graduate Fellowship, Dr. Esme Foord Graduate Scholarship, King-Platt Fellowship and Memorial Award, the Randy Baker Memorial Fellowship, and the University of Victoria Graduate Fellowship; and research funding from the USDA Forest Service's Washington Office, the Pacific Southwest Research Station, and the AUCC-LACREG. I also would like to acknowledge and appreciate all the guppies, shrimp and bugs who have assisted me during my research.

Lastly, I would like to thank my family and friends who have been encouraging throughout my Ph.D. years. In particular, I would like to thank my wonderful partner, Kevin Yongblah, who has been very caring, patient, and supportive during some of the most challenging parts of my Ph.D. Finally, I would like to express a special gratitude towards Piatã Marques, who has started and ended this journey with me at the same time, in the same lab. Not only has he been an amazing lab mate and collaborator, but he has been an invaluable friend! He has managed to literally save my life twice in the field and countless times figuratively by keeping me sane during panic moments. Without Piatã, my Ph.D. experience would not have been the same and surely would have been only half as fun. Saúde to many more well-hydrated and squishy guppy years to come!

Dedication

To Chango and all the wild animals

Chapter 1: Introduction

Freshwater systems are critical because they provide important ecosystem services such as supplying clean drinking water and food, and offering habitat to a diversity of animals. Rivers and lakes host the highest number of described species per area globally (Strayer & Dudgeon, 2010), and are very sensitive to human-related stressors. They have the highest number of imperilled species per area compared to other ecosystems (Strayer & Dudgeon, 2010), where 84% of freshwater species have declined rapidly since 1970 (Living Planet Index, IPBES, 2019). Since biodiversity enhances ecosystem function (Lefcheck *et al.*, 2015), the number and quality of ecosystem services provided by freshwater ecosystems have also decreased (Isbell *et al.*, 2017). Global climate change and species introductions are considered to be among the top five anthropogenic threats that streams and lakes face and both are expected to drastically alter structure and function of freshwater ecosystems (Bellard, Leclerc & Courchamp, 2015; IPBES, 2019). This dissertation examines the consequences of climate change and species introduction individually and combined for tropical island streams by empirically measuring changes in resources, macroinvertebrate communities, and nutrient recycling.

1.1 Climate change and streamflow

The most recent Intergovernmental Panel on Climate Change (IPCC) report has concluded that there is a 95% probability that human activities over the past 50 years have warmed our planet (IPCC, 2014). Humans are estimated to have caused an observed warming of approximately 1.0°C by 2017 relative to pre-industrial levels, with average temperatures over the past 30 years rising by 0.2°C per decade (IPBES, 2019). We know

that increases in temperature can alter freshwater species composition, production, and dispersal patterns through long-term monitoring (e.g. Haase *et al.*, 2019), theoretical models (e.g. Patrick *et al.*, 2019), and experiments (e.g. Yvon-Durocher *et al.*, 2011; Polato *et al.*, 2018). The IPCC panel also concluded that there is a > 95% probability that human-produced greenhouse gases such as carbon dioxide have caused this increase in temperature (IPCC, 2014). Industrial activities have raised atmospheric carbon dioxide levels from 280 parts per million to 400 parts per million in the last 150 years (IPCC, 2014). A recent study shows that these increases in carbon dioxide not only lead to ocean acidification, but they have also lowered the pH of inland waters in the past 35 years (Weiss *et al.*, 2018). It is expected that these changes in carbon dioxide and pH have similar effects on freshwater species and their environments as found for marine ecosystems (Woodward, Perkins & Brown, 2010b).

Current climate models note that the frequency and intensity of extreme weather events, and the associated floods and droughts, have increased in the past 50 years (IPCC, 2014; Donat *et al.*, 2016). Increases in temperature can alter the amount of moisture evaporating (thermodynamic effect) and shift the circulation patterns in the atmosphere, enhancing the intensity and variability of storm and drought events (Trenberth, Fasullo & Shepherd, 2015). Compared to temperature, changes in precipitation are predicted to be an equally important driver of climate change in stream ecosystems, because precipitation is one of the main drivers of streamflow (Pyne & Poff, 2017). The natural flow regime (i.e. magnitude, frequency, duration, and variation of streamflow over time) is essential for the ecological integrity of lotic systems (Poff *et al.*, 1997; Jardine *et al.*, 2015). The forecasted changes in intensity, timing, and quantity of precipitation all control

streamflow rates (IPCC, 2012). Yet the majority of studies focus on the effects of increasing temperature, followed by changes in carbon dioxide (Bale *et al.*, 2002; Rosenblatt & Schmitz, 2014). Therefore, one of this dissertation's objectives is to examine the effects of climate-driven changes in precipitation on ecosystem structure and function.

1.2 Introduced species and guppies

Species are being transferred between regions faster and farther than ever, causing substantial changes to ecosystems worldwide (Ricciardi, 2007). We know that introduced species can affect ecosystem structure by decreasing native populations (via predation, competition, introducing diseases) and ecosystem function by altering production, nutrient cycling, and trophic interactions (Gallardo *et al.*, 2016). These impacts have been detected at the levels of individuals, populations, communities, and ecosystems (reviewed by Vilà *et al.*, 2011; Thomsen *et al.*, 2011). Among these, individual and population-level impacts of non-native species are commonly studied, whereas ecosystem-level impacts are less frequently reported and rarely quantified (Ricciardi *et al.*, 2013). In addition, the mechanisms that drive these impacts are still relatively unknown (Thomsen *et al.*, 2011; Ricciardi *et al.*, 2013). Studies have suggested that both individual (e.g. traits) and population characteristics (e.g. density) of an introduced species play important roles (Franzese *et al.,* 2017; Jackson et al. 2017); yet the relative importance of each and their interaction in reshaping ecosystem dynamics has not been measured. In particular, we do not understand how these characteristics and effects change through time as a result of plasticity, evolution, or the demographic response to environmental change.

Guppies (*Poecilia reticulata*) are a model species to explore the impacts and drivers of an introduced species through time, because the evolution of life histories has been extensively studied for this species. Guppies are native to the Caribbean and the north-east coasts of South America. In Trinidad, guppies historically exist either with or without predators. These guppies vary in a wide range of traits (e.g. life history, morphology, excretion rates), as well as population properties like density and size structure (Reznick *et al.*, 1997). The absence of predators is thought to be a major driver of these trait and population changes. Guppy introduction experiments, where guppies are transported from downstream, high-predation pressure locations to upstream predator-free locations in the same river, have been widely used to study the evolution of phenotypic traits as guppies are released from predators (Reznick *et al.*, 1997). These guppy introduction studies show that the release from predation pressure affects plastic traits (Ghalambor *et al.*, 2015), heritable traits, and population characteristics (Reznick *et al.*, 1997; Reznick, Butler IV & Rodd, 2001). This plasticity and adaptability has likely enabled guppies to be an invasive species in many parts of the world (Deacon, Ramnarine & Magurran, 2011).

Guppies have been transported globally for two main reasons: 1) they are a popular aquarium species, and 2) they are commonly used as a method of controlling mosquito populations in many tropical countries (Deacon *et al.*, 2011). In regions where the prevalence of mosquito-borne illnesses such as dengue fever and malaria are high, guppies can depress the risk of an infection by feeding on the aquatic larvae of mosquitoes (Kusumawathie *et al.*, 2008). However, the effectiveness of guppies as a mosquito control is equivocal (El-Sabaawi *et al.*, 2016), and their use has led to guppies

invading local aquatic ecosystems (Magurran, 2009; Deacon *et al.*, 2011). They have established populations in at least 69 countries outside of their native range (Deacon *et al.*, 2011), depleted native fauna, and altered structure and function of ecosystems (reviewed by El-Sabaawi *et al.* 2016). However, the drivers of these changes are unknown. Therefore, one of this dissertation's objectives is to explore the impacts of guppies both as an introduced species in Trinidad (introduced within the native range) and as an invasive species in Hawaii (introduced within the non-native range resulting in negative impacts on the local environment).

1.3 Anthropogenic stressors through time

Anthropogenic impacts are rarely static through time and as a result, temporal sampling is an integral part of assessing anthropogenic impacts. Understanding the impacts of introduced species through time is ideally accomplished with long-term sampling of an introduced population. Long-term experiments are the most realistic form of understanding the effect of a perturbation through time, but they require extensive logistical support and are often unfeasible. However, the vast majority of studies documenting the effects of introduced species offer a snapshot in time, making it difficult to assess the mechanisms of ecosystem impact.

For stressors like climate change, temporal dynamics are of critical importance, because we need to make predictions in deep time, which are not possible without detailed mechanistic models. A space-for-time substitution approach allows us to test long-term, integrative effects of climate without compromising realism (Fukami & Wardle, 2005; Blois *et al.*, 2013). It is a sampling design where a spatial gradient mimics

a forecasted or historical change over time. A space-for-time substitution is an innovative way to characterize ecological dynamics that occur over time-scales beyond the duration of conventional experiments, especially when infrastructure required for long-term monitoring is lacking (Fukami & Wardle, 2005). Such substitutions have been successful in terrestrial ecosystems, accurately predicting ~72% of forecasted change scenarios (Blois *et al.*, 2013). However, application in aquatic ecosystems remains limited, except for a few studies investigating effects of invasive species (e.g. Thomaz *et al.*, 2012). This dissertation utilizes both time series and space-for-time substitutions to study the effects of climate change and introduced species through time.

1.4 Stream structure and function

Stream structure is comprised of resources and consumers, and is characterized by measuring standing stocks and diversity. This dissertation focused on stream invertebrate consumers, because they are an important food resource for animals inside (e.g. fish) and outside (e.g. birds) the stream. Changes to invertebrate abundance and diversity are likely to have cascading effects on aquatic and terrestrial ecosystems (Wallace & Webster, 1996). Invertebrates also play a major role in ecosystem processes such as nutrient recycling, decomposition, and ecosystem metabolism (Wallace & Webster, 1996), which are important functions for maintaining healthy, productive, and stable ecosystems. Since invertebrates are very sensitive to environmental changes, they act as ecosystem indicators, meaning they are often the first organisms to respond to environmental stress (Feld & Hering, 2007). Studies have shown that invertebrate abundance, production, and behaviour respond to changes in flow within a single stream over short time periods (e.g.

Rempel, Richardson & Healey, 2000; Hoover & Mackenzie, 2009; Scholl *et al.*, 2016). However, we do not understand climate-driven changes in flow and species introductions can affect these important species.

Ecosystem function is characterized by measuring rates and fluxes of materials. The dissertation focused on nutrient recycling because it is an important component of stream function (Vanni, 2002). It is defined as nutrients excreted or egested by organisms and is often studied using the framework of ecological stoichiometry. The stoichiometric framework expresses ecological processes as ratios of multiple essential elements (e.g. carbon (C), nitrogen (N) and phosphorus (P)) maintained by a mass balance (Sterner & Elser, 2002). Aquatic organisms sequester nutrients through growth and reproduction, and remineralize nutrients via excretion and egestion. Body elemental composition reflects animal traits and diet, and is sensitive to changes in phenotype and environmental conditions (e.g. El-Sabaawi *et al.*, 2012a, 2012b; Costello & Michel, 2013). Body elemental composition and size, diet, growth rate, and assimilation efficiency all determine the amount of nutrients recycled by consumers (Elser *et al.*, 1996; Sterner & Elser, 2002; Vanni *et al.*, 2002). Nutrients excreted by an organism should be negatively correlated with the elemental concentration in the body tissue and positively correlated with the elemental concentration of the diet (Elser *et al.*, 1996; Vanni *et al.*, 2002). Nutrients sequestered are important because they provide new tissues for the consumer and for higher trophic levels. Excreted waste contains inorganic nutrients in form of ammonium and phosphate that are readily available for primary producers (e.g. macrophytes, algae) and microbial communities (e.g. bacteria, fungi), stimulating productivity at the base of the food web. Fish contribute on average 5 – 30% of nutrients

required by a stream ecosystem (Vanni, 2002), but invertebrates can also play a significant role in nutrient recycling as they often have a large biomass and their smaller size leads to larger mass-specific excretion rates (Sterner & Elser, 2002). For example, in a desert stream, invertebrate assemblages provided 70% of the N required by the stream biota (Grimm, 1988). Fish can also indirectly affect nutrient recycling rates by controlling invertebrate abundance and composition (Bassar *et al.*, 2012). However, the relative importance of consumer-mediated nutrient recycling depends on time (e.g. season, time of day), ambient nutrient concentrations, ecosystem size, species involved, and most importantly, the demand of the system (Benstead *et al.*, 2010; Griffiths & Hill, 2014).

In order to assess the importance of nutrient recycling in the ecosystems, it is often compared to measurements of ecosystem demand. Nutrient demand is defined as the concentration of nutrients (N and P) required by the stream ecosystem. If consumers contribute fewer nutrients than the stream's demand, excreted N and P will be taken up by microbial and plant communities within the reach. If, however, consumers contribute more than the demand, labile nutrients will be exported to stimulate downstream, estuarine, and coastal productivity (Atkinson *et al.*, 2017). As nutrient demand is affected by both abiotic (e.g. background nutrients, disturbance frequency, temperature, channel geomorphology, flow obstructions) and biotic (e.g. abundance, community composition of primary producers and microbes) factors (Allan & Castillo, 2007), the demand is expected to vary with climate-driven changes in precipitation regimes and species introduction.

1.5 Dissertation goals and structure

The goal of this dissertation was to determine the individual and combined effects of climate change and introduced guppies on stream structure and function on tropical islands. To achieve this goal, we first developed a method that determines the drivers of changes in ecosystem function over time after species introduction (Chapter 2). We demonstrate this method by examining how nutrient recycling changes over the first 6 years after guppies were introduced into previously guppy-free reaches of streams in their native range in Trinidad. From there we determined if individual and/or population characteristics of guppies drive these changes in nutrient recycling. In the third chapter, we switched the setting to Hawaii, where we investigate how a space-for-time substitution approach helps us characterize the effects of climate change on tropical stream structure. This chapter involves sampling stream resources and invertebrates along rain shadow gradient, which mimics forecasted changes in rainfall and streamfow. Sampling stream ecosystem structure along the gradient allows us to make predictions on how climate change will affect these streams. In chapter four, we build on this work by looking at climate-change effects on ecosystem function, specifically nutrient recycling along the rainfall gradient. Lastly, we wanted to assess if the effects of climate change differ if a non-native fish also invaded streams. To do so we examined the impacts of guppies on resources, macroinvertebrates, and nutrient recycling along the rainfall gradient in Hawaii.

The following four chapters are written like manuscripts and adhere to the general format of a manuscript. Chapter 2 has been given feedback from journal reviewers and revisions are in progress, while chapter 3 has been published in Global Change Biology

(DOI: 10.1111/gcb.14584). Although all of this is my own work and writing, it is important to note that it would have not been possible without my collaborators. As such, I use the pronoun “we” rather than “I” throughout my dissertation. I have noted at the beginning of the subsequent data chapters the contributions of each of my collaborators and co-authors.

Chapter 2: Partitioning method exposes how traits and demographic characteristics change the contribution of an introduced population to ecosystem function over time

Therese C. Frauendorf [1], Andrés López-Sepulcre [2,3], Alexander E.G. Lee [2], Michael C. Marshall [4], and Rana W. El-Sabaawi [1]

[1] Department of Biology, University of Victoria, Victoria, British Columbia, V8W 3N5, Canada

[2] Department of Biological and Environmental Science, University of Jyväskylä, Jyväskylä, 40014, Finland

[3] Institute of Ecology and Environmental Sciences of Paris, Sorbonne Université, Paris, 75252, France

[4] Center for Applied Isotope Studies, University of Georgia, Athens, GA 30602, USA

Author contributions: TCF designed and implemented the study. RES, AEGL, and contributed to the intellectual development of the method. The mathematical components and the R code were build by ALS, AEGL, and TCF. Data were collected by TCF and MCM. TCF wrote the manuscript. RES, ALS, AEGL, and MCM contributed substantially to the edits of previous versions of this manuscript.

2.1 Abstract

Ecosystem structure and function change over time and space as a result of evolving populations and communities. Studies have suggested that both phenotypic traits and demographic structure of a population play important roles in ecosystem function; yet the relative importance of each characteristic and their interaction in reshaping ecosystem dynamics has not been measured. We derived a simple algebraic partitioning method (based on scaling equations) to decompose change in any size related ecosystem function of a population into the relative individual and demographic contributions. This population partitioning method (PoPaM) estimates proportional contributions of an effect trait, the population size distribution, and population density to ecosystem function across space and time. We illustrate the method using longitudinal data from a series of guppy (*Poecilia reticulata*) introduction experiments performed in Trinidadian streams to partition guppy population nutrient recycling (ecosystem function) into individual excretion rate (effect trait) and population size structure and density. Using PoPaM we found that when guppies establish in a new environment, they show considerable variation in population nutrient recycling through time. This results from changes in density during the early years, and changes in individual excretion in the later stages. We also show that changes in guppy population excretion depend on the environmental context. PoPaM is simple and easy to apply to data collected by most field studies in ecology. The decomposition will facilitate the understanding of the drivers behind changes in ecosystem function in the context of eco-evolutionary dynamics and anthropogenic changes.

2.2 Introduction

Ecosystems are made up of individuals, organized in populations that are assembled into communities, which are embedded in an abiotic environment. Individual, population, and community components interact with the abiotic environment and can change over time and space. Ecosystem structure and function arise from the interactions of these components. However, in recent history, anthropogenic activities have been causing unprecedented changes in ecosystem structure globally, with major consequences for ecosystem function (Hooper *et al.*, 2012; De Laender *et al.*, 2016). Under this scenario, understanding how ecosystem structure and function are interrelated has become a major objective in ecology (De Laender *et al.*, 2016). Since changes at the individual, population, and community levels occur simultaneously, it is difficult to separate their relative importance to ecosystems without manipulative experiments. Mathematical methods that partition the variation in ecosystem function into individual- and population-level effects can be important when examining the relationship between ecosystem structure and function. For example, if a plant population changes their contribution to carbon fixation, it is important to determine if these changes are a result of shifts in individual photosynthetic rates or shifts in population size structure or density.

Partitioning methods have been widely used when investigating the effects of biodiversity on ecosystem function (McGlinn *et al.*, 2019). Many of these methods are based on the Price equation, which decomposes evolutionary change of a phenotype into natural selection and transmission bias (Price, 1970; Price, 1972). Recent studies have adapted this additive model to estimate the effects of species loss and/or gain on ecosystem function by decomposing changes into species richness, species composition,

and context dependent effects (Fox, 2006; Fox & Kerr, 2012). Loreau and Hector (2001) adapted the Price equation to decompose ecosystem function of a community by comparing the components to a null model. This approach has later been expanded to include weighed coefficients to represent species specific contributions to ecosystem function (Grossiord *et al.*, 2013). However, to date most of ecological partitioning methods have been applied to understand community-level contributions to ecosystem function. In contrast, quantitative methods that measure the contribution of traits and demographic properties to population-level effects on ecosystem function are limited (Rudolf & Rasmussen, 2013). Only a few Price equation-based partitioning derivations include individual (Fox & Harpole, 2008) or demographic components (Ellner, Geber & Hairston, 2011), but they determine the absolute relationship of various components to the change in ecosystem function rather than estimating the relative contribution of each component. One exception is a study that has used bioenergetics modeling to estimate the relative effects of biomass, size structure, growth, and elemental allometry to nutrient recycling of a fish population at a single point in time (Tuckett *et al.*, 2014).

Population level effects on ecosystem function arise from variation in individual traits and demographic characteristics (size structure and density). Ecosystem effect traits are defined as individual characteristics that affect ecosystem function (Violle *et al.*, 2007). Body size of an individual plays an important role, because many ecological effects scale allometrically (Brown *et al.*, 2004; Allgeier *et al.*, 2015). Studies in ecosystem ecology are increasingly recognizing that, in addition to density, the variation in body size across a population (i.e. the frequency distribution of body size, herein size structure/distribution) is important when measuring population level effects on ecosystem

function (Fritschie and Olden 2016). However, there is no consensus on how to incorporate size structure into population level effects. In trait based ecosystem ecology, integration functions are used to scale individual and demographic characteristics to the population and community level (Violle *et al.*, 2007), but they have had limited application. In addition, these scaling equations have not been used to partition the population-level effect on ecosystem function, even though the interest in understanding the relative contributions of traits and demographics has grown, in particular for eco-evolutionary studies (Hendry, 2016; El-Sabaawi, 2017).

In this paper, we propose a method, based on scaling equations, to partition population-level effects of a species through time. We first define and derive a simple algebraic partitioning method that decomposes change in any size related ecosystem function of a population into relative individual and demographic contributions. We then illustrate the method using longitudinal data from a series of guppy (*Poecilia reticulata*) introduction experiments performed in montane streams of the Caribbean island of Trinidad (Travis *et al.*, 2014) to partition guppy nutrient recycling (ecosystem function) into per-capita excretion (effect trait), size structure, and density. Since this method is adapted from scaling equations, which are simple and easy to use, it can be applied to data collected by most field studies in ecology. This method can be used for step-wise and continuous time data sets. In addition, this method is flexible to numerous ecological scenarios because it can include interactive and additive interaction factors between demographic and individual traits. We have created R functions to facilitate the application of this method (Appendix 2.1). We have also provided alternate derivations to demonstrate the power and flexibility of our method.

2.3 Population partitioning method (PoPaM)

2.3.1 Mathematical derivation

The effect of a population on an ecosystem process is the product of an ecosystem effect trait, body size, and density. Most ecosystem effect traits (e.g. excretion, respiration, nutrient uptake) scale allometrically with body size following a power law function

$$E = a\,(z)^{\,b}, \tag{1}$$

where E is the per-capita trait, z is body size, and a and b are, respectively, the normalization (i.e. intercept) and scaling (i.e. slope) coefficients. Populations have a size distribution, where varying proportions of individuals are distributed in size categories, and the population density is the sum of all individuals in that population per unit area. Thus, the population effect (R) on an ecosystem process is calculated as

$$R = \int E_{(z)} P_{(z)} N\, dz = \int a(z)^b P_{(z)} N\, dz, \tag{2}$$

where $E_{(z)}$ describes the trait at a given size z, $P_{(z)}$ depicts the proportion of individuals in the population with the size z, and N is the population density. Since the population effect at a given time is the integral of the trait, size structure, and density, the proportional change ($\frac{R_{t2}}{R_{t1}}$) from the given time ($t1$) to the next sampling time ($t2$) is

$$\frac{R_{t2}}{R_{t1}} = \frac{\int E_{(z,t2)} P_{(z,t2)} N_{(t2)} dz}{\int E_{(z,t1)} P_{(z,t1)} N_{(t1)} dz}. \tag{3}$$

To estimate the contribution of each component we based our approach on the differential sensitivity analysis (Hamby, 1994). We calculate a proportional difference that divides the measured change in the ecosystem function by a hypothetical scenario where the component in question did not change. For example, to calculate the contribution of size

structure to an observed ecosystem change, the hypothetical scenario is calculated by holding size structure constant across time points, while allowing the individual trait and density to vary as observed between the time points. The product of each proportional contribution (trait (A), size structure (S), and density (D)) and the interaction between them ($I_{A,S}$) equals the total proportional change in population-level effect ($\frac{R_{t2}}{R_{t1}}$):

$$\frac{R_{t2}}{R_{t1}} = ASDI_{A,S}, \tag{4}$$

where the proportional contribution of change in the effect trait is

$$A = \frac{\int E_{(z,t2)} P_{(z,t2)} N_{(t2)} dz}{\int E_{(z,t1)} P_{(z,t2)} N_{(t2)} dz} = \frac{\int E_{(z,t2)} P_{(z,t2)} dz}{\int E_{(z,t1)} P_{(z,t2)} dz}, \tag{5}$$

the proportional contribution of change in size structure is

$$S = \frac{\int E_{(z,t2)} P_{(z,t2)} N_{(t2)} dz}{\int E_{(z,t2)} P_{(z,t1)} N_{(t2)} dz} = \frac{\int E_{(z,t2)} P_{(z,t2)} dz}{\int E_{(z,t2)} P_{(z,t1)} dz}, \tag{6}$$

the proportional contribution of change in density is

$$D = \frac{\int E_{(z,t2)} P_{(z,t2)} N_{(t2)} dz}{\int E_{(z,t2)} P_{(z,t2)} N_{(t1)} dz} = \frac{N_{(t2)}}{N_{(t1)}}, \tag{7}$$

and the proportional contribution of the interaction between the trait and size structure $I_{A,S}$ is

$$\begin{aligned} I_{A,S} &= \frac{\int E_{(z,t2)} P_{(z,t2)} N_{(t2)} dz}{\int E_{(z,t1)} P_{(z,t1)} N_{(t2)} dz} \cdot \frac{\int E_{(z,t1)} P_{(z,t2)} dz}{\int E_{(z,t2)} P_{(z,t2)} dz} \cdot \frac{\int E_{(z,t2)} P_{(z,t1)} dz}{\int E_{(z,t2)} P_{(z,t2)} dz} \\ &= \frac{\int E_{(z,t1)} P_{(z,t2)} dz}{\int E_{(z,t1)} P_{(z,t1)} dz} \cdot \frac{\int E_{(z,t2)} P_{(z,t1)} dz}{\int E_{(z,t2)} P_{(z,t2)} dz} = \frac{R_{t2}}{R_{t1}} : (ASD). \end{aligned} \tag{8}$$

This interaction accounts for both the additive and interactive effects of A and S. In the first term of the interaction the proportional change is estimated where both components remain constant (E and P) while N varies, and the subsequent two terms of the interaction are needed to balance the first (i.e. $1/A$ and $1/S$). In this model density does not interact

with the trait, because density, unlike body size, has only a scaling effect (Appendix 2.2). However, if traits are density dependent, this term can be added much like it was for the interaction of body size and excretion.

2.3.2 Statistical Implementation

When scaling per-capita effects to the population level, it is important to propagate the errors associated with the trait measurements and allometric relationship between trait and size. Monte Carlo simulations are a common approach to propagate the error from individual to community levels (Manly, 2006). Therefore, we can estimate the allometric coefficients (a and b) for the effect trait a given number of times (e.g. 1000 times), where the trait is estimated from parameter values drawn from a multivariate normal distribution with means and variances taken as the coefficients and variance-covariance matrix of the allometric models.

2.4 Applying PoPaM to introduced guppy populations in Trinidad

We chose the Trinidadian guppy to test our method, because it is a well-studied species when examining the evolution of traits and demographic characteristics and their effect on ecosystem function, and guppies are also used to model the dynamics of species introduction (Travis *et al.*, 2014). In Trinidad, guppy populations exist in the same river (separated by waterfall barriers) with predators (high predation sites, HP) and without predators (low predation sites, LP). These guppies vary in a wide range of traits (e.g. life history, morphology, excretion rate), as well as population properties like density and size structure (Reznick, Shaw, Rodd, & Shaw, 1997). The evolution of the LP phenotype can

be induced by transporting guppies from downstream to upstream guppy-free environments (Reznick *et al.*, 1997). There have been several guppy introduction studies, which have shown that the release from predation pressure affects trait plasticity (Ghalambor *et al.*, 2015), heritable traits, and demographic properties (Reznick *et al*., 1997; Reznick, Butler IV, & Rodd, 2001). Understanding the ecological effects of guppies after they are introduced to a predator free environment is important because eco-evolutionary interactions might explain the LP phenotype (Travis *et al.*, 2014), and because guppies are an invasive species globally with negative effects on local communities and ecosystems (Deacon *et al.*, 2011; El-Sabaawi *et al.*, 2016). However, we have yet to understand how changes in guppy traits, size structure, and densities combine to contribute to changes in ecosystem function throughout the course of establishing in a new environment (El-Sabaawi, 2017).

Nutrient recycling is an important ecosystem function in which consumers can control resource dynamics by remineralizing nitrogen and phosphorus through excretion (Atkinson *et al.*, 2017). Excreted waste from organisms contains inorganic nutrients in the form of ammonium and phosphate that become an important nutrient supply to primary producers and microbial decomposers (Augustine & McNaughton, 2006; Coetsee, Stock & Craine, 2011). Nutrient recycling can be influenced by individual traits (body size, diet, elemental composition, growth rate, and assimilation efficiency) as well as population properties (density and size class distribution) (Allgeier *et al.*, 2015; Fritschie & Olden, 2016; Atkinson *et al.*, 2017). Previous guppy introduction experiments found that guppies from LP sites excrete less nitrogen per individual than guppies from HP sites, due to a dietary shift towards lower quality food (Zandonà *et al.*, 2011; El-

Sabaawi *et al.*, 2015). However, as a population, guppies in LP sites contribute more excreted nitrogen than in HP sites, because populations attain higher densities and larger average body sizes in the absence of predators (Bassar *et al.*, 2010; El-Sabaawi *et al.*, 2015).

We utilized data from four recent guppy introduction experiments on the island of Trinidad (Travis *et al.*, 2014) and applied PoPaM to ask: (a) how do the effect trait (per-capita excretion) and/or population dynamics (size structure, density) contribute to ecosystem function (nutrient recycling); (b) do their relative contributions change throughout the early stages of their establishment; and (c) if the impacts of the traits and demographics are context specific to the environment. We predicted that density would be the primary contributor of population excretion during the early phases of the invasion, because the removal of natural enemies (e.g. predators) can cause rapid increases in species abundance (enemy release hypothesis) (Liu & Stiling, 2006). As the population stabilizes and guppies acclimate and potentially adapt physiologically to their new environment, we expected that that per-capita excretion rate would play an important role in determining population excretion, because it is sensitive to diet and life-history changes (Sterner & Elser, 2002) and might evolve to be lower in LP guppies (Dalton *et al.*, 2017). Therefore, we predicted that guppy per-capita excretion rate would decline after introductions, causing the population excretion to decline as well. Population size structure is linked to life history traits of female guppies and changes in female size have been reported to evolve by 7.5 years (Reznick *et al.*, 1997). However, rapid plastic changes in body size are also possible after species establish, but little is known about

them in guppies. Therefore, we expected population size structure to vary within the first six years, possibly towards a larger average body size.

To address if the relative contribution of each component varies across environmental conditions, we compared the results from the above analysis with two introduction streams where riparian canopy was thinned to allow more light to reach the streambed. In stream ecosystems, light increases resource quality and quantity (Kohler *et al.*, 2012; Travis *et al.*, 2014), which affect key guppy traits and population dynamics (El-Sabaawi *et al.*, 2015). Therefore, we predicted that the impact of traits and demographic properties of a guppy population would be context specific and would vary with light availability. Specifically, we hypothesized that light would increase population excretion in the guppy by increasing guppy densities, per-capita excretion rate, and average size.

2.5 Methods

2.5.1 Description of the guppy introduction data

The methods described herein have already been reported in published studies, but the relevant details are summarized here. Guppies from the downstream high predation pressure sites of the Guanapo river were introduced to four first order streams in the Guanapo watershed that were relatively undisturbed, guppy-free, low in predators, and similar in geology and riparian vegetation (Travis *et al.*, 2014). Males and females that were mated in the laboratory, were introduced at even sex ratios into the Lower La Laja (LOL, 75 individuals, 0.18 ind/m^2) and Upper La Laja (UPL, 74 individuals, 0.14 ind/m^2) in March 2008, and into the Caigual (CAI, 127 individuals, 0.62 ind/m^2) and Taylor (TAY, 102 individuals, 0.67 ind/m^2) in March 2009 (Handelsman *et al.*, 2013).

One year before the guppy introductions, riparian canopy was experimentally thinned along a 200 m reach by 4% at UPL and 28% at TAY (Kohler *et al.*, 2012). No canopy manipulations were conducted at LOL and CAI stream reaches. The canopy treatments were maintained and light levels were monitored to ensure they remained at similar levels throughout the sampling period (Kohler *et al.*, 2012; Collins *et al.*, 2016). In each stream, guppy nutrient excretion rates were measured within a 60-80 m reach during the dry season (March - May) in years 1-3 and additionally in year 5 for CAI and 6 for LOL. For each of these sampling events population density and size structure was obtained from monthly censuses carried out routinely for a parallel capture-mark-recapture study (Travis *et al.*, 2014).

Nitrogen recycling rates of individual guppies were sampled across the full range of the observed body size distribution ($N = 386$; 20-35 individuals per stream and year). Individual guppies were placed in sealable containers filled with a known volume of filtered stream water. Containers were positioned in stream water to maintain similar temperature. Water was sampled from the container before the introduction of the guppy, after 20 min, and after 40 min of incubation. Wet body mass (0.35 – 1.75 g) of each individual was measured, and water samples were analyzed for ammonium concentration using a fluorometric method (Holmes *et al.*, 1999). Guppies with ammonium excretion levels below the detection limit of the fluorometer were removed from all analyses (18/386). Per-capita excretion rates (µg N/h) were calculated by subtracting the initial ammonium concentration from the final, and adjusted for the volume of water in the container, incubation time, and background water concentration.

2.5.2 Calculating the population-level effect and contributions of each component

We established an allometric relationship between the logarithm of the individual body mass and logarithm of the per-capita nitrogen excretion rates. This relationship is defined by equation (1). To estimate coefficients *a* and *b*, we fit linear models to the log-excretion against log-size data for each of our four focal streams and time points (N_{LOL} = 104; N_{UPL} = 104; N_{CAI} = 95; N_{TAY} = 65). We extracted the mean estimates and the variance-covariance matrix for each allometric relationship from the output.

We applied a Monte Carlo simulation to generate 1000 slopes and intercepts for each allometric relationship between size and the individual trait (e.g. per-capita excretion). With the data on population structure and density, we calculated population excretion rates according to equation (2) for each of the 1000 combinations of allometric parameters. With this distribution of 1000 results, we obtained the mean guppy population-level excretion rates (i.e., amount of nutrients excreted by all individuals within a population per unit time and area (μg N/h/m^2)) with the associated 95% confidence intervals for each stream and time point. Lastly, we decomposed population level effect into trait and demographic components using equations (3-8), to estimate the proportional contribution of per-capita excretion, size structure, density, and the interaction to the change in guppy population excretion for each stream and time point. These calculations were done on all 1000 Monte Carlo simulations, to calculate the associated 95% confidence intervals.

We created five functions in the statistical program R in conjunction with the "tidyverse" environment (Wickham, 2017), to facilitate the application of the PoPaM.

These functions, along with the R code, and an example on how to use them, are available in Appendix 2.1 and 2.3.

2.5.3 Statistical analyses of results

We ran linear models to determine the significant relationships between size and per-capita excretion. We ran the Kruskal-Wallis test to determine if there was a significant difference between mean size across time and space. We applied the Dunn test, using the package "FSA" in R (Ogle, Wheeler & Dinno, 2018), to determine which population size structure was different. We included baselines in the population excretion plot, which were extracted from El-Sabaawi *et al.* (2015), a study that compared guppies from naturally low (LP) and high predation (HP) areas in the Guanapo River. Since guppies from our study came from the same high predation source population, these baselines gave us the opportunity to check if and how guppy characteristics were shifting relative to the naturally low predation guppy phenotype from the same river.

2.6 Results

2.6.1 Traits and population properties

Per-capita excretion rates varied through time since guppy introduction, and increased with size, which was a consistent trend across time and streams (Fig. 2.1, Appendix 2.4) and expected according to metabolic theory (Brown *et al.*, 2004). The overall average metabolic scaling coefficient was 0.66, which is close to the 2/3 power law, but coefficients ranged between 0.5 and 0.99 across sites and years, as is common for intraspecific vertebrate scaling coefficients (Glazier, 2005). Per-capita excretion ranged

between 0.03 – 47.78 μg N/fish/h and was quite variable between years. There was no consistent difference in per-capita excretion rates between high and low light availability.

Guppy density increased considerably in the first year of the introduction and leveled off within three years (Fig. 2.2), while population size structure varied through the years (Fig. 2.3). In streams with low light conditions (CAI and LOL), guppies increased their densities up to 2.5 individuals per m^2 and then remained relatively consistent across time since introduction. Under higher light conditions guppies increased densities up to 4 (UPL) and 6 (TAY) individuals per m^2 within the first two years, but decreased to around 2.5 individuals in year three. This dip in density from year two to three was also apparent in LOL. Densities were between 1.5 to 3 times larger in high light streams compared to streams with less light availability. The average size based on guppy weight varied between 0.17 and 0.22 g per individual across streams. While there were some significant differences in average size across time and between streams, the general size structure of the guppy populations did not vary in a consistent patter between light treatments and with time since introduction (Fig. 2.3, Appendix 2.5).

2.6.2 Population excretion and relative contribution of components across time

Guppy populations added up to 41.5 μg/h/m^2 of nitrogen via excretion to previously guppy-free streams, where rates initially increased but then declined across the years of post-guppy introduction (Fig. 2.4). Within the first two years after the introduction, nitrogen levels excreted by guppy populations were 5 to 10-fold higher than the baseline for guppies under naturally high predation pressure (3.82 μg/h/m^2) and 1 to 2-fold higher than guppies under naturally low predation pressure (14.74 μg/h/m^2, Fig. 2.4; El-Sabaawi

et al., 2015). Between years two and three post-introduction, population excretion rates sharply declined. LOL increased again thereafter at a slower rate, compared to the first two years. The slower increase in population excretion was not as apparent in CAI, because we did not see the significant drop in population excretion in year three. The general pattern of population excretion did not change between light treatments, however, population excretion rates doubled in high light compared to low light conditions.

Initial population excretion increases were almost entirely driven by density (Fig. 2.5). However, per-capita excretion, which declined within the first year, was also an important contributor of change in population excretion (contributed up to 80%). Therefore, within the first year, density and per-capita excretion had opposing effects on population excretion; density drove population excretion up as per-capita excretion rates declined. However, between years one and two both density and per-capita excretion increased population excretion. In addition, concurrent declines in density and per-capita excretion reduced population excretion during the second year, except for TAY, which decreased during the first year. After year three, per-capita excretion was the main contributor of population excretion increases. This result indicates that the variation in per-capita excretion drove a lot of the variability both among years and between sites. Guppy size structure and the interaction of size structure and per-capita excretion contributed at most 25% to changes in guppy population excretion. These patterns were consistent between the intact and thinned canopy treatments.

2.7 Discussion

2.7.1 PoPaM in relation to the guppy study

PoPaM allowed us to calculate excretion rates of an introduced population and evaluate how they change through time. Nutrient recycling by guppy populations varied substantially within the first six years post-introduction. This is not surprising since the effect of a newly established species can vary considerably through time (Vilà *et al.*, 2011; Strayer, 2012). Guppy population excretion rates generally increased rapidly within the first two years (up to 28-fold) but then declined in year three (up to 80%, Fig. 2.4). In addition, when comparing our results to excretion rates from guppies under natural low and high predation pressure (El-Sabaawi *et al.*, 2015), we do not see our values consistently shifting from the high to low predation phenotype over time. Instead we see dynamic shifts, which could indicate that when a new species establishes the ecosystem level impacts are not linear through time.

PoPaM also allowed us to discover which components (traits and/or population demographics) drove the overall change in population excretion. As we predicted, guppy density and per-capita excretion mainly contributed to changes in population excretion during the first six year post-introduction, while population size distribution and the interaction factor played small roles. Guppy density increased substantially in the first two years, which is likely a result of the predation pressure release (Liu & Stiling, 2006). However, sharp increases in abundance can lead to reduced offspring numbers and increased adult mortality (Reznick, Bassar, Travis, & Helen Rodd, 2012), which likely explains the decline in guppy abundance after year two. Per-capita excretion is a variable trait that responds to changes in diet quantity, quality, consumption rate or changes in

nutrient demand (Sterner & Elser, 2002; El-Sabaawi *et al.*, 2012b). Therefore, declines in per-capita excretion can result from guppies switching to a lower quality resource when under low predation pressure (Zandonà *et al.*, 2011); while high densities in low predation environments could elevate stress levels of fish, which can increase per-capita excretion rates (Whiles *et al.*, 2009).

Lastly, PoPaM allowed us to test if population excretion patterns are context specific. We saw evidence that light increased population excretion by increasing guppy density and elevating per-capita excretion rates. Light increases algal production in Trinidadian streams (Kohler *et al.*, 2012), which expands resource availability, increasing guppy densities and subsequently population excretion rates in streams with less canopy cover. This indicates that some aspects of population excretion are context specific. However, the overall direction of guppy population excretion over time and relative contribution of each component did not differ with the light treatments, indicating that other aspects of population excretion do not vary with specific environmental condition.

Traits and population properties that allow introduced species to establish are relatively well defined, but components that drive subsequent ecosystem-level changes are still debated (Ricciardi *et al.*, 2013). Studies have suggested that both traits and demographic properties of introduced populations play important roles (Ricciardi *et al.*, 2013; Fritschie & Olden, 2018); yet the relative importance of each and their interaction in reshaping ecosystem dynamics have not been measured. Although the guppy data used here is not meant to draw exhaustive conclusions about the effects of guppy introductions on ecosystem function, it demonstrates the potential and power of this method to answer questions about the effects of an introduced species.

2.7.2 Broader considerations of PoPaM

PoPaM is based on scaling equations, which are algebraically simple, making this method relatively easy to apply. In addition, the method estimates change in ecosystem function as a proportional difference between two populations in space and/or time. Proportional differences have the advantage to estimate the relative differences of each component in relation to the total change and the change of the other components. When using the absolute change in ecosystem function (e.g. Price equation adaptations), the effect size of each component needs to be calculated separately. On the other hand, community-level partitioning methods that are derived from the Price equation account for context dependent effects (Fox, 2006), which PoPaM cannot directly estimate (i.e. the relative contribution of environmental variation in relation to individual and demographic components). However, it can estimate if context dependence matters to ecosystem function and its components, if the experimental design is set up as such. If context dependence is not taken into consideration, PoPaM will operate under the assumption that all other environmental variables are similar across space and time. Lastly, PoPaM has the advantage that it is not dependent on a null hypothesis, which is what any method related to Loreau and Hector's equation requires (2001). Nevertheless, we want to emphasize that we consider PoPaM to be a complementary population-level approach to the already existing community-level partitioning methods and suggest utilizing both methods in conjunction to estimate the drivers and their contributions to ecosystem function change on both the population - and community-level.

PoPaM is simple, powerful, and adaptable and can therefore be applied it to a variety of field study scenarios. The method can be expanded and contracted, depending on the set up of the study. For example, if there is no allometric relationship between the body size and effect trait, the same but simplified framework can be applied to scale the individual trait to the population level and then decompose trait and density into proportional contributions (see Appendix 2.6). On the other hand, some studies have suggested that density dependence of an individual trait might vary once populations have evolved (Bassar *et al.*, 2010). This means that a density-trait interaction factor may be necessary, which can easily be added to this framework. In addition, this method can be informative at different continuous or discrete time scales or at different spatial scales/gradients (e.g. space-for-time substitution, Chapter 4). With PoPaM's simplicity and adaptability the method can be applied in the context of several ecological questions.

2.7.3 Broader applications of PoPaM

Since PoPaM is adaptable to any rate-based ecosystem function (e.g. metabolism, production) that changes over time and/or space, this method can be applied to other questions outside the realm of species introductions. PoPaM can be applied to any biodiversity-ecosystem function question that is interested in the contributions of functional traits and demographic properties. For example, scientists and managers can use it to understand which characteristics within a population changes ecosystem function as a result of anthropogenic disturbances (e.g. species introduction/ removal, climate change, urbanization). In addition, eco-evolutionary studies are realizing that traits are important for ecosystem function and that they interact with demographics, but these

interactions have not been quantified or deciphered yet (Hendry, 2016; El-Sabaawi, 2017). PoPaM would be able to identify which functional traits and demographic components are driving ecosystem function change through time.

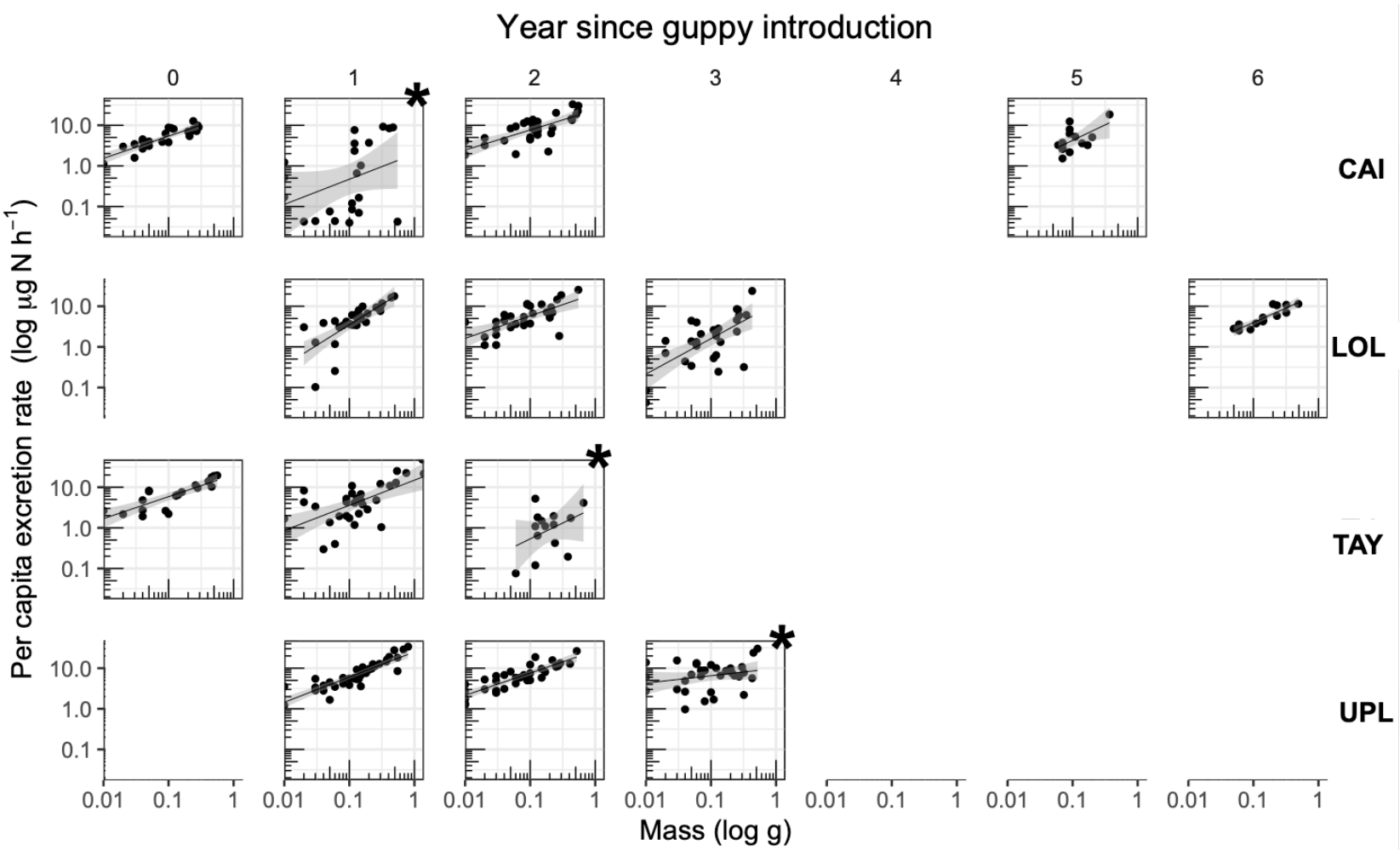

Figure 2.1: Per-capita excretion rates of guppies (log of µg nitrogen excreted individual^{-1} hour^{-1}) across body size (log of mass in grams) over time since guppy introduction. CAI and LOL streams were under low light conditions, while TAY and UPL had higher light conditions. The lines represent model fits with 95% CI, and asterisks indicate the relationships that were not significant. There was no consistent difference between years and streams.

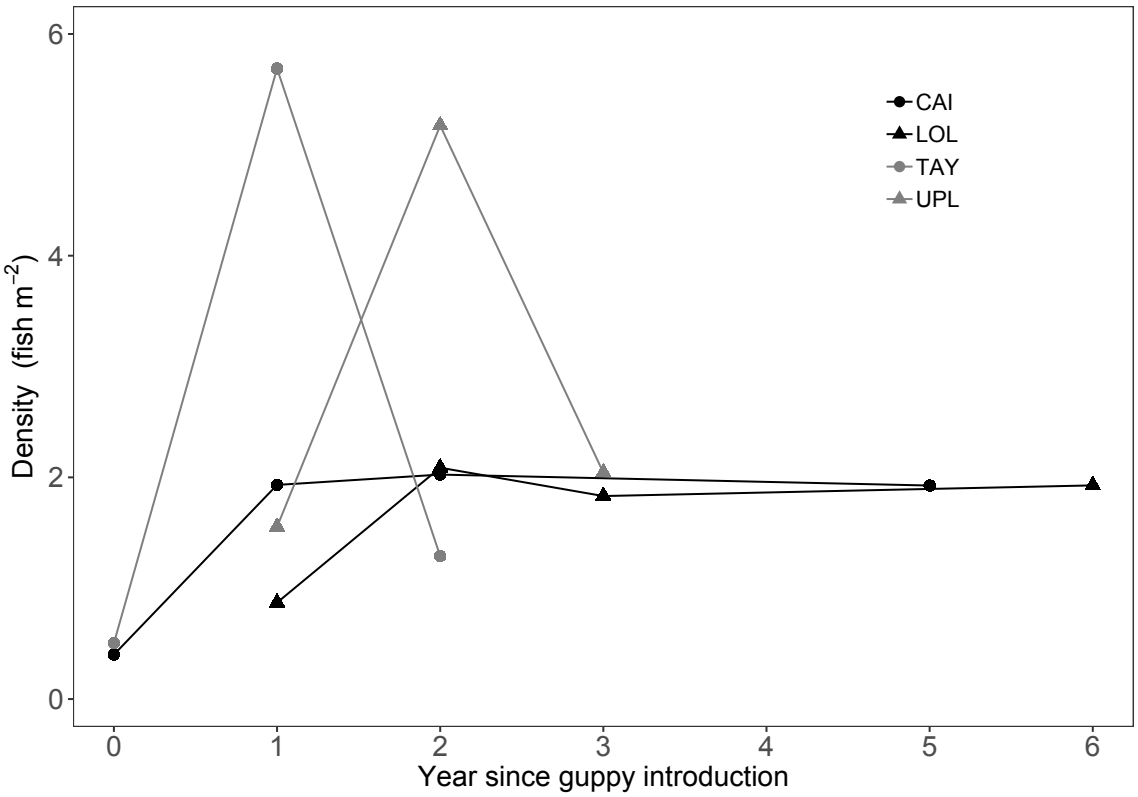

Figure 2.2: Guppy population density (fish m^{-2}) across years since guppies were introduced from a high predation pressure environment into an environment with little predation. TAY and UPL stream reaches have 28% and 4% reduced canopy cover, respectively, while CAI and LOL canopy cover remained intact.

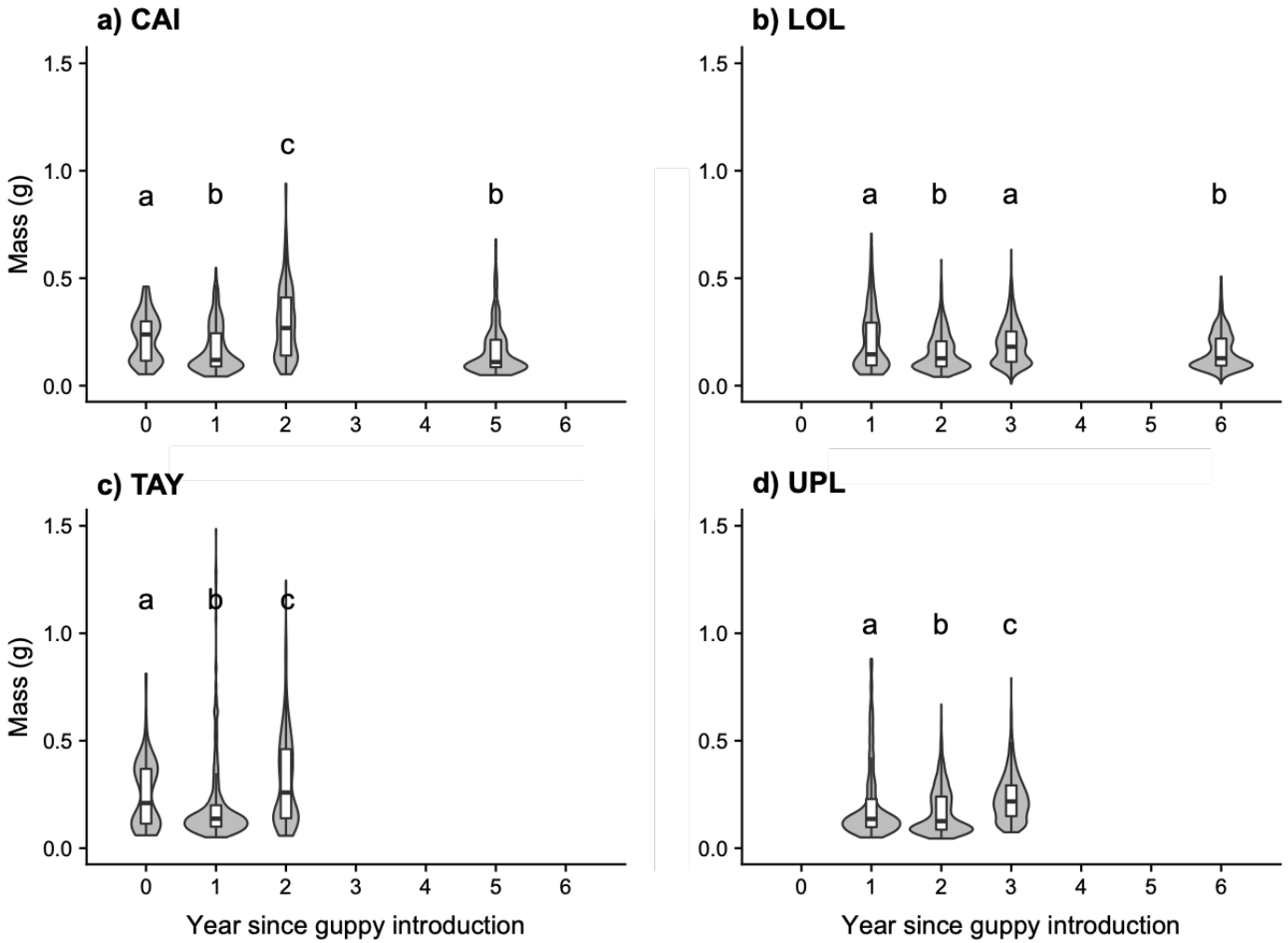

Figure 2.3: Violin plots of the size frequency distribution of guppy populations over years since guppy introduction at low (a and b) and high (c and d) light condition in streams. While there were some significant differences in average size across years since introduction (indicated by letters from Kruskal-Wallis test, $p \leq 0.05$), the size distribution varied little across years and streams.

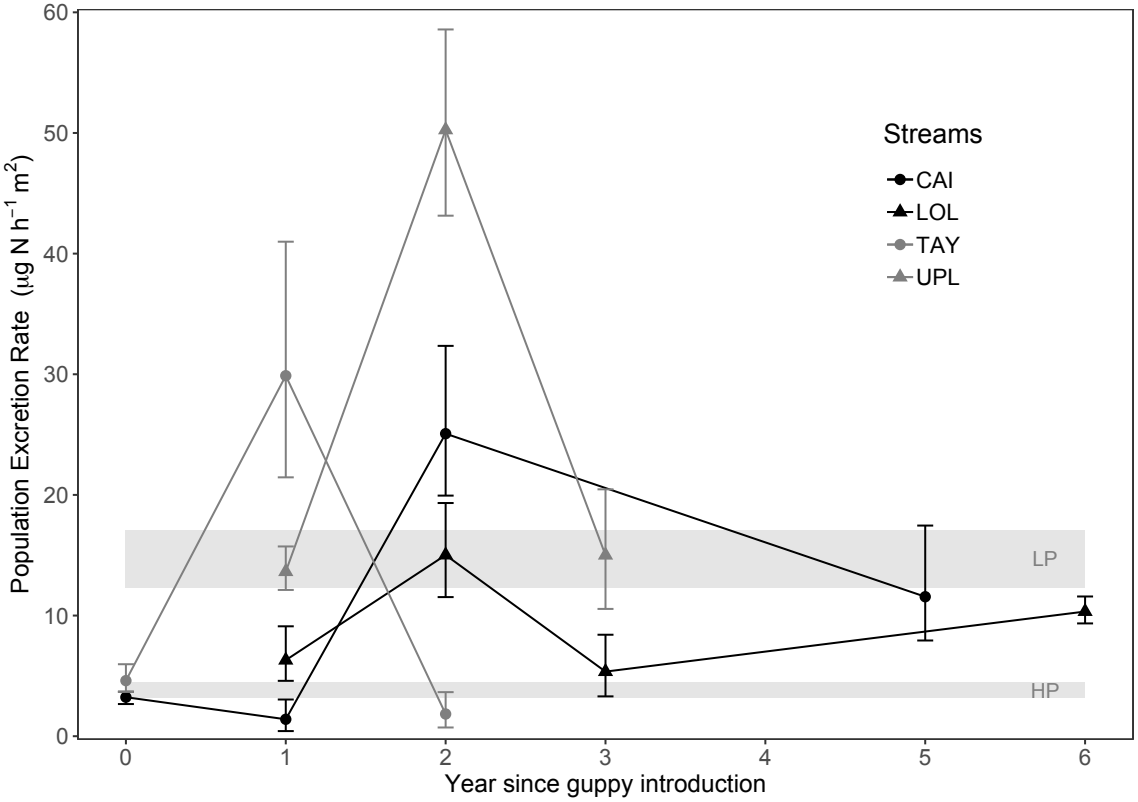

Figure 2.4: Guppy population excretion (µg of N h^{-1} m^{-2} with 95% confidence intervals) varied over time since guppies were introduced from a high predation pressure environment into an environment with little predation. TAY and UPL stream reaches had 28% and 4% reduced canopy cover, respectively, while CAI and LOL canopy cover remained intact. The upper and lower gray lines represent excretion rates from guppy populations that naturally experience low (LP) and high predation (HP) pressure with 95% CI.

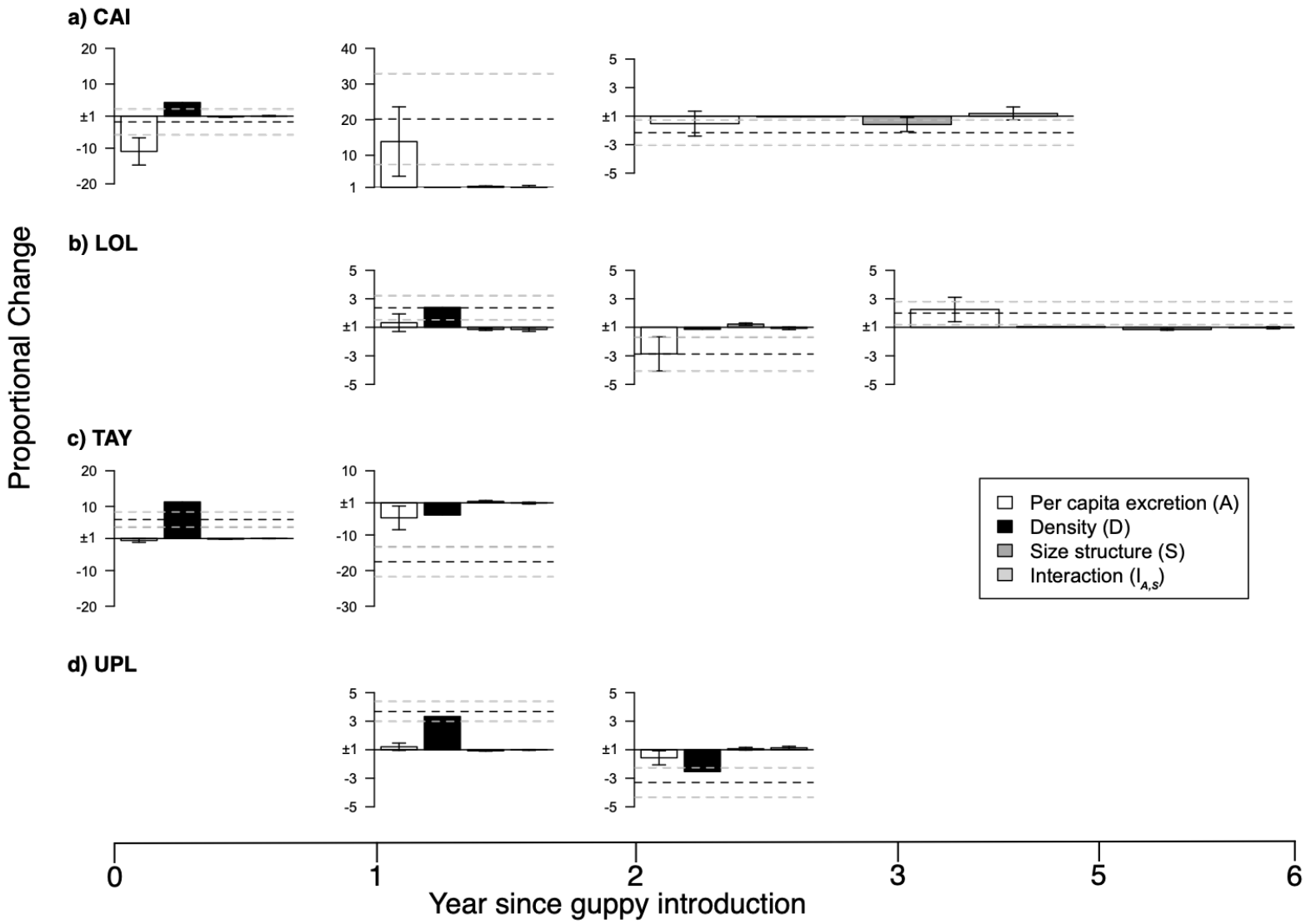
a) CAI
b) LOL
c) TAY
d) UPL
Proportional Change
Per capita excretion (A)
Density (D)
Size structure (S)
Interaction ($I_{A,S}$)
0
1
2
3
5
6
Year since guppy introduction

Figure 2.5: Each bar represents the contribution of a component (i.e. per-capita excretion (A), density (D), population size structure (S) and the interaction of A and S) ± 95% confidence intervals (CI) to the proportional change in population-level excretion from one post-guppy introduction year to the next for two low ((a) and (b)) and high ((c) and (d)) light streams. For each plot the sum of all components equals the proportional change in population excretion, which is represented by the black dotted line (grey dotted lines represent 95% CI). Positive entries (y-axis > 1) represent proportional increases, while negative entries (y-axis < -1) represent decreases. For example, TAY population excretion increased 6x between year 0 and 1, which mainly resulted from the 11x increase in density and the 1.5x decline in per-capita excretion. Overall guppy density and per-capita excretion drove changes in population excretion throughout the six years post-guppy introduction. Note: Y-axes have different scales. The third graph in (a) and (b) are stretched out because no data were collected during year 3 and 4, and 4 and 5 post-guppy introduction.

Chapter 3: Evaluating ecosystem effects of climate change on tropical island streams using high spatial and temporal resolution sampling regimes

Adapted from: Therese C. Frauendorf [1], Richard A. MacKenzie[2], Ralph W. Tingley III[3], Abby G. Frazier[4], Michael H. Riney[5], and Rana W. El-Sabaawi[1]. 2019. *Global Change Biology (25)*,1344-1357.

[1] Department of Biology, University of Victoria, Victoria, British Columbia, V8W 3N5, Canada

[2] Institute of Pacific Islands Forestry, Pacific Southwest Research Station, USDA Forest Service, Hilo, Hawaii 96720, USA

[3] Missouri Cooperative Fish and Wildlife Research Unit, The School of Natural Resources, University of Missouri, Columbia, Missouri 65211

[4] East-West Center, Honolulu, Hawaii 96848, USA

[5] Shasta Valley Resource Conservation District, Yreka, California 96097, USA

Author contributions: TCF conceived and designed the experiment, with intellectual contributions from RAM and RES. TCF and MHR gathered the raw field data and analyzed the resource and invertebrate data. AGF and RWT collected and analyzed the rainfall and streamflow data. TCF wrote the manuscript. RES, RAM, RWT, AGF and MHR all provided editorial advice.

3.1 Abstract

Climate change is expected to alter precipitation patterns worldwide, which will affect streamflow in riverine ecosystems. It is vital to understand the impacts of projected flow variations, especially in tropical regions where the effects of climate change are expected to be one of the earliest to emerge. Space-for-time substitutions have been successful at predicting effects of climate change in terrestrial systems by using a spatial gradient to mimic the projected temporal change. However, concerns have been raised that the spatial variability of these models might not reflect the temporal variability. We utilized a well-constrained rainfall gradient on Hawaii Island to determine a) how predicted decreases in flow and increases in flow variability affect stream food resources and consumers and b) if using a high temporal (monthly, 4 streams) or a high spatial (annual, 8 streams) resolution sampling scheme would alter the results of a space-for-time substitution. Declines in benthic and suspended resource quantity (10-40 fold) and quality (shift from macrophyte to leaf litter dominated) contributed to 35-fold decreases in macroinvertebrate biomass with predicted changes in the magnitude and variability of flow. Invertebrate composition switched from caddisflies and damselflies to taxa with faster turnover rates (mosquitoes, copepods). Changes in resource and consumer composition patterns were stronger with high temporal resolution sampling. However, trends and ranges of results did not differ between the two sampling regimes, indicating that a suitable, well-constrained spatial gradient is an appropriate tool for examining temporal change. Our study is the first to investigate resource to community wide effects of climate change on tropical streams on a spatial and temporal scale. We determined that predicted flow alterations would decrease stream resource and consumer quantity and

quality, which can alter stream function, as well as biomass and habitat for freshwater, marine, and terrestrial consumers dependent on these resources.

3.2 Introduction

Climate change is threatening ecosystems, yet our understanding of the effects of precipitation change on ecosystem structure and function remains limited. Temperature, atmospheric carbon dioxide, and precipitation are altered simultaneously by climate change, yet the majority of studies focus on the effects of increasing temperature, followed by changes in carbon dioxide (Bale *et al.*, 2002; Rosenblatt & Schmitz, 2014). Current climate models project global and regional changes in precipitation quantity, variability, and timing (Chadwick, Boutle & Martin, 2012; IPCC, 2014; Donat *et al.*, 2016). However, most experimental studies emphasize the effects of changes in precipitation quantity, rather than changes in intensity, timing and frequency of precipitation events (Wu *et al.*, 2011). In addition, studies measuring impact of changes in precipitation related to climate change are primarily focused on terrestrial ecosystems, while studies in freshwater systems remain limited (Wu *et al.*, 2011). However, effects of changes in precipitation are especially important to understand in lotic systems, as precipitation is one of the main drivers of streamflow.

Changes in rainfall patterns driven by global climate change are likely to have severe impacts on stream structure and function. A recent model estimated that predicted changes in streamflow and warming are equally important risks to stream community composition in different ecoregions (Pyne & Poff, 2017). The magnitude, variation, and duration of streamflow are essential for the ecological integrity of stream systems (Poff *et*

al., 1997; Jardine *et al.*, 2015). Natural flow disturbances regulate habitat structure, population size, and species diversity (Lytle & Poff, 2004). It is highly likely that the projected changes in precipitation can all affect streamflow magnitude, timing, and variation simultaneously. For example, projections indicate that in northern temperate regions warming will cause snowmelt-driven streams to switch into rainfall-driven streams, shifting the timing and magnitude of peak flows from summer to winter (Zwiers, Schnorbus & Maruszeczka, 2011). In many tropical regions, the frequency and intensity of flash flood events is expected to increase, but overall streamflow is predicted to increase or decrease depending on the region-specific precipitation projection (IPCC, 2012).

Studies on the effects of precipitation changes are concentrated in temperate ecosystems (Wu *et al.*, 2011), yet tropical regions are expected to be one of the first to be impacted by climate change (Mora *et al.*, 2013). In addition, tropical biomes are considered especially sensitive ecosystems to climate variability, because they are often already approaching ecological tipping points (Seddon *et al.*, 2016). Tropical islands, in particular, are at the forefront of changes in precipitation. In Hawaii, for example, studies have documented significant drying trends statewide since 1920 (Frazier & Giambelluca, 2017) with an increase in the number of dry days in the last 50 years (Chu, Chen & Schroeder, 2010) and long-term stream gauging showing a 23 percent reduction of flow over the past 100 years (Bassiouni & Oki, 2013). However, the ecological response to these changes in flow is not well understood. One of the reasons for this paucity in both tropical and temperate systems is that streamflow, in particular flow variability, is

difficult to experimentally manipulate *in situ* and the results are often measured over a short time frame (Poff *et al.*, 2018).

Predicting long-term ecosystem responses to changes in precipitation and streamflow is uniquely challenging, because we lack the data required to mechanistically model ecosystem processes in most aquatic ecosystems. Such a challenge can only be currently met by observational studies that substitute spatial variations in environmental conditions for temporal variation. A space-for-time substitution is an experimental design where a spatial gradient mimics a projected or historical change over time. It is an innovative way to characterize ecological dynamics that occur over time-scales beyond the duration of conventional experiments, without compromising realism (Fukami & Wardle, 2005). They have accurately predicted approximately 72% of real time scenarios in terrestrial systems (Blois *et al.*, 2013) and have been used for quantitative predictions in data-poor regions like the tropics (Lester *et al.*, 2014). They allow us to examine impacts of changes in precipitation quantity and variability across terrestrial gradients. However, the utilization of space-for-time substitutions in aquatic ecosystems is rare (Thomaz *et al.*, 2012), despite the presence of appropriate gradients (e.g. Strauch *et al.*, 2015).

Here, we use a space-for-time substitution approach in order to investigate how tropical island stream ecosystems will respond to projected changes in precipitation. We utilize a rainfall gradient on Hawaii Island that mimics projected decreases in seasonal precipitation and increases in precipitation variability (Zhang *et al.*, 2016; Jackson *et al.*, 2017). The mean annual rainfall (MAR) along a 20 km long stretch of the North Hilo coastline has a range of approximately 3500 - 7000 mm yr^{-1} (Giambelluca *et al.*, 2013),

while mean annual temperature, riparian plant community structure, land use, soil type, and geologic age show little variation at similar elevations. The strong decline in rainfall across this MAR gradient results in concomitant declines in stream baseflow and flow stability (Strauch *et al.*, 2015). The precipitation trend across these streams follows the historical trends and future projections of streamflow for high-gradient streams of the Hawaii islands (Bassiouni & Oki, 2013; Strauch *et al.*, 2015). Therefore, the streams along the North Hilo coast offer an excellent model ecosystem to test hypotheses about the response of stream resource and consumer dynamics to projected changes in precipitation and flow.

The first objective of this study was to determine how basal resources and consumers in streams respond to predicted changes in flow during the dry season (May to September) in eight streams across our rainfall-flow gradient. First, we wanted to test if the rainfall pattern during our seasonal sampling was representative of long-term conditions along our gradient (Giambelluca *et al.*, 2013) and test if those changes in rainfall led to the predictable changes in streamflow quantity and variability that have been established previously (Strauch *et al.*, 2015). We repeated this analysis for three years in order to assess interannual variability. Second, we tested how the resources and macroinvertebrate consumers responded to projected changes in flow. We predicted that climate-driven changes in flow would increase detrital resources (e.g. leaf litter) at the expense of autochthonous (e.g. macrophytes) resources, because reduced streamflow can increase detrital standing stocks (Jones, 1997). In other words, detrital resources will dominate towards the dry end of the gradient. Macrophytes are a higher quality food resource compared to leaf litter, because they have lower carbon:nitrogen ratios (Dodds *et*

al., 2004). Therefore, with declines in resource quality and changes in flow, we hypothesized that invertebrate consumer biomass will decline. We also predicted that species with faster turnover rates would become dominant at the dry end of the gradient as a result of high-flow variability.

Our second objective was to determine the sensitivity of predictions generated from a space-for-time study to changes in sampling scheme. When establishing a space-for-time-substitution, studies need to balance the number of sites representing a gradient of interest and the frequency of sampling events (Gonzalez *et al.*, 2016). In tropical stream ecosystems, there are considerable short-term temporal variations in precipitation and flow due to seasonal changes in rainfall (i.e., dry vs. wet season dynamics) or interannual variability that results from influences of El Niño and La Niña events. Sampling across seasons along the gradient helps frame forecasted changes in flow to the seasonal cycle, but there is often a logistical tradeoff between sampling frequently in time and sampling frequently in space. To answer this question in the context of climate change, we collected resources and macroinvertebrate consumers in 4 of the 8 streams across the MAR gradient, monthly for one year. This created two sampling schemes, where one has a high spatial (8 streams) and lower temporal resolution (1x per year for 3 years), which will be referred to as HSR; while the other has a high temporal (12x per year for 1 year) but lower spatial resolution (4 streams), which will be referred to as HTR. This allowed us to compare the resource and consumer response to flow change between the two sampling schemes and determine if the magnitude and variability of the response variables are similar between the HSR and HTR sampling.

3.3 Materials and methods

3.3.1 Study sites and rainfall data

Streams along the north east coast of Hawaii Island are characterized by narrow gulches, riparian vegetation comprised of native ʻŌhiʻa trees (*Metrosideros polymorpha*), Uluhe fern (*Dicranopteris linearis*), and non-native strawberry guava (*Psidium cattleyanum*), and young geologic substrate that was formed from a similar aged lava flow (<100,000 years). The slopes of the streams are comparable along the gradient (Table 3.1, Strauch *et al.*, 2015). Eight streams were selected along the rainfall gradient spanning a range of ~3000 mm mean annual rainfall (Honolii (HON), Kapue (KAP), Kolekole (KOL), Umauma (UMA), Manoloa (LOA), Makahiloa (MAK), Pahale (PAH), and Kaawalii (KAA)) for the high-spatial-resolution (HSR) sampling scheme and sampled once during the dry season of 2015 and 2016 (Fig. 3.1). In addition, four of the eight streams (KOL, UMA, MAK, and KAA) were selected for monthly sampling between April 2012 and March 2013 to represent the high-temporal-resolution (HTR) sampling.

We attributed 30-year mean annual rainfall estimates to all local catchments (see Tingley *et al.* 2018) for details on catchment delineation) within the study area by using the Rainfall Atlas of Hawaii (Giambelluca *et al.*, 2013). We then used an aggregation tool, described in Tsang *et al*. (2014), to calculate the area-weighted average of rainfall in the upstream catchment of each sample site. Since both local and upstream rainfall influence the availability of fluvial habitat within the channel, we averaged upstream and local estimates of rainfall. In addition, we calculated 2012, 2015, and 2016 dry season rainfall using the same procedure. Monthly rainfall data were available 2012 (Frazier *et al.*, 2016), while the 2015 and 2016 rainfall data were collected from all nearby stations

and interpolated using an optimized Inverse Distance Weighted (IDW) technique (see Longman *et al.* (2019) for method details). Rainfall totals were summed from May 1 through September 30 to obtain the dry season values for each year.

3.3.2 Stream parameters

For each study stream, streamflow was compiled from a continuous dataset that uses in-stream data loggers to collect flow measurements at 15-minute intervals (Strauch *et al.*, 2015). Any interruptions in the continuous data set that resulted from logger malfunction or complete loss of logger due to strong flash flood events were supplemented with values from a distributed hydrology model (DHSVM), which was specifically developed for streams along the North Hilo coast (Povak *et al.*, 2017). We calculated base- (Q_{90}), median- (Q_{50}), and storm flow (Q_{10}) based on mean daily flow and adjusted these values for the watershed area of each stream (L s^{-1} km^{-2}). From these values, flow variability (Q_{10}/Q_{90}) and flood intensity (peak flow/Q_{50}) were estimated. For HSR sampling, these flow variables were averaged from May through September of each year, while for the HTR sampling scheme flow variables were averaged across each month sampled.

Study reaches of each stream were dominated by riffle/run systems, and began and ended with large waterfall/plunge pool complexes. Since deep plunge pools are difficult to sample using the same methods and comprised only about 10% of the habitat, we focused our collections on riffle/run sites within a 100 m study reach. All the sampling reaches were at similar elevation between sites (Table 3.1). For each HSR and HTR sampling event, we selected three random sites within the reach to obtain one collection of each resource and consumer variable and averaged these three replicates. In

addition to these variables, percent substrate composition was visually estimated within a 0.1 m^2 sampling area and canopy cover was estimated using a densiometer at each of these three random locations. Resources and consumers were collected using the same methods for both HSR and HTR sampling schemes.

3.3.3 Benthic and suspended resource biomass and composition

Benthic organic matter was collected at three random sites within the reach using a Surber sampler (250 μm mesh size, 0.1 m^2 sampling area). Samples were dried to a constant weight at 65 °C (≥ 48 hours)**,** combusted at 550 °C for 3 hours, and reweighed to obtain ash-free dry mass (AFDM; Hauer & Lamberti, 2011). In 2012 and 2015 benthic samples were sorted into macrophyte, leaf litter, wood, seeds, grass, and miscellaneous (unidentified ≤ 1 mm detritus) categories before they were combusted to determine the dominant resource types. Suspended organic matter was collected using a drift net (250 μm mesh size, 0.1 m^2 sampling area) which was secured at the water surface for ~ 30 min during baseflow conditions. To estimate drift concentration (mg AFDM L^{-1}), volume of water passing through the net was calculated by accounting for water velocity across the net, area of submerged net, and time that the net was submerged.

Benthic biofilm was collected using a modified Loeb sampler (Loeb, 1981) and scrubbing between 1-7 subsamples from one rock area, which were homogenized into one sample. A subsample of the slurry was filtered through a glass-fiber filter and combusted to approximate total biofilm biomass (mg AFDM m^{-2}). To estimate the photosynthetic component, an additional subsample of slurry was filtered and standard EPA methods were used to calculate chlorophyll *a* (mg Chl *a* m^{-2}) concentrations (Arar &

Collins, 1997). In addition, for the HTR sampling scheme only, annual net benthic primary production (mg Chl *a* m^{-2} yr^{-1}) was calculated by summing the average differences between each month for one year.

3.3.4 Macroinvertebrate biomass and composition

We focused on macroinvertebrates, because they are a major component of animal biomass in streams and they are critical for ecosystem function (Wallace & Webster, 1996). In addition, macroinvertebrates are often the first organisms to respond to environmental stress and therefore used as biotic indicators of stream health (Feld & Hering, 2007). Many species have adapted to the predictability of natural flow regimes and prolonged deviations may threaten the local persistence of species and even entire communities (Poff & Ward, 1989; Poff *et al.*, 2018). Macroinvertebrates were sampled at three random locations within each stream reach with a Surber net and preserved in 70% ethanol. Invertebrates were counted, measured to the nearest millimeter, and identified to the lowest feasible taxonomic level, generally genus. Biomass of macroinvertebrate taxa that represented >1% of the total abundance in each stream was calculated by using our own length-mass relationships (Appendix 3.1) with methods adapted from Benke *et al.* (1999).

3.3.5 Statistical Analyses

Generalized linear models were run to determine the relationships between rainfall, streamflow metrics, resource quantity and quality, and invertebrate biomass, using the "lme4" and "pscl" (to extract R^2 values) packages from the statistical program R (Bates *et*

al., 2015; Jackman, 2017). To explore how flow drives changes in resources and consumers, we first had to select an appropriate flow predictor variable since median flow, flow variability, and flood intensity were all strongly correlated with baseflow (R^2 of Q_{90} vs. Q_{50} = 0.88, Q_{10}/Q_{90} =0.92, peak flow/Q_{50} = 0.88, analyses not shown). We chose baseflow (Q_{90}) as the main flow predictor variable because it is a more direct driver of resources and consumers in streams than median flow (Pyrce, 2004). Our choice was confirmed in an exploratory analysis where we used the "relaimpo" package in R (Grömping, 2006) to estimate the relative importance of each of the flow variables to changes in resource and consumer biomass (using the following linear model (lm): resource or consumer biomass ~ baseflow + flow variability + flood intensity; lm resource: $R^2 = 0.63$, $p = 0.002$; lm consumer: $R^2 = 0.68$, $p \leq 0.001$). We found that baseflow was the main driver of both resource and consumer biomass changes (61-72%) followed by flow variability and flood intensity.

To address potential temporal pseudo replication in our HTR sampling scheme (i.e. repeated monthly measurements within one stream), we ran generalized mixed effect models with months as a random factor to determine the relationship between flow and the response variables (Bolker *et al.*, 2009). For the HSR sampling scheme we ran generalized linear models separately for each of the three years. Based on the distribution of the data and the model fit (residual and Q-Q plots), we selected the Gaussian, Gamma or Gamma (link = log) family for our generalized models. The parameters and output of each model are reported in Appendix 3.2.

For each sampling scheme (i.e., HTR, HSR), we plotted the macroinvertebrate community data (based on abundance) across streams in a NMDS plot using the "vegan"

package in R (Oksanen *et al.*, 2017). If the stress value of the plots were ≤ 0.2, we used the "clustsig" package (Whitaker & Christman, 2014) to determine any clusters in the data and ran an analysis of similarity (ANOSIM) to establish if these clusters were significantly different ($p \leq 0.05$). Finally, we performed a SIMPER test with the "vegan" package to determine which species were driving these significant differences.

3.4 Results

3.4.1 Rainfall and stream parameters

Rainfall during the dry season (May-September) generally related with the 30-year mean annual rainfall and streamflow (Fig. 3.2). The total rainfall during the dry season sampling period in 2012 (lm: $R^2 = 0.95$, $p < 0.001$) and 2016 (lm: $R^2 = 0.79$, $p = 0.003$) followed the same general upward trend as the long-term rainfall (Fig. 3.2a). The year 2012 was the 8th driest in 60 years (NOAA, 2013), while 2015 had statewide the highest dry season rainfall in 30 years (NOAA, 2017). Baseflow (Q_{90}) increased with seasonal rainfall in 2012 (lm: $R^2 = 0.72$, $p = 0.008$), 2015 (lm: $R^2 = 0.76$, $p = 0.005$), and 2016 (lm: $R^2 = 0.76$, $p = 0.005$) (Fig. 3.2b), a trend that was mirrored by median- (Q_{50}) and storm flow (Q_{10}, Table 3.1). On the other hand, streamflow variability (Fig. 3.2c; Q_{10}/Q_{90}) and flood intensity (Fig. 3.2d; peak flow/Q_{50}) exponentially decreased with increasing seasonal rainfall in 2012 (generalized linear model (glm): $R^2 = 0.78$, $p = 0.005$; $R^2 = 0.96$, $p = 0.022$, respectively), 2015 (glm: $R^2 = 0.99$, $p = 0.002$; $R^2 = 0.98$, $p = 0.019$, respectively), and 2016 (glm: $R^2 = 0.81$, $p = 0.002$; $R^2 = 0.91$, $p = 0.001$, respectively)**.**

Canopy cover decreased with increasing baseflow (lm: $R^2 = 0.70$, $p = 0.010$), likely because higher flow creates wider streams, decreasing canopy cover. Substrate type

within the streams varied across the streamflow gradient (Table 3.1). The driest and wettest sites were mostly composed of bedrock and boulder, while intermediate flow sites had smaller substrate present (e.g. sand, gravel, cobble). These substrate patterns are expected, because strong flash floods at dry sites and higher flow in wet streams scour smaller substrate to downstream areas.

3.4.2 Resource availability

Benthic and suspended resources increased with baseflow (Fig. 3.3). Benthic organic matter standing stocks increased ten-fold with increasing baseflow in 2015 (lm: R^2 = 0.90, p = 0.001) and in 2016 (lm: R^2 = 0.77, p = 0.004) (Fig 3.3a). However, this pattern was not significant for the HTR sampling scheme (Fig. 3.3b; generalized linear mixed model (glmm): p = 0.068). Suspended material (g AFDM day^{-1}) was 40x greater at higher baseflow for both HSR (Fig 3.3c; glm 2012: R^2 = 0.62, p = 0.052; glm 2015: R^2 = 0.62, p = 0.031; and lm 2016: R^2 = 0.79, p = 0.003) and HTR (Fig. 3.3d; glmm: R^2 = 0.29, p = 0.004) sampling schemes.

Macrophyte and miscellaneous organic material (unidentified ≤ 1mm detritus) were the most abundant resources in high-flow streams, while in low-flow streams leaf litter and miscellaneous organic material dominated (Appendix 3.3). Since macrophytes and leaf litter were the two most abundant resource types, we calculated their percent contribution to the total benthic resource availability and regressed the percentages against baseflow (Fig. 3.4). Macrophyte presence increased up to 80% with higher baseflow for HSR (Fig. 3.4a; lm 2012: R^2 = 0.97, p = 0.016; lm 2015: R^2 = 0.88, p = 0.002) and HTR (Fig. 3.4b; glmm: R^2 = 0.34, p = 0.001) sampling. Macrophytes

consisted mostly of two native feather moss species (*Glossadelphus zollingeri* and *Eurhynchium mulleri*). Percent leaf litter, on the other hand, exponentially declined with increasing baseflow for HSR (Fig. 3.4c; glm 2012: $R^2 = 0.98$, $p = 0.009$; glm 2015: $R^2 = 0.99$, $p < 0.001$) and HTR (Fig. 3.4d; glmm: $R^2 = 0.22$, $p = 0.007$).

Benthic biofilm did not vary across our sites, but net primary production was greater in high-flow streams. We saw no patterns with the photosynthetic (Chl *a*) and non-photosynthetic (AFDM) component of biofilm across the rainfall gradient on a monthly basis within the year (HTR glmm: $p = 0.83$, $p = 0.47$, respectively) or across sampling years (HSR lm 2012: $p = 0.53$, $p = 0.26$; glm 2015: $p = 0.39$, $p = 0.23$; and lm 2016: $p = 0.27$, $p = 0.19$). However, net benthic primary production was ten-fold higher with increases in flow within the year 2012 (lm: $R^2 = 0.99$, $p = 0.003$).

3.4.3 Macroinvertebrate biomass and composition

Invertebrate biomass increased on average by 35x with baseflow with both sampling schemes (Fig. 3.5). In 2012, invertebrate biomass increased by 28x during the wet season (October – April) and by 42x during the dry season. The increases in 2012 (annual glmm: $R^2 = 0.73$, $p < 0.001$, dry season glm: $R^2 = 0.74$, $p = 0.028$), 2015 (glm: $R^2 = 0.74$, $p = 0.014$), and 2016 (glm: $R^2 = 0.61$, $p = 0.024$) biomass along the gradient were driven by an increase in caddisfly and midge biomass in wetter streams (see Appendix 3.4 for detail).

Macroinvertebrate community composition changed significantly across the streams, even though richness did not (glm: $p = 0.20$ - 0.60). The NMDS plots had stress values of 0.15 and we therefore ran a cluster analysis and ANOSIM on both sampling

schemes. Invertebrate taxa did not cluster significantly for the HSR sampling (Fig. 3.6a), while HTR had three significant clusters (Fig. 3.6b; $R = 0.48$, $p = 0.001$). The three clusters in the HTR NMDS plot separated low, intermediate, and high-flow sites (Fig. 3.6b). Macroinvertebrate communities were 23 - 38% dissimilar (SIMPER) between the driest stream and the other paired sites (Appendix 3.5). Higher abundances of snails, mosquitoes, and copepods at the driest sites contributed to 26 - 70% of that difference, while higher abundance of caddisflies and damselflies in the wetter streams contributed to 29 - 70% of the difference.

3.5 Discussion

Climate models project increases in precipitation extremes and decreases in total mean annual rainfall for many areas of Hawaii (Zhang *et al.*, 2016). Our study is unique because it attempts to quantify the effects of both of these climate variables on stream structure simultaneously, by using a natural rainfall gradient as a space-for-time substitution. Flow patterns along this gradient have been previously studied, and are thought to mimic the predicted effects of climate change (Strauch *et al.*, 2015), providing an important opportunity to test the effects of climate-driven changes in flow on stream ecosystems. In addition, we compared high spatial resolution (HSR) and high temporal resolution (HTR) sampling efforts within the space-for-time substitution model and determined that there are few differences between the results of the two sampling schemes. Both sampling designs indicated that resource quantity and quality and consumer biomass in tropical island streams generally declined by at least ten-fold with predicted changes in streamflow. In addition, macroinvertebrate composition switched to

species with higher turnover rates. Not only are many of the variables we measured related with streamflow, several of these relationships are exponential, suggesting rapid changes in ecological parameters in response to changes in precipitation. These results provide important insight into the effects of climate change on these vulnerable tropical island ecosystems and improve our understanding of how to apply a space-for-time substitution more effectively when estimating climate change impacts.

Benthic and suspended resource availability declined with decreasing streamflow. A 40-fold decline in suspended organic material can have a stark impact on filter feeding species like endemic shrimp, which depend on suspended resources for more than 30% of their diets (Riney, 2015). In addition, decreases in flow have shown to reduce the quality of the suspended material (Atkinson *et al.*, 2009), which can have further implications for these native filter feeders. Benthic resource availability declined with changes in flow as well; a trend that is supported by studies that investigate the relationship of flow and resource availability in temperate (Jones, 1997) and tropical (MacKenzie *et al.*, 2013) streams. These declines in benthic resources are driven by reduced macrophyte biomass in drier systems.

Our results suggest that climate change will tip the balance between autochthonous and allochthonous resources in tropical stream ecosystems. Lower light availability (i.e. high canopy cover) and higher frequency of scouring events (Salas & Dudgeon, 2003; Kohler *et al.*, 2012) likely decreased macrophyte biomass and periphyton production towards the drier end of the gradient. Evidence suggests that tropical stream consumer rely more strongly on authochthonous resources compared to their temperate counterparts (Neres-Lima *et al.*, 2016). An over 10-fold decline in

macrophytes and periphyton resources can therefore have stark consequences for higher trophic levels. In addition, consumers may utilize certain macrophyte types (e.g. moss) not only for direct consumption, but also for shelter and refugia during high flow events (Jansson, Nilsson & Malmqvist, 2007).

Our study suggests that extended low-flow periods associated with declines in rainfall are likely to increase allochthonous resources in tropical streams. Leaf litter accumulation increased towards the drier end of our flow gradient (Fig. 3.4 c, d; Appendix 3.3). This result was further highlighted by increased detrital storage during 2012, which was one of the driest years in the past 60 years. Increases in allochthonous resource availability with climate driven changes in flow have recently been reported in high elevation temperate streams as well (Larson *et al.*, 2018). However, it is important to note that the contribution of macrophytes to total resource biomass is larger in high flow streams (maximum 49.12 mg AFDM m^{-2}) than the contribution of leaf litter in low flow streams (up to 9.48 mg AFDM m^{-2}, Appendix 3.3). This results in the overall decline in available benthic resources at the drier end of the gradient, despite the increase in allochthonous resources. The shift from a macrophyte to detrital dominated carbon system decreases resource quality (i.e. low C:N macrophytes to high C:N detritus), which can increase consumer feeding rates in order to maintain a similar nutritional intake (Jochum *et al.*, 2017). Therefore, declines in both resource quantity and quality can adversely impact consumer biomass.

As predicted, we found a consistent decrease in invertebrate biomass with projected declines in flow rates and increases in flow variability, suggesting that climate change will affect the standing stocks of these important stream consumers. Previous

studies have shown that flow alterations triggered by climate change can decrease invertebrate abundance by using predictive models (Kakouei *et al.*, 2018) and long-term monitoring of two Costa Rican streams (Gutiérrez-Fonseca, Ramírez & Pringle, 2018). In our study, we found that both abundance and biomass of invertebrates declined up to 20x and that caddisflies and midges were the dominant invertebrate taxa that drove these changes in biomass and abundance (Appendix 3.4). In comparison, two studies conducted on Maui Island, Hawaii, found a 44-60% decline in invertebrate abundance and biomass as a result of flow reduction by river dams, but did not attribute the decline to certain taxa (McIntosh *et al.*, 2008; Gorbach *et al.*, 2014). In addition, a congruent study along this rainfall gradient shows that the endemic shrimp, *Atyoida bisulcata,* has lower average biomass in streams with low baseflow (Tingley III, 2017). We speculate that the drop in consumer biomass results from both direct (i.e. scouring from increased flood intensity and flow variability) and indirect (i.e. lower food resource availability and quality) effects of changes in flow. We encourage future studies to investigate the relative contribution of each effect on invertebrate biomass.

While we did not see dramatic changes in invertebrate richness along the gradient, we saw a shift towards species that tolerate flow variability and changes in resource quantity and quality. Caddisflies and damselflies dominated invertebrate communities at the wet end of the gradient, while snails, mosquitoes and copepods were more abundant at the dry end. This pattern suggests that climate change will shift community composition towards organisms with shorter life histories. Studies from semi-arid boreal ecosystems have shown that macroinvertebrate community composition changes with elevated numbers of drying (Eady, Hill & Rivers-Moore, 2014) and extreme hydrological

events (Sarremejane *et al.*, 2018). Increases in magnitude and variation of streamflow can lead to species with shorter larval life cycles, smaller body size, and low oxygen tolerance (Poff & Ward, 1989; Bunn & Arthington, 2002). In addition, a mesocosm study demonstrated that functional redundancy in macroinvertebrate communities increases with habitat contraction and fragmentation (Boersma *et al.*, 2014), indicating that predicted decreases in flow may not only affect stream structure, but also function (Boersma *et al.*, 2014; Pyne & Poff, 2017).

Downscaled climate projections for Hawaii and other parts of the Tropics indicate that certain regions will likely experience simultaneous declines in precipitation quantity and increases in extreme events (Rauscher, Kucharski & Enfield, 2010; Elison-Timm, Giambelluca & Diaz, 2015; Zhang *et al.*, 2016). Our results raise the question whether changes in flow rates or flow variability are the main driver of resource and consumer patterns along our gradient. Previous studies have shown that declines in flow (Northington & Webster, 2017) and increases in variability (Ohlberger *et al.*, 2018) can each affect stream resources and consumers separately. However, our rainfall gradient presented us with the unique opportunity to estimate ecosystem effects of flow magnitude and variation alteration combined. Our preliminary models speculate that the decline in flow is the strongest driver of decreases in resource and consumer biomass (61-72%) compared to increased flow variability and flood intensity (see methods). However, further flow manipulation studies are necessary to tease apart how much each flow variable drives the predicted changes in resources and consumers. Overall, we conclude that predicted declines in streamflow quantity and changes in variability will result in decreased freshwater resource and invertebrate biomass, which can have negative

repercussions for higher trophic levels such as predatory fish, birds, and mammals that rely on this important food resource.

Globally, extreme precipitation events have increased and are projected to continue to intensify in the future (IPCC, 2013). However, it is necessary to recognize that the projections for total precipitation change vary across regions, and a large amount of uncertainty still exists for the tropics and subtropics, both in models and observationally-constrained datasets (Kent, Chadwick & Rowell, 2015; Bador *et al.*, 2018). For example, recent evidence shows that there has been little change in total precipitation in wet regions of the world, although these results were less robust for tropical regions (Donat *et al.*, 2017). On the other hand, regional calculations for Meso-America (Rauscher *et al.*, 2010) and Central America (Diffenbaugh & Giorgi, 2012) project a reduction in precipitation. In addition, the downscaled projections available for the Hawaiian Islands vary spatially, depending on local air temperature, evapotranspiration, ocean water surface temperature, and wind speed and direction (Zhang *et al.*, 2016). While there are uncertainties and variation in estimates of total precipitation change across the Tropics, declines have been projected in several cases and the implications of our results can be applied to other tropical areas where similar precipitation projections have been made.

The high spatial resolution (HSR) sampling scheme allowed us to evaluate interannual variability, while high temporal resolution (HTR) sampling efforts demonstrated little differences in patterns within the year. We were able to capture a relatively dry, extremely wet, and an average rainfall year with the HSR sampling regime, which allowed us to evaluate if resource and consumer patterns are altered by

extreme years. The seasonal rainfall patterns of 2012 and 2016 were strongly related with the 30-year long-term rainfall trend, but this relationship did not hold up during the extremely wet season in 2015. This is likely because the drier end of the gradient received an increased number of short but extreme rainfall events, inflating the average rainfall estimates in these areas. However, the flow pattern of 2015 was similar to 2012 and 2016, because baseflow estimates avoid the artificial inflation by extreme flood events. Since baseflow is a direct driver of stream resources and consumer, we saw little difference in the ecological response patterns (biomass and composition) between the 2015 and the 2012/2016 years. This agreement indicates that this space-for-time substitution is a robust sampling model that can be useful in quantifying long-term responses, even in years that involve extreme events. The HTR sampling regime also demonstrated that there was little difference in the resource and consumer response patterns between the months. Nevertheless, when averaged, the resource and consumer biomass patterns were stronger during the dry season (e.g. invertebrate biomass 28x decline in wet vs. 42x in dry season, analyses not shown), which mimicked the overall biomass patterns we observed in the eight streams sampled for the HSR along our rainfall gradient. This indicates that the flow variability within the year (HTR) simulates the flow range along our rainfall gradients (HSR).

There was little difference in the direction and strength of the resource and consumer response pattern to variation in flow between the two sampling schemes, suggesting that both schemes provide similar predictions about how climate change will affect tropical communities. Baseflow, and resource and consumer response variables had very similar ranges between the HTR and HSR sampling schemes, indicating the

difference between monthly sampling events (e.g. wet vs. dry season) mirrored interannual variation in rainfall events (e.g. El Niño-Southern Oscillation). The only difference between the two schemes was in the response of community composition to changes in flow. The HTR sampling scheme detected a significant separation of communities between wet, dry, and intermittent streams, indicating that there are significant shifts in macroinvertebrate community composition with changes in flow. These patterns did not significantly cluster out with the HSR sampling scheme (Fig. 3.6a), although the wet, dry, and intermittent streams grouped similarly to HTR sampling. The lack of separation is likely because there were only two to three points per stream for the HSR sampling regime. Therefore, the HTR sampling captured the community structure more effectively and we suggest using this method when answering consumer and resource composition questions. However, overall, we deem both sampling strategies comparable when answering ecosystem questions where a space-for-time substitution approach is appropriate.

Although using a space-for-time substitution approach to estimate effects of climate change can have some drawbacks, it has been a valuable tool when used in the right context. Space-for-time substitutions have the benefit of capturing long-term environmental responses within a reasonable sampling time scale without losing realism. However, there are three main criticisms of this method: site and species histories can vary or are unknown, biotic and abiotic factors vary along the spatial gradient, and the spatial variability may not represent the temporal variability (Fukami & Wardle, 2005; Johnson & Miyanishi, 2008). Since our predictive rainfall gradient was formed along a short distance (~20 km) and from the same lava flow, it presented us with the unique

opportunity to have similar site and species history. In addition, we reported many of the biotic and abiotic factors to ensure they are not a cofactor driving our results. By comparing our two sampling regimes (HTR vs. HSR), we were able to conclude that the spatial variability generally represented the temporal variability well. In addition, a recent long-term study (15 years) in Costa Rica, where the projected changes in precipitation variability aligned with ours, reported similar declines in macroinvertebrate abundance (Gutiérrez-Fonseca *et al.*, 2018). We conclude that a space-for-time substitution approach is a valuable tool to assess climate impacts on the whole ecosystem if the limitations of the approach are addressed by the study design. We encourage other climate studies to include landscape gradients to address anthropogenic impacts in a timely manner.

Table 3.1: Physical characteristics of 8 streams across the North Hilo rainfall gradient. Mean annual rainfall (MAR) was gathered from the Rainfall Atlas of Hawaii (Giambelluca *et al.,* 2013). Baseflow (Q_{90}), median flow (Q_{50}), stormflow (Q_{10}), flow variability (Q_{10}/Q_{90}), flood intensity (peak flow/Q_{50}), as well as canopy cover and substrate composition were averaged for the sampling periods (May-September) across 3 years.

DRY **WET** →

Stream	HON	KAP	KOL	UMA	LOA	MAK	PAH	KAA
MAR (mm y^{-1})	5764	5868	6520	5178	5168	4748	4527	3703
Elevation (m)	470	460	500	490	420	400	510	475
Mean Slope (%)	6.2	6.7	6.1	8.5	8.8	8.8	8.9	9.9
Stream Order	2	2	3	2	1	2	1	2
Canopy Cover (%)	35.6	34.5	36.3	25.7	65.7	60.6	70.4	78.2
Flow Metrics:								
Q_{10} (L $s^{-1}km^{-2}$)	261.1	628.7	293.2	619.3	87.26	273.1	122.7	22.14
Q_{50} (L $s^{-1}km^{-2}$)	53.07	57.22	46.77	42.09	10.59	16.52	4.11	0.18
Q_{90} (L $s^{-1}km^{-2}$)	26.43	18.87	20.92	11.27	5.19	3.67	0.32	0.06
Flow variability	10.87	37.11	15.06	66.76	23.05	78.47	36924	71995
Flood intensity	24.17	59.47	34.26	225.6	230.6	422.6	1117	402819
Substrate Comp. (%):								
Bedrock	33.3	76.7	54.2	0.6	3.3	11.9	76.7	73.1
Boulder	66.7	23.3	2.8	13.9	25	3.1	0	0
Cobble	0	0	20.4	48.2	63.3	37.5	0	14.9
Gravel	0	0	17.2	29	8.3	34.2	23.3	11
Sand	0	0	5.4	8.3	0	13.3	0	1.1

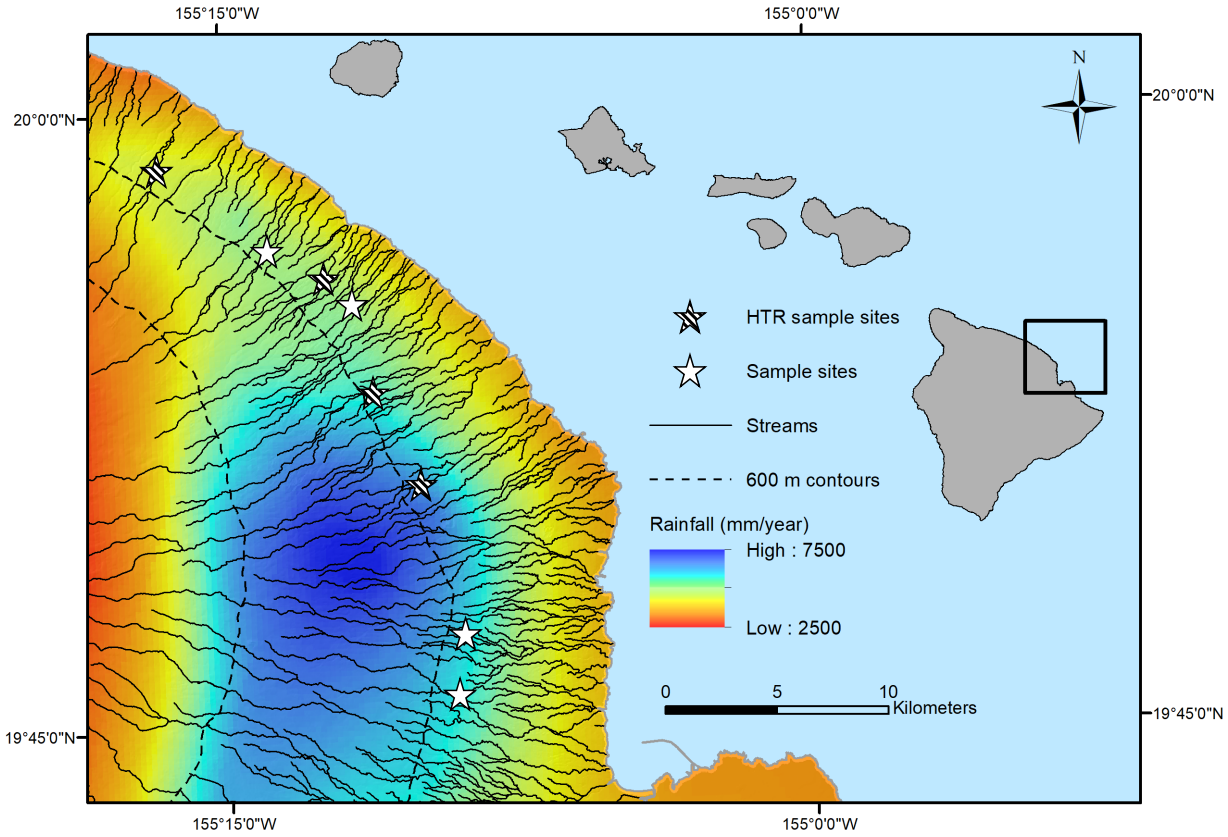

Figure 3.1: Eight sample stream sites (stars) located along the northeast coast of Hawaii Island with similar environmental characteristics except for the difference of ~3000 mm mean annual rainfall. The striped stars indicate sites sampled at high temporal resolution (HTR). Data for this map were generated from the Rainfall Atlas of Hawaii (Giambelluca *et al.,* 2013).

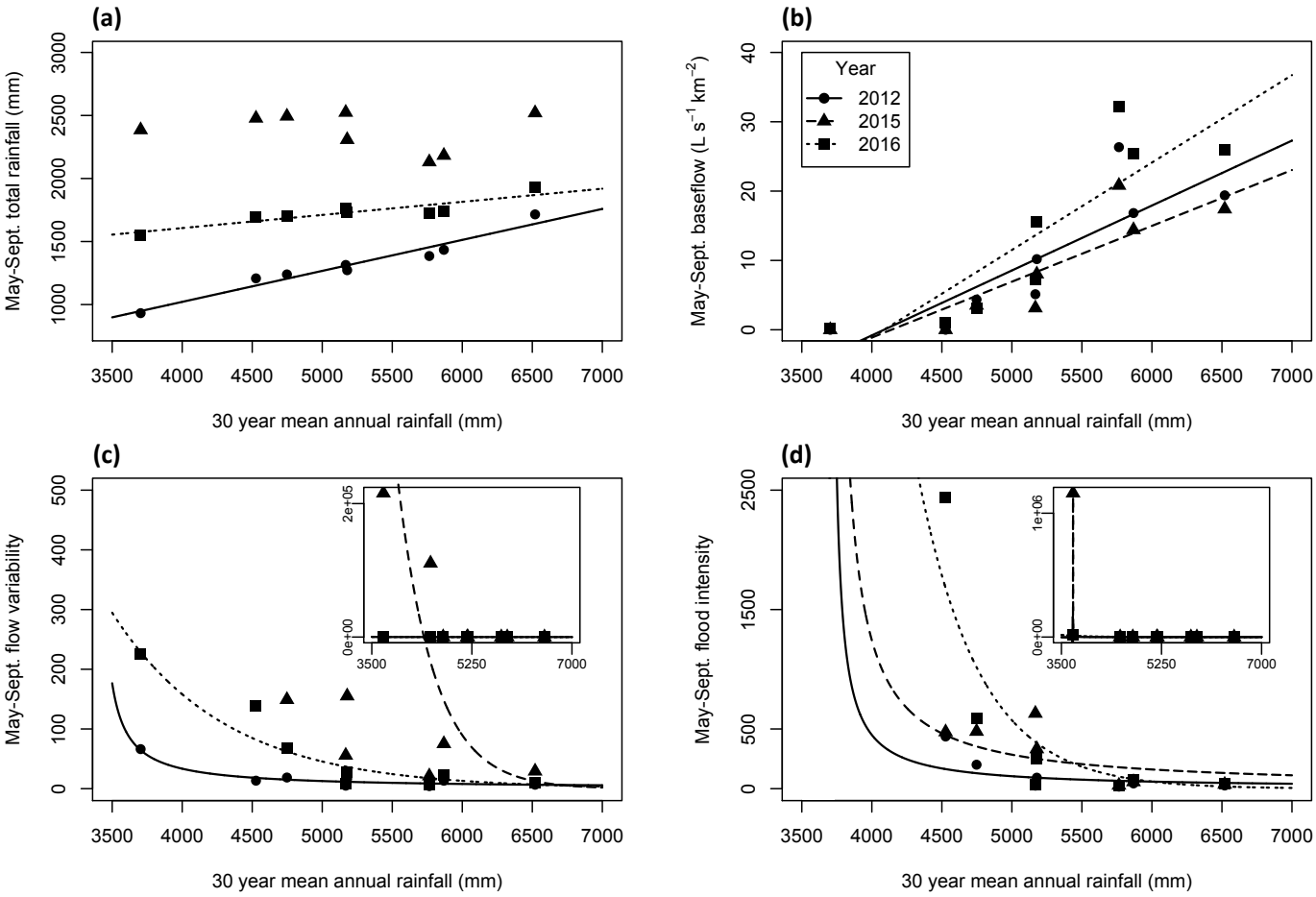

Figure 3.2: Rainfall and streamflow variables of eight sites (one point per stream) across the three sampling years. The 30-year mean annual rainfall average related to the total rainfall during the sampling period in years 2012 and 2016 (a). Baseflow ((b); Q_{90}) increased with rainfall; while streamflow variability ((c); Q_{10}/Q_{90}) and flood intensity ((d); peak flow/Q_{50}) exponentially declined with rainfall. Lines indicate the significant model output of each relationship ($p \leq 0.05$).

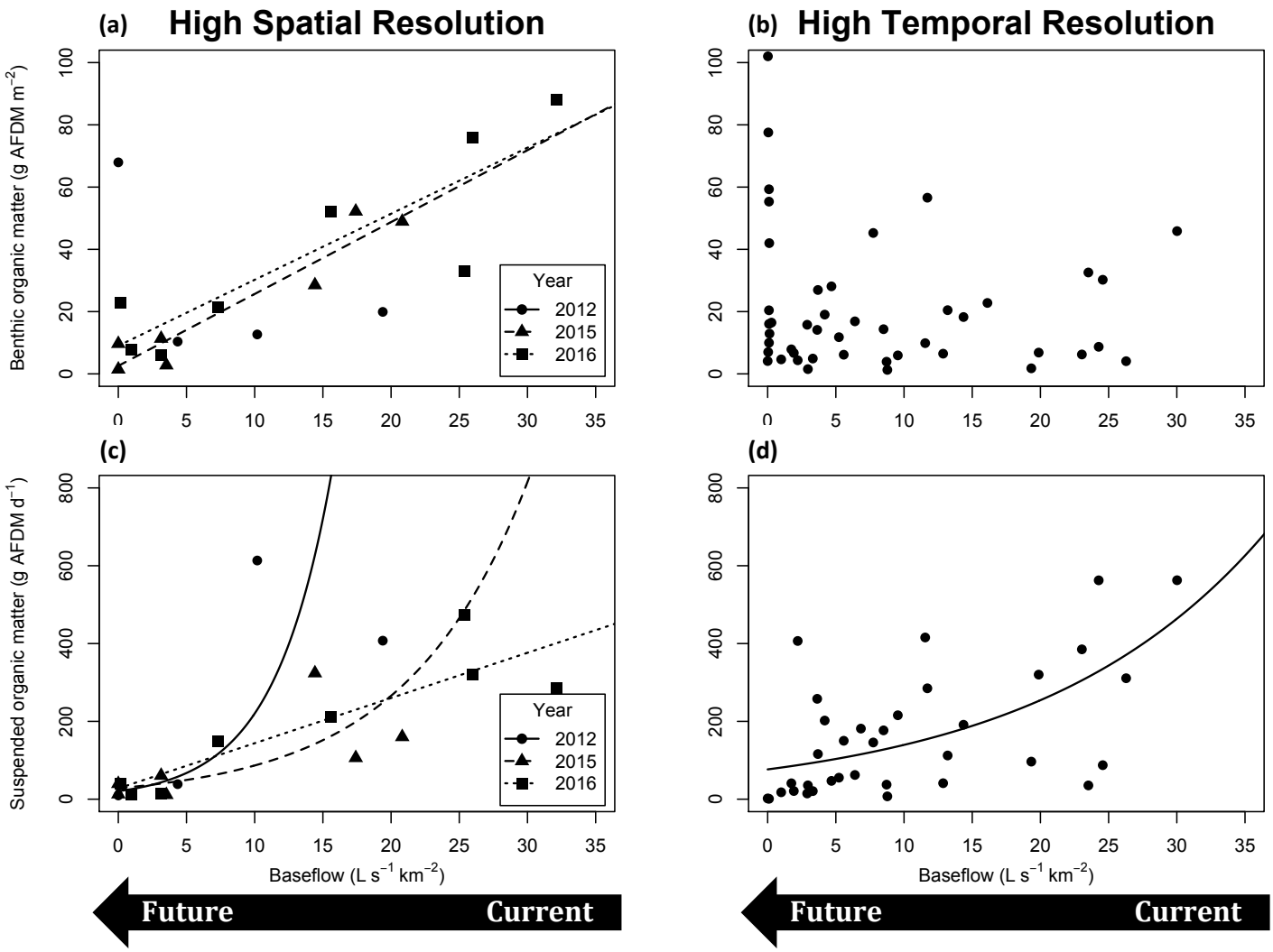

Figure 3.3: Responses of stream resource quantity to predicted decreases in base flow when sampling under higher spatial ((a) and (c); up to 8 streams per year) and temporal ((b) and (d); 4 streams per month, 12 months) resolution. Benthic organic matter ((a); g Ash-free dry mass (AFDM)/m^2) increased significantly with baseflow across years. However, this pattern was not significant within the year 2012 (b). Suspended material (g AFDM day^{-1}) increased with base flow across years (c) and within the year (d). Lines indicate the significant model output of each relationship ($p \leq 0.05$).

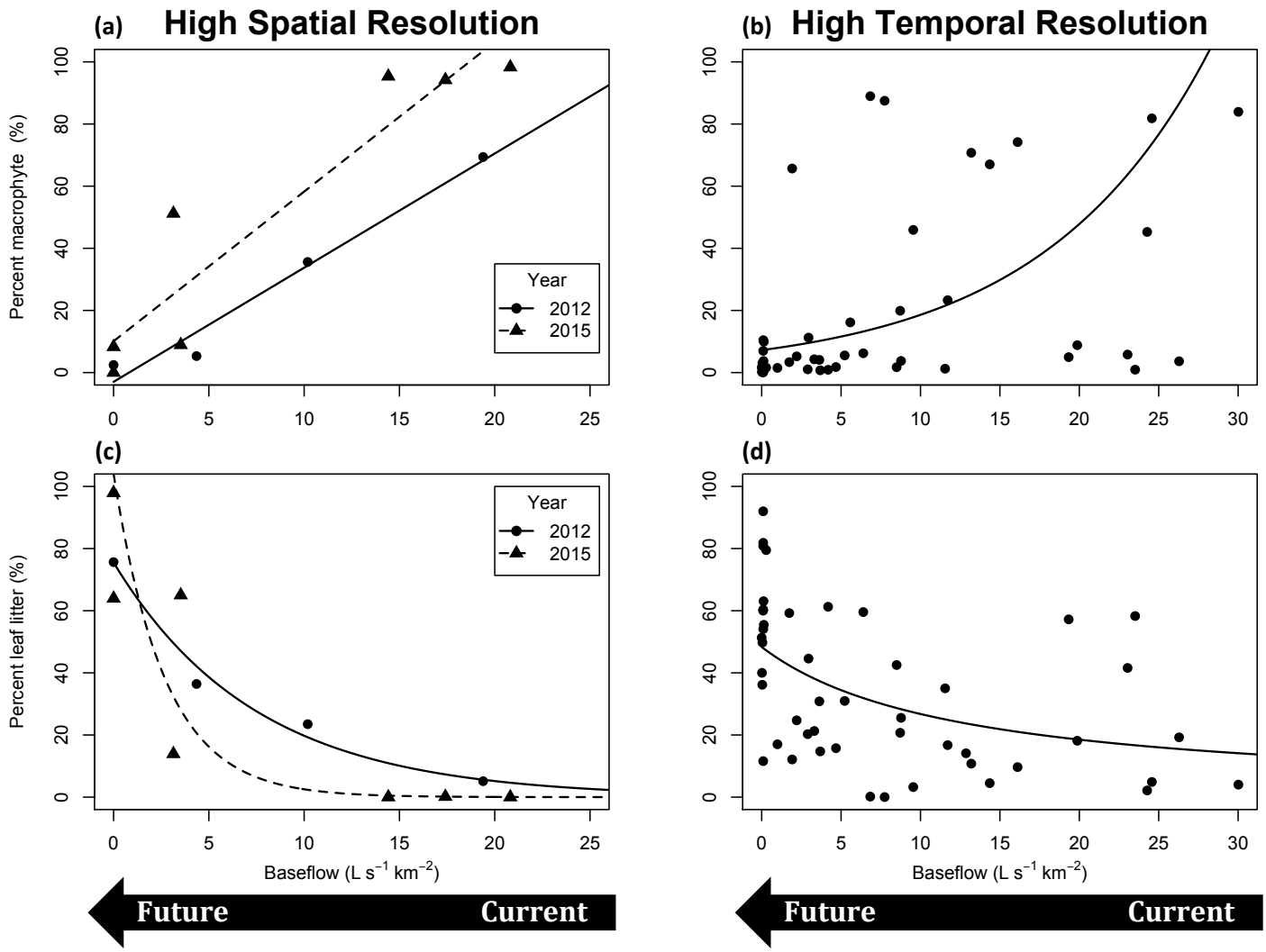

Figure 3.4: High spatial ((a) and (c); up to 8 streams per year) and high temporal ((b) and (d); 4 streams per month, 12 months) sampling of percent availability of dominant stream resource types across base flow. Macrophyte presence increased with higher baseflow across years (a) and within the year 2012 (b), while percent detritus decreased with increased baseflow across years (c) and within the year (d). Lines indicate the significant model output of each relationship ($p \leq 0.05$).

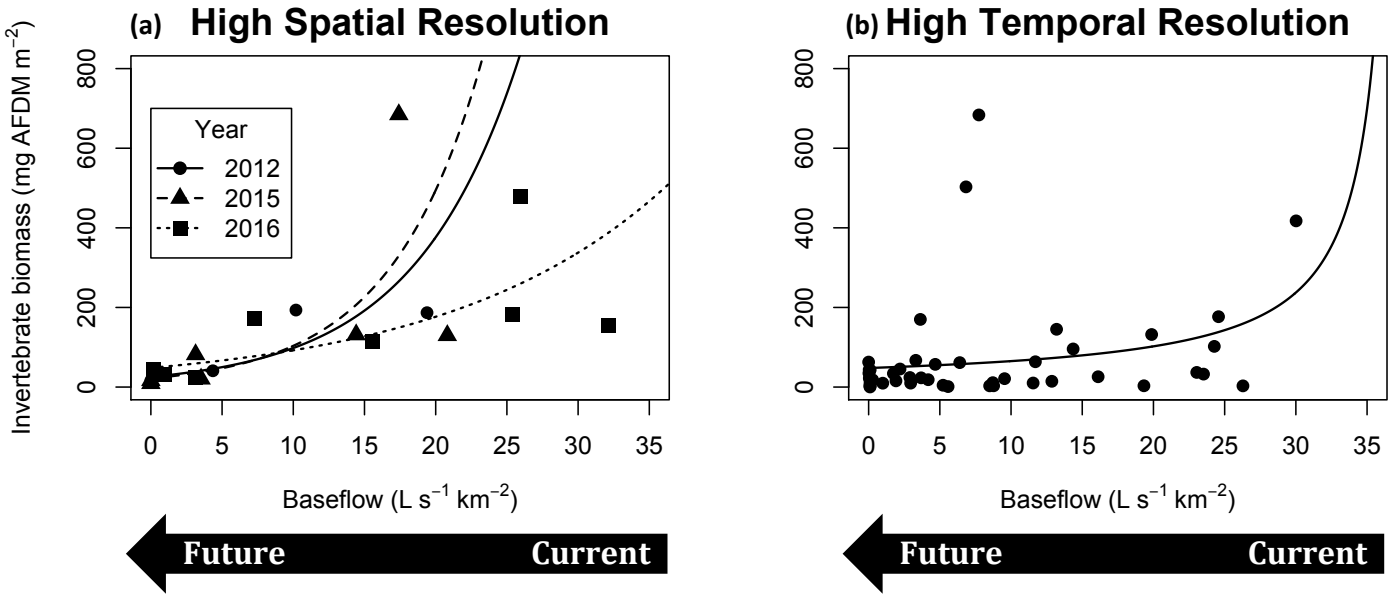

Figure 3.5: Stream invertebrate biomass (mg ash-free dry mass (AFDM) per m^2) across baseflow sampled under high spatial ((a); up to 8 streams per year) and temporal ((b); 4 streams per month, 12 months) resolution. Invertebrate biomass increased with higher baseflow across years and within the year 2012. Lines indicate the significant model output of each relationship ($p \leq 0.05$).

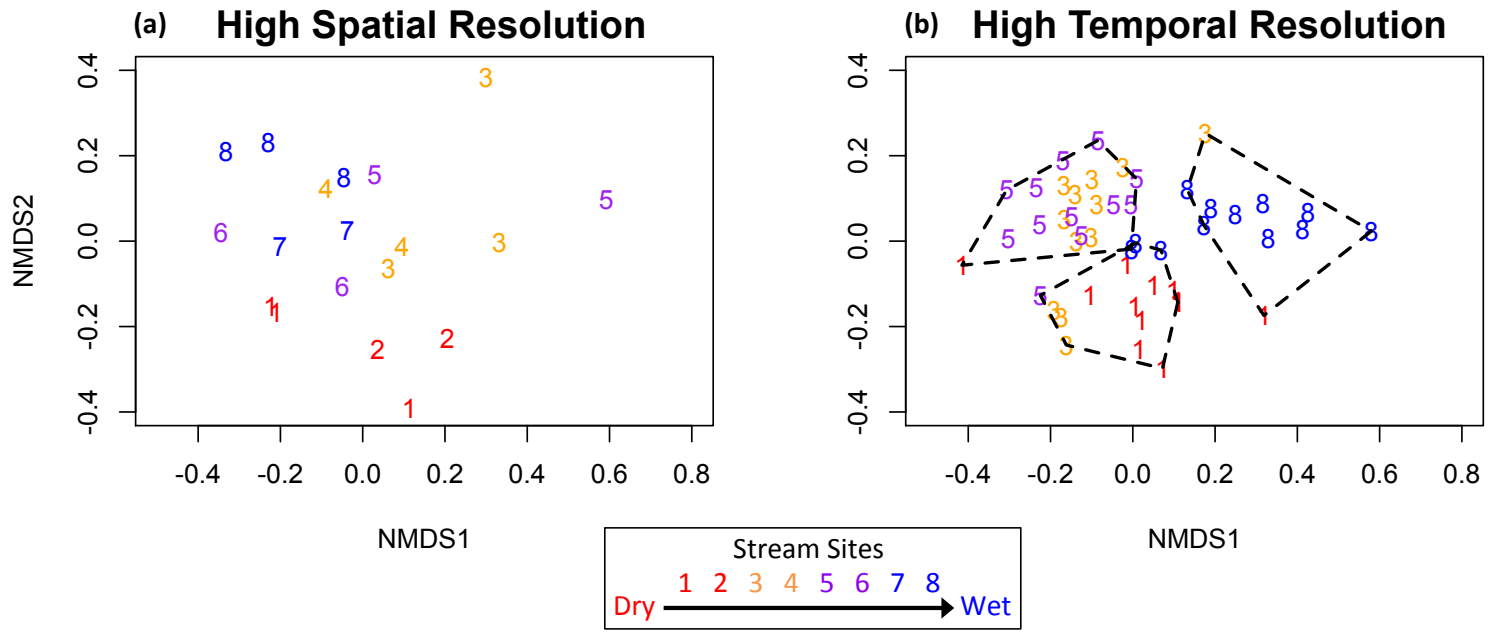

Figure 3.6: Ordination plots of invertebrate taxa when using the high spatial ((a); n= 2 or 3 years) and high temporal ((b); n=12 months) sampling scheme, where each point represents one stream, sampled at one time point. Streams are labeled from low (1) to high (8) flow using average annual flows (1. KAA, 2. PAH, 3. MAK, 4. LOA, 5. UMA, 6. HON, 7. KAP, 8. KOL). The stress value for each plot was 0.15. The driest and wettest sites separated out significantly from the intermediate flow streams with high temporal resolution sampling, but this separation was not significant with high spatial resolution sampling.

Chapter 4: Using a space-for-time substitution approach to predict the effects of climate change on nutrient cycling in tropical island stream ecosystems

Therese C. Frauendorf[1], Richard A. MacKenzie[2], Ralph W. Tingley III[3], Dana M. Infante[4], and Rana W. El-Sabaawi[1]

[1] Department of Biology, University of Victoria, Victoria, British Columbia V8W 3N5 Canada

[2] Institute of Pacific Islands Forestry, Pacific Southwest Research Station, USDA Forest Service, Hilo, Hawaii 96720 USA

[3] Missouri Cooperative Fish and Wildlife Research Unit, The School of Natural Resources, University of Missouri, Columbia, Missouri 65211 USA

[4] Department of Fisheries and Wildlife, Center for Systems Integration and Sustainability, East Lansing, Michigan 48823 USA

Author contributions: TCF designed and implemented the study, based on the gradient proposed by RAM, with intellectual contributions from RES. TCF collected and analyzed the data. RWT and DMI provided raw shrimp density and size distributions along the gradient. TCF wrote the manuscript with editorial input from RES, RAM, RWT, and DMI.

4.1 Abstract

Climate change is expected to alter precipitation patterns worldwide, which can have direct effects on streamflow dynamics. In many tropical regions, climate-driven changes in rainfall are predicted to decrease streamflow and increase flash flooding, but the ecological implications of these changes for stream ecosystem function are poorly understood. We used a rainfall gradient along the northeast coastline of Hawaii Island that mimics projected changes in rainfall and streamflow in order to estimate how climate change affects nutrient recycling. We selected eight streams along the gradient and measured per-capita excretion (nitrogen, phosphorus) and egestion rates of three dominant taxa (shrimp, caddisfly, midge) across three years. We scaled these rates to the population and community levels and measured nitrogen and phosphorus demand of the ecosystem to estimate if the relative contribution of nutrients supplied by invertebrates changes along the gradient. Across all three taxa, population egestion and excretion rates were ten-fold lower at the drier end of our rainfall gradient. These declines were driven by a smaller population density, rather than differences in per-capita rates. Under the current climate scenario, community excretion supplied up to 70% of the nitrogen demand, which declined ten-fold with projected changes in rainfall. Conversely, community excretion supplied up to 5% of the phosphorus demand, which did not vary across the rainfall gradient. This difference indicates that climate change may exacerbate nitrogen limitations in tropical streams, and change the balance of nitrogen and phosphorus dynamics. Our study demonstrates that space-for-time substitutions are a valuable tool to examine implications of climate change on ecosystem function in freshwater systems.

4.2 Introduction

Climate models forecast regional and global changes in precipitation (IPCC, 2014; Donat *et al.*, 2016), which are predicted to alter structure and function, particularly for lotic ecosystems (Heino, Virkkala & Toivonen, 2009; Dudgeon, 2014). The consequences of precipitation changes are important to understand in stream systems because precipitation is one of the main drivers of streamflow. Forecasted changes in precipitation can alter the magnitude, timing, and variation of streamflow simultaneously (e.g. Strauch *et al.,* 2015), and each of these components are important for the integrity of stream ecosystems (Poff *et al.*, 1997; Jardine *et al.*, 2015). Tropical regions often receive higher amounts of precipitation, which can lead to more variable flow regimes compared to their temperate counterparts (Dudgeon, 2011). The Tropics are also expected to be one of the earliest regions to deviate from the normal climate variability (Mora *et al.*, 2013). Recent studies have proposed that forecasted changes in streamflow can alter ecosystem structure by decreasing abundance and biomass of fauna, and change community composition in tropical island streams (Gutiérrez-Fonseca *et al.*, 2018; Frauendorf *et al.*, 2019). However, implications of predicted changes in flow for stream ecosystem function (i.e. biological, geochemical or physical processes) are still unknown.

Ecosystem function and structure are linked because the role of organisms in ecosystem processes depends on their traits, population characteristics, and community composition (Woodward *et al.*, 2010b; El-Sabaawi, 2017). In order to accurately forecast the effects of global change on ecosystem function, it is important to assess impacts of climate change across scales of ecological organization. For example, body size is an important trait for predicting the effects of biological change on ecosystem function

(Fritschie & Olden, 2016; Carlson & Langkilde, 2017). However, studies have shown that population properties (e.g. density, size structure) also play an important role in altering ecosystem function (Chapter 2, Jackson *et al.*, 2017). In addition, the composition and structure of communities can be a key factor in influencing stream ecosystem function (Vanni *et al.*, 2002; McIntyre *et al.*, 2008). Therefore, the impacts of climate-driven changes in streamflow on ecosystem function need to be scaled from the individual to the ecosystem level, taking into account salient variation at each level.

Nutrient cycling, defined as the flux of nutrients between biotic and abiotic compartments, is a critical component of ecosystem function in streams (Sterner & Elser, 2002). Nutrient cycling can be affected by animals through direct (e.g. consumer-mediated recycling processes such as excretion, egestion) and indirect (e.g. grazing, soil compaction, bioturbation) pathways (Sterner & Elser, 2002). Aquatic organisms sequester nutrients in their tissue because of growth and reproduction, and recycle nutrients back to the ecosystem through excretion (Atkinson *et al.*, 2017). Excreted waste contains inorganic nutrients in the form of ammonium and phosphate that are readily available for primary producers (e.g. macrophytes, algae) and microbial communities (e.g. bacteria, fungi), supporting productivity at the base of the food web (Zimmer, Herwig & Laurich, 2006; Atkinson *et al.*, 2017). Compared to excreted waste, egested material cannot be easily taken up by primary producers, but microbial breakdown and direct consumption of the egested material makes this waste product more accessible (Joyce, Warren & Wotton, 2007; Halvorson *et al.*, 2015). Stream invertebrates can play a large role in nutrient cycling, as they often have large standing stocks and their smaller size leads to larger mass-specific excretion rates compared to fish (Vanni, 2002; Atkinson

et al., 2017). For example, in a desert stream, invertebrate assemblages provide 70% of the nitrogen required by the stream biota (Grimm, 1988). Body elemental composition, size, and diet of the consumer are important factors that determine the amount of nutrients excreted (Elser *et al.*, 1996; Sterner & Elser, 2002; Vanni *et al.*, 2002), but these characteristics are sensitive to changes in environmental conditions (e.g. El-Sabaawi *et al.*, 2012a; Costello & Michel, 2013; Griffiths & Hill, 2014).

The importance of excreted nutrients in the broader nutrient cycle depends on the demand of the ecosystem and how much of this demand is supplied by the consumers. Nutrient demand is defined as the amount of nutrients (i.e. nitrogen (N) and phosphorus (P)) required by the stream biota. If the supply of recycled nutrients is less than the demand, then recycled nutrients will be consumed within the ecosystem. Conversely, if supply of recycled nutrients exceeds the demand, then ecosystems can become net exporting, influencing the productivity of adjacent ecosystems (Covino, Bernhardt & Heffernan, 2018). Nutrient demand might also vary with climate change because it is the product of both abiotic (e.g. background nutrients, disturbance frequency, flow obstructions) and biotic (e.g. abundance, community composition of primary producers and microbes) factors (Allan & Castillo, 2007).

Our goal is to explore how nutrient cycling in tropical stream ecosystems might be altered under the projected climate-change scenario. To do so we used a space-for-time approach, which exploits a natural gradient that mimics a forecasted change over time (Woodward *et al.*, 2010b). In Hawaii, studies have forecasted a decline in rainfall and an increase in flash flooding in response to climate change. Indeed, studies have documented significant drying trends statewide since 1920 (Frazier & Giambelluca,

2017), which have translated into declines in baseflow and increases in streamflow variability (Bassiouni & Oki, 2013). These patterns are predicted to continue and intensify with climate change (Elison-Timm *et al.*, 2015; Zhang *et al.*, 2016). For our study we sampled a rainfall gradient along the North Hilo coastline on Hawaii Island. The mean annual rainfall (MAR) decreases along the North Hilo coastline from approximately 7000 to 3500 mm yr^{-1} (Giambelluca *et al.*, 2013) within 20 km (Fig. 4.1), which corresponds to the forecasted climate-driven decline in rainfall (Elison-Timm *et al.*, 2015; Zhang *et al.*, 2016) and the resulting streamflow changes for Hawaii (Strauch *et al.*, 2015). We and others have previously utilized this MAR gradient as a space-for-time substitution to investigate how predicted changes in precipitation alter stream ecosystem structure (e.g. Strauch *et al.,* 2014; Tingley III. 2017; Frauendorf *et al*., 2019). However, the implications for ecosystem function remain unclear.

To address our goal we quantified nutrient supply (N and P excretion; egestion) by dominant stream consumers and nutrient demand (N and P uptake) across eight streams along the North Hilo MAR gradient. We used these data to make predictions about the effects of climate change on stream ecosystem function in tropical streams. Previously, we showed that the decline in streamflow along the MAR gradient reduces the quality and quantity of benthic and suspended resources and changes benthic resource composition from being primarily macrophyte based to leaf litter based (Frauendorf *et al.*, 2019). Ecological stoichiometric theory predicts that because consumers have strict elemental homeostasis, decreases in food resource quality will force them to excrete less N and P in order to conserve their elemental composition (Sterner & Elser, 2002). Therefore, we hypothesized that a reduction in food quality and quantity in drier and

more variable streams will lower the excretion and egestion rates of individual invertebrates. Our previous work showed that macroinvertebrate biomass also declines with decreasing streamflow (Frauendorf *et al.*, 2019). As a result, we predicted that the concomitant declines in individual excretion and egestion rates, as well as population biomass, will cause an overall reduction in consumer-mediated recycling along the gradient. In contrast, we expected nutrient uptake to remain constant along the gradient, because losses in primary producers may be compensated by increases in microbial decomposers present with higher detrital resources. Since we expected nutrient demand to remain constant, but the nutrient supply by community excretion to decrease, we predicted that net export of nutrients would decline along the gradient as well. In other words, we predicted that climate change would increase the importance of consumer-mediated nutrient recycling within the stream reach, while decreasing the capacity of streams to export nutrients downstream.

4.3 Methods

4.3.1 Study system, rainfall and streamflow parameters

Streams along the northeast coast of Hawaii Island are characterized by narrow gulches and young geologic substrate that was formed from a similar-aged lava flow (<100,000 years) (Vitousek, 1995). Besides the mean annual rainfall, characteristics like the slope, elevation, mean annual temperature, riparian vegetation, and soil age and type were similar at each stream sampling site (Strauch *et al.*, 2015). Eight streams were selected along the rainfall gradient spanning a range of ~3000 mm mean annual rainfall (Honolii

(HON), Kapue (KAP), Kolekole (KOL), Umauma (UMA), Manoloa (LOA), Makahiloa (MAK), Pahale (PAH), and Kaawalii (KAA)) (Fig. 4.1).

Previous studies along this rainfall gradient have established that flow patterns along the gradient mimic the forecasted effects of climate change, and showed that changes in rainfall and flow alter the structure in streams. Decreases in MAR result in concomitant declines in stream baseflow and flow stability (Strauch *et al.*, 2015), which mimic the historical trends and climate change driven predictions of flow for high-gradient streams of the Hawaiian islands (Bassiouni & Oki, 2013). Declines in streamflow along this gradient have decreased the amount of particulate organic carbon (Strauch *et al.*, 2018), and benthic and suspended resource quantity and quality (Frauendorf *et al.*, 2019). As a result, the endemic and dominant shrimp in these streams have a smaller average body size and are in poorer condition in streams with lower baseflow (Tingley III, 2017). Overall invertebrate biomass was 35-fold lower in drier streams, which was apparent in both seasonal and inter-annual sampling regimes (Frauendorf *et al.*, 2019). For this study we sampled across three dry seasons (2014, 2015, 2016) to test how stable the ecosystem function patterns were when taking interannual variation into account.

Tropical streams often have seasonal cycles in rain. Since we sampled during the dry season, we began by comparing how well rainfall and streamflow patterns during a sampling season reflected broader patterns along the gradient. In other words, we wanted to ensure that flow variation among the sites in the dry season reflected long-term patterns. These patterns have already been verified for 2015 and 2016 (Frauendorf *et al.*, 2019), and therefore only needed to be confirmed for the 2014 sampling year. The 30-

year mean annual rainfall (MAR) and the seasonal rainfall data of each sampling year was calculated by using the Rainfall Atlas of Hawaii (Giambelluca *et al.,* 2013) to average the area-weighted upstream and local rainfall of the catchment for each sample site (Frauendorf *et al.*, 2019). For each study stream, streamflow was compiled from a continuous dataset that uses in-stream data loggers to collect flow measurements at 15-minute intervals (Strauch *et al.*, 2015). We calculated base- (Q_{90}), median- (Q_{50}), and storm flow (Q_{10}) based on mean daily flow and adjusted these values for the watershed area of each stream (i.e. unit area discharge, L s^{-1} km^{-2}). From these values, we estimated flow variability (Q_{10}/Q_{90}) and flood intensity (peak flow/Q_{50}). These flow variables were then averaged from May through September of each year.

4.3.2 Consumer excretion, egestion, and tissue composition

Individual excretion rates of the three dominant consumer taxa were measured across the full range of the observed size distributions in each of the eight study streams. Shrimp (*Atyoida bisulcata*), caddisflies (*Cheumatopsyche analis*), and midges (Chironomidae) were the three dominant consumers that represented in total between 70-98% of the animal biomass in each of the streams (estimated from Tingley III. 2017; Frauendorf *et al.,* 2019). Each individual (20 individuals per species, per stream, per year) was placed in a sealable container filled with a known volume of filtered stream water (scaled to the size of the organism). We added 3-5 control containers per species and sampling event, which were filled with the same amount of filtered stream water, but did not hold an organism. Containers were positioned in stream water to maintain similar temperature and incubated between 30 to 90 minutes. At the end of the incubation, the individual was

removed and the water sample was filtered through a 0.7 μm pore sized glass fiber filter to separate any material egested. Water samples were immediately put on ice until nutrients were analyzed. After euthanasia, the standard body length of each invertebrate was measured (to the nearest 0.01 mm), the gut was removed, and the remaining tissue was dried and analyzed for the carbon (C) and nitrogen (N) content using a Carlo Erba NA1500 CHN analyzer. From these data we calculated molar tissue C:N ratios to examine elemental homeostasis of invertebrates across the gradient.

We measured ammonium concentration of the excretion water samples for all three years, but only determined the phosphate and nitrate concentrations in 2014 and 2015. We measured ammonium concentrations with a Turner Design Trilogy fluorometer following methods described by Holmes *et al*. (1999), with modifications by Taylor *et al.* (2007). Phosphate concentration was determined by using the ammonium molybdate method and a Shimadzu spectrophotometer (Strickland & Parsons, 1972; Parsons, Maita & Lalli, 1984). Finally, nitrate concentrations of the water samples were estimated by the University of Hilo Analytical Lab, using the cadmium reduction method with a Lachat Quikchem flow injection analyzer. Per-capita excretion rates (μg N or P individual^{-1} hour^{-1}) were calculated by subtracting the background nutrient concentration from the final, and adjusted for the volume of water in the container and incubation time. Mass-specific excretion rates (μg N or P hour^{-1} g of ash-free dry mass (AFDM)$^{-1}$) were then estimated by dividing per-capita excretion rates by the individual's mass (AFDM was estimated from length-mass regressions extracted from Frauendorf *et al.*, 2019 and Tingley III 2017). The excretion rates of the 20 individuals were then pooled to obtain an average per-capita and mass-specific excretion rate per site and year.

Population excretion rates (μg N or P population^{-1} m^{-2} hour^{-1}) are defined as the amount of N and P excreted by all individuals within a population (El-Sabaawi *et al.*, 2015). Consequently, population excretion is the product of per-capita excretion and the density of the population. Since per-capita excretion often scales allometrically with body size (Sterner & Elser, 2002), the size distribution of a population can also influence population excretion (Fritschie & Olden, 2016). Thus, we first ran a linear model for each taxon to determine if per-capita excretion related to body size. If an allometric relationship was present, we calculated population excretion (R) using the following equation adapted from chapter 2:

$$R = \int E_{(z)} P_{(z)} N \, dz, \quad (1)$$

where $E_{(z)}$ is the per-capita excretion rate at a given size z, $P_{(z)}$ is the proportion of individuals in the population with the size z, and N is the population density. If there was no allometric relationship present, we simply multiplied the average per-capita excretion rates by the population density for each taxon and site:

$$R = E\,N \quad (2)$$

Densities and size distributions were obtained from Frauendorf *et al*. (2019) for the caddisflies and midges, and from Tingley III (2017) for the shrimp. Both studies collected these data from the same sampling streams, season, and years, with the exception of the shrimp. Shrimp density and size distribution sampling only overlapped during the dry season of 2014. However, the same study found little difference in shrimp density and size between years along this rainfall gradient (Tingley III, 2017). Lastly, we calculated the community excretion rate (C, μg N or P m^{-2} hour^{-1}), defined as the amount

of N and P excreted by all the populations in a community, by summing the population excretion rates from the three dominant taxa in our streams:

$$C = R_{Shrimp} + R_{Caddisfly} + R_{Midge} \quad (3)$$

During 2014 and 2015, filters from the individual excretion trials with the egested material were dried, weighed, ashed at 550 °C, and reweighed to obtain an estimate of the amount of particles egested per individual (µg AFDM). This estimate was adjusted by the incubation time (µg AFDM/hr), and any weight from the control container filters was subtracted from these estimates. Due to the small amount of egested material, we were not able to obtain midge egestion rates. We estimated the shrimp and caddisfly population and community level egestion using the same calculations as for excretion.

4.3.3 Nutrient uptake

We measured uptake using an instantaneous nutrient release method adapted from Covino *et al.* (2010) in each of the eight streams along the gradient. We released a conservative tracer (NaCl) and measured the time and change in specific conductivity in a 100 meter reach. The change in conductivity over time curve was then integrated to calculate the exact flow for the reach. Based on this flow rate, the appropriate reach length and salt and nutrient concentrations were calculated to ensure that the nutrient residence time (18-25 minutes) and concentrations (5 g NaCl $L^{-1}s^{-1}$, 300 mg KH_2PO_4-P $L^{-1}s^{-1}$, 200 mg KNO_3-N $L^{-1}s^{-1}$, and 100 mg NH_4Cl-N $L^{-1}s^{-1}$) were constant across the streams. Sodium chloride acted as the conservative tracer to account for any non-biological nutrient loss, while ammonium chloride, potassium nitrate, and potassium

phosphate are biologically active and are taken up by microbial and plant communities. After the salts were dissolved and released at the top of the reach, 30 filtered water samples spanning the breakthrough curve were collected at the bottom of the reach. Samples were placed on ice until the nutrient analyses, which followed the methods described above. Nutrient uptake rates (μg N or P m^{-2} hr^{-1}) were then calculated by taking the slope of the difference between the initial and final nutrient concentration to conservative tracer ratio of each of the 30 collected samples (Covino *et al.*, 2010). We calculated percent contribution of excreted nutrients to the demand across the flow gradient by dividing the community excretion rate by the nutrient uptake of the stream and multiplying the result by 100.

4.3.4 Statistical analysis

To explore how flow drives changes in nutrient dynamics, we selected baseflow (Q_{90}) as the main flow response variable, because previous research along this rainfall gradient shows that baseflow is the strongest driver of resource and consumer dynamics (Frauendorf *et al.*, 2019). Furthermore, there was a correlation between Q_{90} and other flow metrics, meaning that they all capture the same patterns (Frauendorf *et al.*, 2019). In addition, in an exploratory analysis we used the "relaimpo" package in R (Grömping, 2006) to estimate the relative importance of each flow variable (i.e. baseflow, flow variability, flood intensity) to changes in excretion and uptake. We confirmed that baseflow was the main driver of population excretion and nutrient uptake (55-93%), followed by flow variability (4-25%) and flood intensity (3-20%) (analyses not shown).

Generalized linear models were run to determine the relationships between rainfall, streamflow, population density, average population size, and nutrient metrics (excretion and uptake), using the "lme4" and "pscl" (to extract R^2 values) packages from the statistical program R (Bates *et al.*, 2015; Jackman, 2017).We ran our linear models with Q_{90}, and sampling year as a second fixed effect to examine interannual variation. Based on the distribution of the data and the model fit (residuals and Q-Q plots), we selected the Gaussian, Gamma or Gamma (link = log) family for our generalized models. The parameters and output of each model are reported in appendices 4.2 - 4.6. Gaussian model outputs are reported as linear models (lm), while non-Gaussian models are reported as generalized linear models (glm).

4.4 Results

4.4.1 Rainfall and stream parameters

Total rainfall during the 2014 dry season increased along the MAR gradient as expected and was comparable to the other two years (lm: $R^2 = 0.78$, $p = 0.004$, Appendix 4.1 and 4.2). The year 2015 had the highest rainfall in 30 years (NOAA, 2017) with 1000 mm more rainfall during the dry season compared to 2014 and 2016. As expected, baseflow (Q_{90}) exponentially increased with rainfall along the gradient in 2014 (lm: $R^2 = 0.63$, $p = 0.019$). Streamflow variability (Q_{10}/Q_{90}) and flood intensity (peak flow/Q_{50}) were inversely related to rainfall in 2014 (generalized linear model (glm): $R^2 = 0.99$, $p = 0.003$; $R^2 = 0.90$, $p = 0.002$, respectively). Overall, baseflow, flow variability, and flood intensity patterns during the 2014 sampling season were similar to the patterns in 2015 and 2016 (Appendix 4.1).

Background nutrients at baseflow across streams and years ranged between 4.03 - 8.49 μg N L^{-1} for ammonium, 10.27 - 19.23 μg N L^{-1} for nitrate, and 4.46-7.44 μg P L^{-1} for phosphate (Table 4.1). Ammonium and nitrate were not related to baseflow (lm: $p = 0.84$, $p = 0.47$, respectively), but phosphate significantly decreased with increases in flow (lm: $R^2 = 0.60$, $p = 0.024$).

4.4.2 Individual responses along the rainfall gradient

Contrary to our predictions, average per-capita and mass-specific excretion rates showed weak trends across the streamflow gradient. Shrimp per-capita ammonium and phosphate excretion rates increased with baseflow (lm: $R^2 = 0.74$, $p < 0.001$; glm: $R^2 = 0.68$, $p = 0.003$, respectively), while midge per-capita phosphate excretion declined with baseflow (glm: $R^2 = 0.66$, $p = 0.005$). Other caddisfly (i.e. NH_4, PO_4) and midge (NH_4) per-capita excretion rates remained relatively constant across the gradient (Fig. 4.2 a-c, Appendix 4.3). Per-capita phosphorus excretion ranged between 0.01 and 6.36 μg P hr^{-1} for shrimp, 0.03 - 0.27 μg P hr^{-1} for caddisflies, and 0.01 - 0.13 μg P hr^{-1} for midges. Shrimp excreted on average 0.15 μg NO_3-N hr^{-1} per-capita, which did not vary significantly with baseflow (Appendix 4.3). We did not detect any nitrate excreted from caddisflies and midges (detection limit: 0.07 μM). Mass-specific ammonium and nitrate excretion rates of shrimp declined with baseflow (glm: $R^2 = 0.32$, $p = 0.027$; $R^2 = 0.55$, $p = 0.013$, respectively), as did the midge mass-specific phosphate excretion (glm: $R^2 = 0.51$, $p = 0.048$). Other mass-specific excretion rates did not show a significant pattern across the streamflow gradient (Fig. 4.2 d-f; Appendix 4.3). None of the individual excretion rates significantly varied across years, except for midge mass-specific phosphate excretion (glm: $R^2 = 0.20$, $p =$

0.011; Appendix 4.3). This was caused by higher variability in mass-specific excretion during the wet year in 2015. Overall, our data suggest that climate-induced changes in flow are likely to have weak effects on individual excretion, and cause a decline in per-capita excretion for some taxa but not for others.

Likewise, C:N in the tissues of the three dominant taxa showed little variation across baseflow (Fig. 4.2 g-i), suggesting that tissue stoichiometry was not very sensitive to changes in rainfall. Midges were the only taxon that showed slightly elevated, but significantly different C:N ratios in wetter streams (from 5.02 to 7.05; glm: $R^2 = 0.70$, $p = 0.035$), while shrimp and caddisfly ratios ranged between 4.13 and 5.84, without a consistent pattern with baseflow.

4.4.3 Population responses along the rainfall gradient

The density of all three dominant taxa increased with baseflow and body size of shrimp was higher in wetter streams (Fig. 4.3, Appendix 4.4). The average body size of shrimp was higher with flow (lm: $R^2 = 0.64$, $p = 0.017$, Fig. 4.3a). However, there were little differences in the size distributions for caddisfly and midge populations across the MAR gradient (Fig. 4.3b and c). Overall, per-capita excretion scaled with body size for shrimp (glm: p-values between < 0.001 and 0.057), but not for caddisflies (glm: p-values between 0.18 and 0.82) or midges (glm: p-values between 0.26 and 0.76). Densities of all three taxa were exponentially higher with streamflow (Fig. 4.3 d-f). Shrimp density doubled in wetter streams (glm: $R^2 = 0.73$, $p < 0.001$), while the density of caddisflies was up to 2000x higher (glm: $R^2 = 0.30$, $p = 0.016$) and midges up to 100x (glm: $R^2 =$

0.58, $p < 0.001$). Therefore, body size of shrimp and density of all dominant taxa were lower with projected climate-driven changes in streamflow.

As we predicted, population excretion rates generally increased exponentially with elevated streamflow (Fig. 4.3 g-i). Shrimp ammonium (Fig. 4.3g), phosphate (0.01 - 64.4 μg P m^{-2} hr^{-1}), and nitrate (0.01 – 104.3 μg N m^{-2} hr^{-1}) population excretion were all significantly and positively related to baseflow (Appendix 4.4). Midge and caddisfly ammonium population excretion was also significantly higher in wetter streams, but the phosphate population excretion of both taxa showed no significant trends across the gradient (midge: 1.7-52.5 μg P m^{-2} hr^{-1}; caddisfly: 0.64 - 178.6 μg P m^{-2} hr^{-1}; Appendix 4.4). Based on our results, we expect population excretion to exponentially decline with climate-driven changes in rainfall, but these effects will be stronger for nitrogen compared to phosphorus.

4.4.4 Community and Ecosystem responses along the rainfall gradient

Midge population excretion rates supplied on average 60% of ammonium and 55% of phosphate to community excretion. Caddisfly populations contributed on average 30% to the ammonium and 41% to the phosphate community excretion, while shrimp contributed only 10% and 4%, respectively. However, these relative contributions varied across baseflow. Midges contributed up to 99% in the driest and wettest streams along the gradient, while caddisflies supplied up to 80% to the community excretion of intermediate flow streams. Meanwhile, the relative contribution of shrimp population excretion significantly increased with baseflow (NH_4: up to 37%, glm: $R^2 = 0.37$, $p = 0.016$; PO_4: up to 39%, glm: $R^2 = 0.85$, $p = 0.001$). Since shrimp were the only taxon that

had measurable excreted nitrate, they were the predominant contributor to the nitrate community excretion. As predicted, nitrogen recycled by the invertebrate community increased exponentially with baseflow, while nutrient uptake did not vary with streamflow. Community ammonium (Fig. 4.4a) and nitrate (0.01 – 104.3 μg N m^{-2} hr^{-1}) excretion rates showed a significant positive relationship with streamflow, yet this pattern was not significant for phosphate (6.72 - 231.3 μg P m^{-2} hr^{-1}; Appendix 4.5).

Ecosystem uptake rates for ammonium (Fig. 4.4b), phosphate (636-5621 μg P m^{-2} hr^{-1}) and nitrate (265-8992 μg N m^{-2} hr^{-1}) were very variable across streams and years, and did not show a consistent pattern with baseflow. The relative amount of nitrogen supplied to the streams by invertebrates was positively related with baseflow, supporting our predictions. Invertebrate communities contributed between 1.6 to 6.9% of ammonium to the nutrient uptake in drier streams, but this number increased 10-fold in streams with higher baseflow (Fig. 4.4c; glm: $R^2 = 0.50$, $p=0.005$). Although percent phosphorus and nitrate supplied by invertebrates increased 10-fold with streamflow as well, the relative contribution of excretion to the demand was comparatively small (PO_4: 0.4-4.4%; NO_3: 0.1 - 1.7%). These small increases were significant for nitrate (glm: $R^2 = 0.80$, $p = 0.001$), but not for phosphate (Appendix 4.5). Therefore, our results suggested that with projected climate-driven declines in streamflow, the nitrogen supply via excretion could decline up to 10-fold.

4.4.5 Egestion rates along the rainfall gradient

Individual, population, and community egestion rates followed similar trends across the rainfall gradient compared to excretion rates. Per-capita egestion rates ranged between

0.001 - 0.854 mg AFDM hr^{-1} for shrimp and between 0.001 - 2.25 mg AFDM hr^{-1} for caddisflies, while mass-specific egestion ranged between 0.02 - 6.58 mg AFDM hr^{-1} g^{-1} for shrimp and between 9.92 - 233.2 mg AFDM hr^{-1} g^{-1} for caddisflies. Per-capita and mass-specific egestion rates did not differ with changes in baseflow (Appendix 4.6). However, population (Fig. 4.5a-b; shrimp glm: $R^2 = 0.74$, $p = 0.014$; caddisfly glm: $R^2 = 0.79$, $p = 0.002$) and community (Fig. 4.5c; glm: $R^2 = 0.79$, $p < 0.001$) egestion rates were significantly higher with baseflow. Differences in community level egestion were driven almost exclusively by changes in caddisfly egestion. There were no significant differences in egestion rates among years, except for caddisfly individual egestion (glm: $R^2 = 0.89$, $p = 0.01$; Appendix 4.6), which scaled up to the population and community level. This difference among years was driven by the large variability in individual egestion rates at the high flow stream (KOL) in 2014. Still, our results suggested that the egestion rates were expected to overall decline with projected climate-driven changes in rainfall, which is driven by changes in caddisfly egestion rates.

4.5 Discussion

Climate change is a prominent and growing threat to freshwater ecosystems. In tropical regions precipitation projections can vary substantially, both by region and by climate models (Bador *et al.*, 2018). Nevertheless, several climate models have projected continued decreases in total mean annual rainfall and increases in precipitation extremes in various tropical regions (e.g. Rauscher *et al,.* 2010; Khalyani *et al.,* 2015) and in Hawaii specifically (Lauer *et al.*, 2013; Lehmann, Coumou & Frieler, 2015). However, our ability to predict the effects of these changes is hindered by the lack of data and

mechanistic models. Space-for-time substitutions are a valuable tool for predicting climate effects without compromising realism. We used a natural rainfall gradient on Hawaii Island that mimics these predicted changes (Fig. 4.1) to quantify the potential effects of climate change on tropical stream ecosystem function. During the dry seasons of 2014-16, we measured excretion rates of shrimp, caddisfly, and midge taxa (representing 70-98% of total consumer biomass) and nutrient uptake in eight streams along the rainfall gradient. We found that the nitrogen and phosphorus supplied by shrimp, caddisfly, and midge populations was all about 10-fold lower at drier sites, suggesting a substantial decline in consumer-mediated recycling with climate change. Egestion rates showed similar patterns to excretion and declined by 10-fold with decreases in streamflow. Most of these patterns did not vary across the three sampling years, even during the extremely wet year in 2015. This is likely because the drier end of the gradient received an increased number of short but extreme rainfall events in 2015, inflating the average rainfall estimates in these areas. However, the flow pattern of 2015 was similar to 2014 and 2016 (Appendix 4.1), because baseflow estimates avoid the artificial inflation by extreme flood events. These results provide important insights into the effects of climate change on ecosystem function in these vulnerable tropical island ecosystems.

We hypothesized that consumers would have lower mass-specific excretion rates at the drier end of the gradient because consumers may need to compensate for lower resource quantity and quality. Previously we showed that resources shift from high quality macrophytes to low quality leaf litter with projected changes in rainfall (Frauendorf *et al.*, 2019). Therefore, consumers might excrete less nitrogen to maintain a

homeostatic balance. Contrary to our prediction mass-specific excretion rates of all three taxa showed weak or no relationships with streamflow. The lack of any pattern in the C:N ratios of shrimp and caddisfly tissue across streamflow indicates that these consumers were homeostatic (Sterner & Elser, 2002). It is possible that shrimp and caddisflies deploy other physiological methods for maintaining homeostatic balance in response to changes in resources, such as increased consumption rate or increased assimilation efficiency (Sterner & Elser, 2002). On the other hand, midges had lower tissue C:N ratios at the drier end of the MAR gradient, suggesting that midges may not maintain a homeostatic balance as streamflow declines. This lack of a homeostatic balance may occur in response to changes in resource quantity and quality across the gradient. It is not uncommon for macroinvertebrate taxa to have non-homeostatic responses when the nutrient content of resources changes (Cross *et al.*, 2003; Small & Pringle, 2009).

As we predicted, population excretion across taxa was lower with projected changes in rainfall, even though mass-specific excretion did not vary. For all three taxa this decrease was more prominent for nitrogen population excretion rates compared to phosphorus. These exponential declines can likely be attributed to the steep drops (up to 200-fold) in invertebrate density with decreases in streamflow. However, in shrimp populations the average body size and per-capita excretion rates also declined at the drier end of the MAR gradient, indicating that size and per-capita excretion play a secondary role in determining the changes in population excretion for some invertebrates. However, for the smaller invertebrate taxa (i.e. midge and caddisfly), body size and per-capita excretion did not contribute substantially to the declines in population excretion. This is because per-capita excretion of midges and caddisflies did not scale with body size.

Consequently, the population size distribution was not incorporated when we scaled individual excretion rates to the population level. Meanwhile, per-capita excretion of caddisflies and midges varied considerably across the MAR gradient, but with no consistent pattern (Fig. 4.2). This contrast among taxa is not surprising as per-capita excretion can be very context specific to the individual and its environment (Atkinson *et al.*, 2017), and we know that streamflow, resources, and consumers all change along this rainfall gradient (Strauch *et al.*, 2015; Frauendorf *et al.*, 2019). We encourage future studies to examine the drivers behind the variability in per-capita excretion rates of midges and caddisflies.

A 10-fold drop in the proportion of consumer-mediated nutrient supply along the gradient was mainly driven by changes in midge, and to some extent caddisfly, contributions. The differences in the relative contribution of each taxon along the MAR gradient can be attributed to the biomass changes of the three dominant taxa (Tingley III, 2017; Frauendorf *et al.*, 2019). As predicted, nutrient uptake varied consistently along the gradient, likely because decreases in primary producers were balanced by increases in fungal and bacterial decomposers. As a result, the relative amount of nutrients supplied by invertebrates declined 10-fold as well. However, our results suggest that projected climate change effects on streamflow will likely have little effect on the phosphate and nitrate budget in these stream ecosystems, because invertebrate excretion contributed less than 5% to the phosphate and nitrate demand across streams. This contrasts to ammonium, where under current conditions invertebrates supply up to 70% of the ammonium demand within a stream.

A 10-fold decrease in consumer nitrogen supply can significantly impact in-stream productivity in the Tropics. Tropical streams are often nutrient poor and limited by nitrogen (Downing *et al.*, 1999). The average nitrogen uptake rates in our streams are comparable to nutrient-limited temperate systems, where some of our rivers require three times as much nitrogen than reported in temperate zones (e.g. Griffiths and Hill 2014). In these high-flow streams consumers supplied up to 70% of the nitrogen demand, which is comparable to the contribution of consumers to nutrient cycling in temperate, low-nutrient streams (Grimm, 1988; Griffiths & Hill, 2014) and other tropical rivers (McIntyre *et al.*, 2008). Therefore, based on our results, climate change can exacerbate the nitrogen limitations in these tropical streams by decreasing the consumer's contribution to the nitrogen cycle 10-fold. Since nutrients affect productivity at the base of a stream food web (i.e. microbes and plants), changes in nitrogen supply rates can potentially have direct and indirect consequences for higher aquatic and terrestrial trophic levels.

When examining nutrient recycling, most studies focus on excretion but some have shown that egestion rates can be as high as excretion rates (Halvorson *et al.*, 2015). Recent research has shown that egested material can become an important food resource for some aquatic organisms and generate sites of enhanced microbial activity (reviewed by Atkinson *et al.,* 2017). The ingestion and mineralization of egested material in return increases the availability of egested nutrients (Joyce *et al.*, 2007). While we could not determine the nutrient content of the egested matter based on the small amount of egested material available, we did determine the egestion rate. As with our excretion results, individual egestion rates did not vary with flow. However, when scaled to the population

and community level, egestion rates declined by 10-fold in low-flow streams because of changes in density and size of the dominant taxa producing the egested material. We conclude that the availability of egested material will also decline with projected changes in rainfall. We recommend further analyses to examine the nutrient content of the egested material to determine the relative importance of lower egestion and excretion rates.

Island streams, like in Hawaii, are relatively short and an alteration to upstream nutrient export can affect rates at which streams deliver nutrients to estuaries and coastal systems (Allan & Castillo, 2007). Streams are continuous systems and changes in the amount of nutrients exported from the study reach can alter downstream labile nutrient availability. In the Tropics, near-shore habitat is often nitrogen limited and up to 80% of phytoplankton productivity can be attributed to stream nutrient supply (Ringuet & Mackenzie, 2005; Hoover & Mackenzie, 2009). Therefore, a 10-fold reduction in nitrogen supply can potentially have direct consequences for the structure and productivity of downstream ecosystems.

Space-for-time substitutions are commonly used in terrestrial systems to estimate implications for ecosystem function. However, in freshwater systems there are few studies that have applied this tool in the context of climate change. These studies focus on implications of temperature changes for ecosystem structure (e.g. Woodward *et al.* 2010a; Stoks et al. 2014), while studies measuring effects of precipitation change, in particular on ecosystem function, are quite rare. We are aware of only one other study that employed a large spatial gradient (i.e. ecoregions) to examine effects of various anthropogenic disturbances on excretion (Moore & Olden, 2017). Therefore, our study is the first to use a space-for-time substitution to assess the effects of precipitation change

on ecosystem function in freshwater systems. There are limitations to the space-for-time substitution approach in that there are often underlying confounding gradients in physicochemistry, biogeography or disturbance that can make it difficult to extrapolate the data (Johnson & Miyanishi, 2008; Woodward *et al.*, 2010b). Nevertheless, if these limitations are addressed, this tool can provide answers to important parts of the research question that cannot be addressed by experiments that often do not capture the complexity of the natural ecosystem. Our rainfall gradient has the advantage that many of these space-for-time substitution limitations are addressed (Frauendorf *et al.*, 2019), and that several studies used this gradient, providing us with substantial background information to make strong predictions. This study shows that there is value and great promise in utilizing space-for-time substitutions as a tool to estimating anthropogenic impacts on freshwater ecosystem function.

Table 4.1: Physical characteristics of 8 streams across the North Hilo rainfall gradient. Mean annual rainfall (MAR) was generated from the Rainfall Atlas of Hawaii (Giambelluca *et al.,* 2013). Baseflow (Q_{90}) and background nutrients (µg molar nitrogen (N) or phosphorus (P) L^{-1}) were averaged for the sampling periods (May-September) across the 3 years.

	WET →							**DRY**
Stream	HON	KAP	KOL	UMA	LOA	MAK	PAH	KAA
MAR	5764	5868	6520	5178	5168	4748	4527	3703
Q_{90}	22.36	15.50	17.56	8.65	4.53	2.56	0.32	0.06
NH_4	5.55	8.49	4.03	4.36	6.93	6.01	4.85	5.13
NO_3	13.70	1.77	13.10	*NA*	17.56	10.27	19.23	18.06
PO_4	4.46	4.94	4.50	5.63	7.01	5.13	5.94	7.44

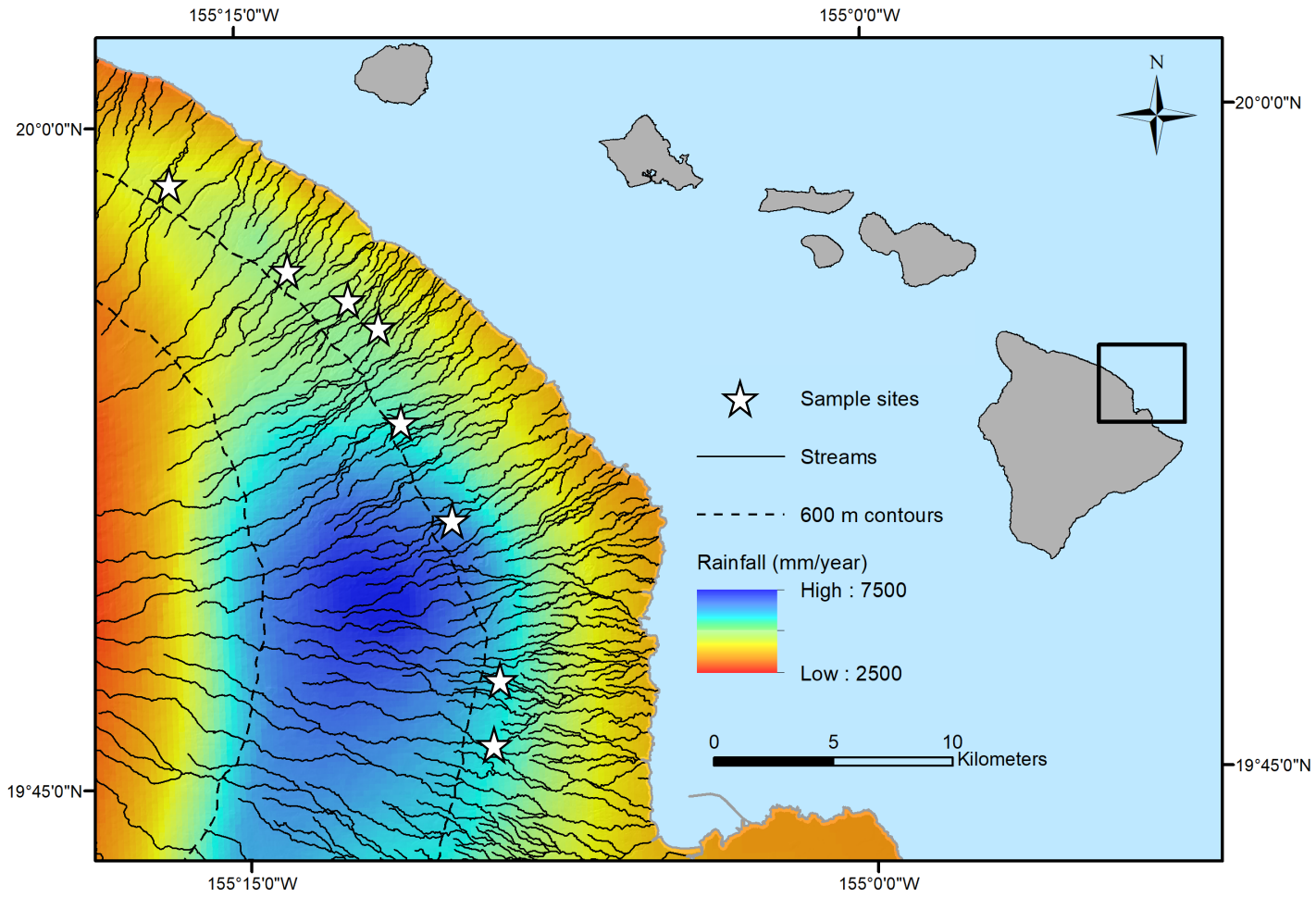

Figure 4.1: Eight stream sites (stars) located along the northeast coast of Hawaii Island with similar environmental characteristics except for the difference in mean annual rainfall. Average rainfall declines from ~ 7000 mm to 3500 mm per year along the coastline, mimicking projected effects of climate change on precipitation and streamflow. Data for this map were generated from the Rainfall Atlas of Hawaii (Giambelluca *et al*., 2013).

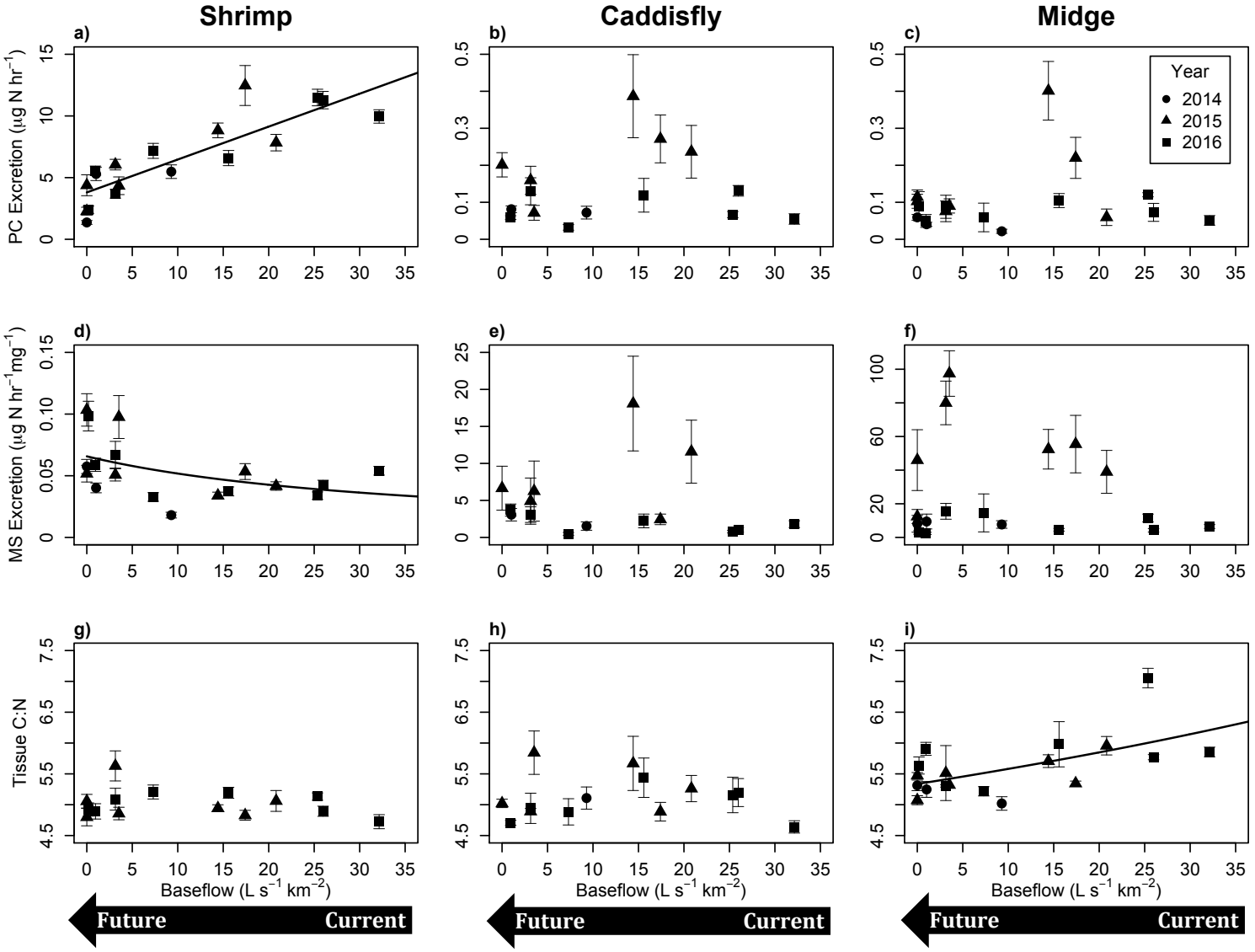
Shrimp
Caddisfly
Midge
a)
b)
c)
d)
e)
f)
g)
h)
i)
PC Excretion (µg N hr^{-1})
MS Excretion (µg N hr^{-1}mg^{-1})
Tissue C:N
Baseflow (L s^{-1} km^{-2})
Year
2014
2015
2016
Future
Current

Figure 4.2: Per-capita ammonium excretion rates increased with baseflow for shrimp (a), while mass-specific excretion declined (d). Per-capita and mass-specific excretion did not vary appreciably across the gradient for caddisflies (b,c) or midges (e,f). Tissue chemistry did not vary for shrimp (g) and caddisflies (h), whereas C:N of midges (i) increased across basefow. Each point represents the average of 20 individuals per taxon (with standard error) in one stream per sampling year. Lines denote significant model output of each relationship ($p \leq 0.05$, see text for modeling details). The x-axes represent baseflow (Q_{90}) averaged for May-September, while block arrows indicate the direction of predicted declines in baseflow with climate change.

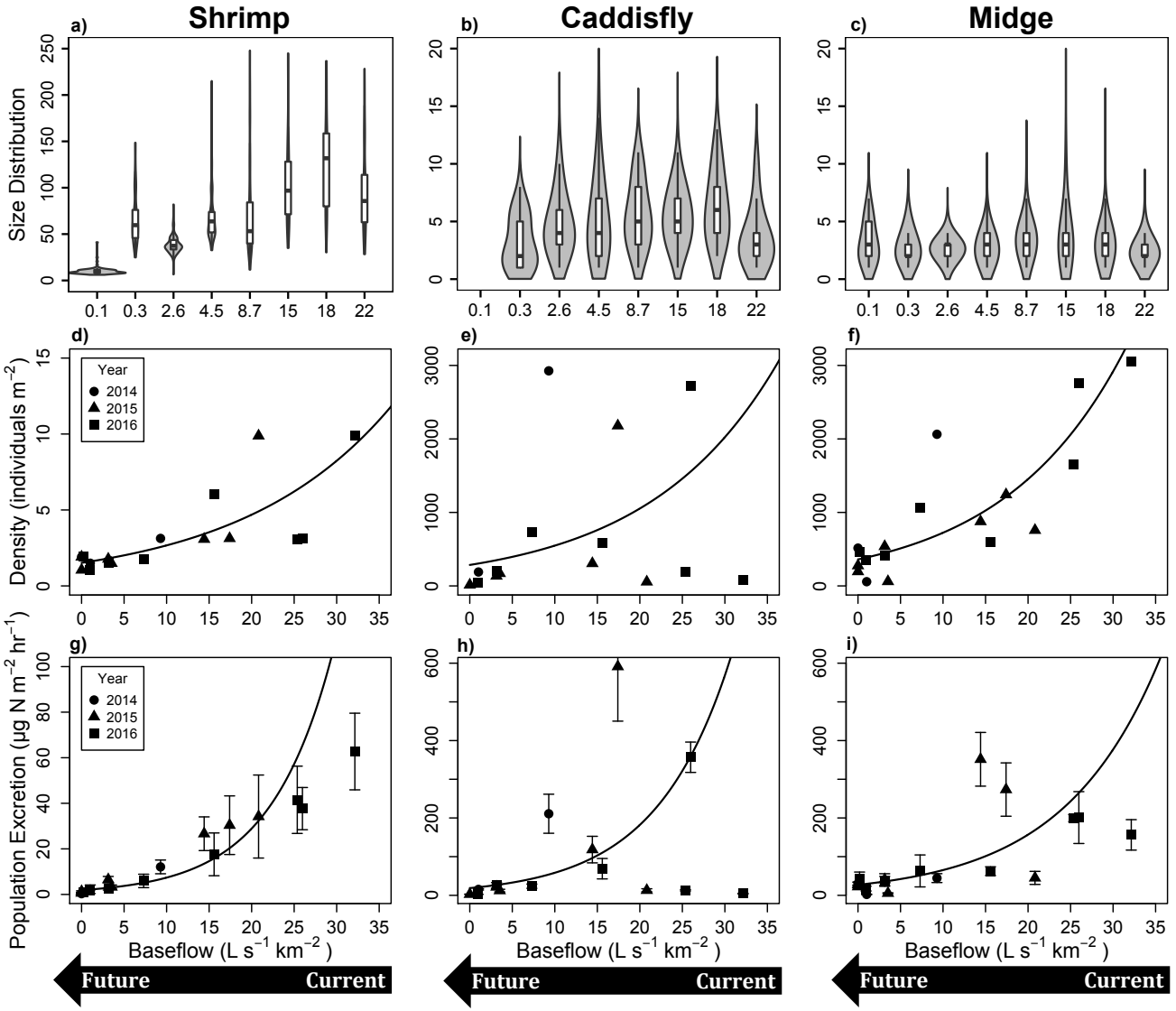
Shrimp
Caddisfly
Midge
a)
b)
c)
d)
e)
f)
g)
h)
i)
Size Distribution
Density (individuals m^{-2})
Population Excretion (µg N m^{-2} hr^{-1})
Year
2014
2015
2016
0.1 0.3 2.6 4.5 8.7 15 18 22
Baseflow (L s^{-1} km^{-2})
Future
Current

Figure 4.3: The violin plots (a-c) display the size distribution of the three dominant taxa across baseflow, where the width of the shaded area indicates the frequency of a particular size class. The average size of shrimp (a; mg AFDM for 2014 only) and caddisfly (b; mm body length average for 2014-16) populations increased significantly with higher baseflow, while the average size of midge populations (c; mm body length for 2014-16) did not vary across flow. Density (d-f) and population-level ammonium excretion (g-i) of all three taxa exponentially increased with higher baseflow streams across all three sampling years. Each point represents the average of 20 individuals per taxon (with standard error) in one stream per sampling year. Lines denote significant model output of each relationship ($p \leq 0.05$, see text for modeling details). The x-axes represent baseflow (Q_{90}) averaged for May-September, while block arrows indicate the direction of predicted declines in baseflow with climate change.

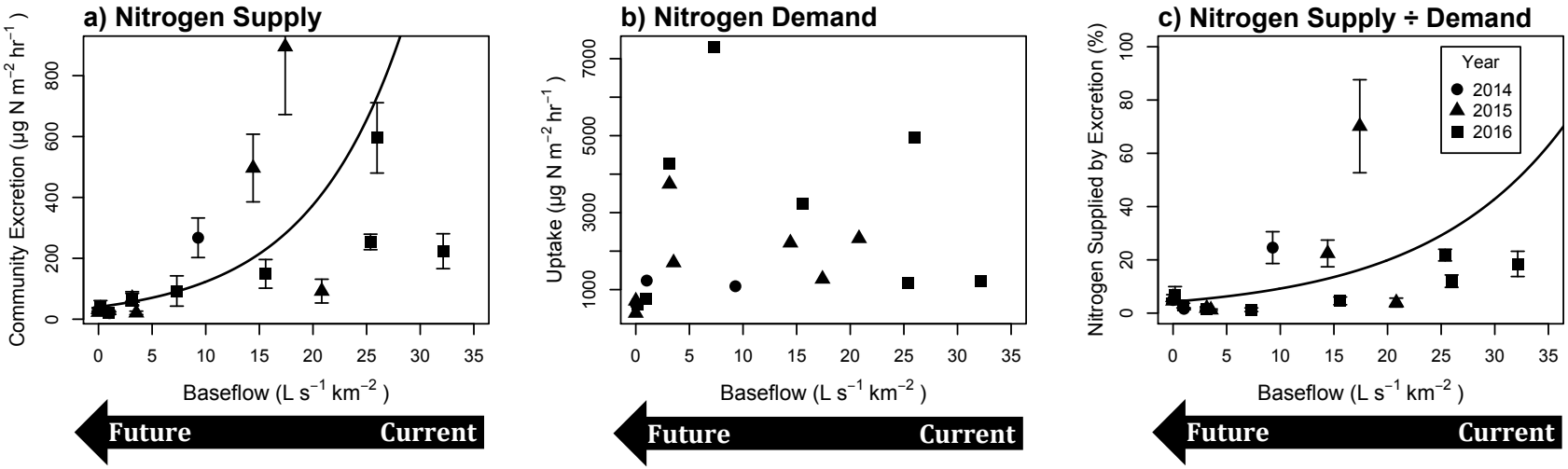

Figure 4.4: Nitrogen supplied by community excretion (a) increased exponentially in streams with higher baseflow, while nitrogen demand (b) did not change. Therefore, the percent of nitrogen supplied by excretion (c) increased by, on average, 10-fold as streams increased in baseflow. Each point represents the average of 20 individuals per taxon (with standard error) in one stream per sampling year. Lines denote significant model output of each relationship ($p \leq 0.05$, see text for modeling details). The x-axes represent baseflow (Q_{90}) averaged for May-September, while block arrows indicate the direction of predicted declines in baseflow with climate change.

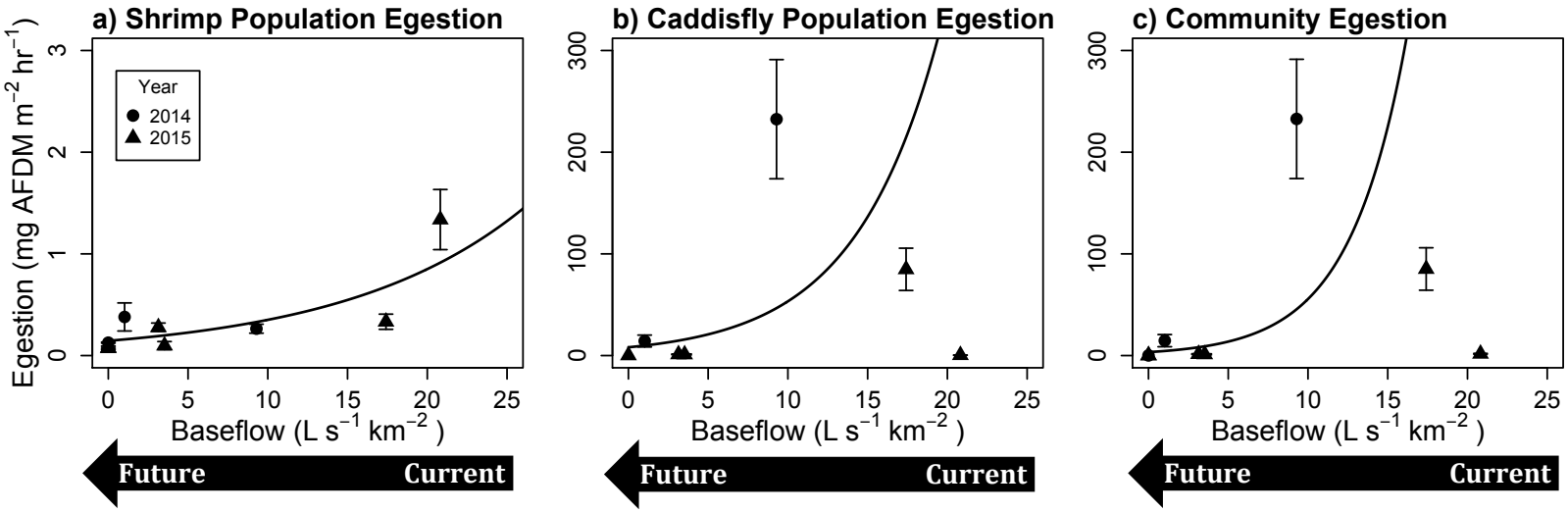

Figure 4.5: Population (a-b) and community egestion (c) increased exponentially with baseflow. Each point represents the average of 20 individuals per taxon (with standard error) in one stream per sampling year. Lines denote significant model output of each relationship ($p \leq 0.05$, see text for modeling details). The x-axes represent baseflow (Q_{90}) averaged for May-September, while block arrows indicate the direction of predicted declines in baseflow with climate change.

Chapter 5: Measuring combined effects of climate change and invasive species on tropical island stream structure and function using a space-for-time substitution approach

Therese C. Frauendorf[1], Richard A. MacKenzie[2], Piatã S. Marques[1], and Rana W. El-Sabaawi[1]

[1] Department of Biology, University of Victoria, Victoria, British Columbia, V8W 3N5, Canada

[2] Institute of Pacific Islands Forestry, Pacific Southwest Research Station, USDA Forest Service, Hilo, Hawaii 96720, USA

Author contributions: TCF conceived the study with intellectual input from RES. TCF collected and analyzed the data with assistance from PSM. TCF wrote the manuscript with editorial contributions from RES, RAM and PSM.

5.1 Abstract

Ecosystems are more often than not affected by multiple threats, such as habitat destruction, overexploitation, climate change, and invasive species. Models predict that multiple anthropogenic stressors will have the greatest impact in freshwater systems, yet verification of these models in natural ecosystems is rare. We used a space-for-time substitution approach to determine the combined effects of invasive fish and climate change on stream ecosystem structure and function in Hawaii. To examine the effects on stream structure, we quantified benthic and suspended resources and macroinvertebrate biomass. To examine the effects on stream function, we determined nitrogen and phosphorus supply rates of dominant consumers via excretion and quantified the stream nutrient demand via uptake. We measured these variables in three guppy-free and three guppy-invaded streams across a rainfall gradient on Hawaii Island that mimics forecasted climate-driven changes in streamflow. Resource patterns resulting from climate-driven changes in flow were not affected by guppy presence. However, the two stressors had additive and synergistic effects on macroinvertebrate biomass and excretion. Climate change enhanced the effect of guppies by lowering native invertebrate biomass and elevating the biomass of a non-native invertebrate species. This same trend was true for the excretion rates of macroinvertebrates, which resulted in consumer nutrient supply exceeding the nutrient demand in guppy-invaded streams under climate-driven changes in flow. We demonstrate that space-for-time substitutions can be a valuable tool to empirically measure the effects of multiple stressors.

5.2 Introduction

Freshwater ecosystems are vulnerable to anthropogenic alterations on both regional and local scales (Dudgeon *et al.*, 2006; Dudgeon, 2014). While the effects of individual anthropogenic stressors (e.g. altered hydrology, temperature, contaminants) on freshwater systems have been investigated in many studies, a growing body of research has shown that the effects of a single stressor are more often than not altered in the presence of another stressor (e.g. Dudgeon *et al.*, 2006; Jackson *et al.*, 2016; Craig *et al.*, 2017). When multiple anthropogenic stressors are combined, the overall effect can be greater than (synergism), less than (antagonism) or equal to (additive) the sum of their individual effects. Concurrent stressors can also manifest in the opposite direction from the sum of the individual effects (reversed; e.g. sum of individual effects is positive but the measured combined effect is negative; *sensu* Christensen *et al.*, 2006; Piggott, Townsend & Matthaei, 2015). A recent synthesis indicated that the net effects of concurrent alterations in freshwater ecosystems were more antagonistic (41%) than synergistic (28%), additive (16%), or reversed (15%) (Jackson *et al.*, 2016). However, empirical evidence of the net effects of multiple stressors on freshwater systems remains limited (Jackson *et al.*, 2016), and understanding the interactive effects of multiple stressors in natural ecosystems remains a central challenge in freshwater science.

Models and mesocosms are common ways of examining the effects of multiple anthropogenic stressors. Mechanistic (mathematical projections) and statistical models (projections based on meta analyses) are important tools for assessing the effects of multiple stressors (e.g. Wenger *et al.*, 2011; Rolls, Hayden & Kahilainen, 2017; Strauch *et al.*, 2017; Denley, Metaxas & Fennel, 2019). However, these projections need to be

verified by studies in natural ecosystems, which are rare in the literature (Craig *et al.*, 2017). Mesocosms are another way of examining multiple stressors, but these studies typically use biomass or abundance of one or two species as the only response variable (Jackson *et al.*, 2016), which can limit the ability to scale the results to the reach, ecosystem, or watershed level (Craig *et al.*, 2017). In addition, mesocosms often last only several weeks, which does not account for the ability of species to adapt to a changing ecosystem. Recently, space-for-time substitutions (i.e. a spatial gradient mimicking a temporal change) have been suggested as a tool that can incorporate plasticity and evolution when measuring a long-term change (Kelly, 2019). A space-for-time substitution can also become an approach for examining the consequences of multiple anthropogenic stressors in natural stream ecosystems, although they have rarely been used in this context. In this study, we demonstrate how a space-for-time substitution approach can be used to assess the effects of climate change and the introduction of an invasive species on tropical island streams.

It is predicted that invasive species and climate change will be among the top five challenges threatening the future of ecosystems (Bellard *et al.*, 2015). Most of the existing knowledge on the combined effects of invasive species and climate change centers around the interactions of the invasive species with temperature (Walther *et al.*, 2009). However, changes in precipitation are an important driver of climate change in stream ecosystems because precipitation is one of the main drivers of streamflow (Pyne & Poff, 2017). Increased flooding can give invasive species access to new habitats, while increased drought events can enhance competitive effects between native and introduced species (Rahel & Olden, 2008). In this study, we focus on tropical island streams,

because tropical areas are considered to be one of the first to experience the effects of climate change (Mora *et al.*, 2013), and remote islands, in particular, are also highly susceptible to species invasion (Moser *et al.*, 2018).

We used a well-described rainfall gradient along the North Hilo coastline on Hawaii Island as a space-for-time substitution model. This rainfall gradient mimics projected precipitation and resulting flow declines and increases in variability (Elison-Timm *et al.*, 2015; Strauch *et al.*, 2015). In addition, guppies (*Poecilia reticulata*) were introduced to several streams along this gradient in the early 1900s, likely as a mosquito control (Holitzki *et al.*, 2013). This study system is unique because the effects of climate change (Frauendorf *et al.*, 2019, Chapter 4) and guppy introductions (Holitzki *et al.*, 2013) have been studied extensively on their own, giving us valuable background information on the effects of each individual stressor independently of the other. These studies show that declines in rainfall will lead to 10-fold declines in resources, consumers, and nutrient supply (Frauendorf *et al.*, 2019, Chapter 4). On the other hand the presence of guppies decreases native consumer (e.g. midge) abundance by 2-fold, while increasing algal resources (i.e. biofilm) by 1.5-fold and nitrogen supply rates by 8-fold (Holitzki *et al.*, 2013). Our goal is to examine the effects of invasive guppies along the gradient in order to specifically ask how their effect is impacted by climate-driven changes in precipitation. Based on the mechanisms described above, we predict that the effects of guppies on biofilm and invertebrate standing stocks will be exacerbated by declines in rainfall. However, because the effect on biofilm and invertebrates will be mediated by increasing guppy density along the gradient, the decline in nutrient supply from changes in rainfall may be balanced by the increases in nutrient supply resulting

from invasive guppies. In other words we predict that climate change and species invasion will have either additive or synergistic effects on stream structure and function.

5.3 Methods

We selected six streams along the North Hilo rainfall gradient and grouped them into dry, medium, and wet based on their annual average streamflow (Fig. 5.1, Table 5.1). Within each category we selected a guppy-invaded and a guppy-free stream. Most of the six streams overlapped with streams from the previous studies (Holitzki *et al.*, 2013; Frauendorf *et al.*, 2019, Chapter 4). The sampling reaches for this study were several kilometers downstream from the Frauendorf *et al.* (2019 and Chapter 4) studies and at similar elevation as the Holitzki *et al.* (2013) study. These six streams (Kolekole, Umauma, Manoloa, Waikamalo, Manowaiopae, and Kaiwilahilahi) are all located within 20 km of each other and have similar characteristics (e.g. temperature, elevation, substrate age and type; Table 5.1; Strauch *et al.* 2015). Besides changes in flow and presence of guppies, the only difference between the streams is the increase in canopy cover at low flow streams (Table 5.1). This is a result of higher flow creating wider streams, which decreases the canopy cover (Frauendorf *et al.*, 2019). However, there are no differences in canopy cover between guppy-invaded and guppy-free streams. Several non-native poeciliid fish are present in other streams along this coastline (Holitzki *et al.*, 2013). However, we selected streams specifically with guppies as the only invasive species to isolate the effect of one introduced species in addition to changes in flow. The endemic goby (*Lentipes concolor*) was the only other fish present in these stream reaches, but their densities were very low (< 0.2 individuals/m^2) and therefore we did not include

them in our study. At each stream we collected the stream structure and function samples in a 100 m reach during the dry season (July-September) of 2015 and 2016.

We quantified benthic and suspended resource availability and macroinvertebrate biomass at three random sites within each reach. Following the methods described in Frauendorf *et al.* (2019), we collected substrate composition (%), suspended material from the water column (g ash-free-dry mass (AFDM)/day), benthic material (g AFDM/m^2), benthic biofilm (biomass (mg AFDM/m^2) and photosynthetic component (mg Chl *a*/ m^2), and macroinvertebrate biomass (g AFDM/m^2). Many of these methods were also similar to the methods described in Holitzki *et al.* (2013). We estimated guppy density following a depletion method (Carle & Strub, 1978). A 30 m stream reach was blocked with fine mesh nets and fished for 45 minutes, three consecutive times. To estimate the size distribution of the population in each stream, we measured the standard length (cm) of around 100 randomly chosen guppies.

We estimated nitrogen (N) and phosphorus (P) supply rates of dominant consumers via excretion. Excretion can transform N and P sequestered from the organic matter of resources to mobile and easily accessible nutrients for uptake by primary producers and microbes (Vanni, 2002). Excretion is often a large component of the N and P budgets in freshwater environments, because excretion stimulates primary production by elevating local nutrient levels. This can potentially create biogeochemical hotspots, where nutrients released exceeds uptake by other organisms (McIntyre *et al*., 2008). Based on previous studies along this coastline (Holitzki *et al.*, 2013; Frauendorf *et al.*, 2019), we knew that midges (Chironomidae) and caddisflies (*Cheumatopsyche analis*) are the dominant taxa in these streams. Therefore, we measured excretion rates of 20

individual midges and 20 caddisflies per stream and sampling year. Excretion rates were measured in the field and in the lab using the same methods as described in Chapter 4. In guppy-invaded streams, we also measured excretion rates of 20 guppies using methods described in Chapter 2. We averaged the 20 individual excretion rates to calculate mean per-capita (ug N or P/hr) and mass-specific (ug N or P/hr/mg of body weight) ammonium and phosphate excretion rates and their 95% confidence intervals. We did not detect any nitrate in the excretion samples of caddisflies, midges, and guppies (detection limit: 0.07 μM). We scaled per-capita excretion rates to the population (μg N or P/hr/m^2) and community levels using the same methods as described in Chapter 4. In addition, we estimated the C:N tissue chemistry of the individuals excreted to determine if the species remained homeostatic. Lastly, we measured nutrient demand via uptake (μg N or P/hr/m^2) using methods explained in Chapter 4, adapted from Covino, McGlynn & McNamara (2010). To estimate the percent of nutrients supplied by excretion (i.e. relative importance of excretion), we divided the community nutrient supply by the nutrient uptake in each stream and multiplied that value by 100.

We averaged the results of 2014 and 2015 for each response variable and calculated 95% confidence intervals (CI). Since we only have two sampling years and low replication by stream, we do not have enough replication for traditional statistical analyses (Amrhein, Greenland & McShane, 2019). We qualitatively (using CIs) examined trends with streamflow to assess if they were similar to patterns observed in previous studies (e.g. Frauendorf *et al.* 2019, Chapter 4), where structure and function were sampled extensively and with good replication along the gradient. Since ultimately our goal was to examine guppy effect, we then used a t-test to examine if overall the

presence of guppies had an effect on the response variable, independently of the flow category (at $\alpha = 0.1$, $n = 6$). If the t-test was significant, we then determined if the effect size between guppy-invaded and guppy-free streams changed across the different flow regimes. We estimated effect size by calculating Hedges' g, using the package "effsize" in the statistical program R (Torchiano, 2018). Hedges' g is calculated like other effect size measurements that use standardized differences (e.g. Cohen's d), where the difference between two means is divided by the pooled standard deviation of the two groups. However, unlike Cohen's d, Hedges' g accounts for a low sample size (< 20) by multiplying the effect size with a correction factor (Durlak, 2009; Hedges & Olkin, 2014). The magnitude of the effect size was then assessed using the thresholds provided by Cohen (1992), where Hedges' $g < 0.2$ is considered negligible, < 0.5 small, < 0.8 medium, and > 0.8 is considered large.

5.4 Results

5.4.1 Effects on stream structure

The effects of streamflow on stream resources were not substantially different with the presence of guppies. As expected, suspended resource biomass was 6-fold lower in drier streams compared to the wetter streams, independently of guppy presence (Table 5.2). Benthic resources biomass did not appear to vary with streamflow (Table 5.2). However, the relative availability of the two dominant resources (macrophyte and detritus represented 80-100% of benthic resources) varied with streamflow. Macrophyte biomass was 10-fold lower, and detrital biomass was 2-fold higher in dry streams compared to the wet streams (Table 5.2). Guppies did not affect suspended ($p = 0.74$) or benthic resource

biomass ($p = 0.23$) in any of the flow treatments (Table 5.2, Appendix 5.1). Guppies also did not affect the relative biomass of different basal resources (macrophyte $p = 0.72$, detritus $p = 0.16$; Appendix 5.1). The only effect that guppies had on benthic resources was increasing higher biofilm chlorophyll *a* (Fig. 5.2a) and biomass (Fig. 5.2b) by 1.5-fold, but this effect was not significant ($p = 0.11$ for both; Appendix 5.1). Lastly, as expected, there was no consistent difference in the substrate composition across streams (Appendix 5.2). The main substrate types at each stream were bedrock, boulder, gravel and cobble. The two dry sites also had some sand present.

In contrast to basal resources, climate and guppies appeared to have synergistic effects on invertebrate biomass. As expected, invertebrate biomass was 2-fold lower in the dry, guppy-free stream (49.5 ± 9.8 (CI) g AFDM/m^2) compared to the wet, guppy-free stream (113.7 ± 20.1 g AFDM/m^2; Fig. 5.2c). Overall, invertebrate biomass was significantly higher when guppies were present ($p = 0.03$, up to 5-fold), but the effect size of guppies was the highest in the dry stream (Hedges' g for dry stream 9.7 vs. wet 0.3; Appendix 5.1).

The taxonomic composition of the invertebrate community did not change noticeably across the different stream categories (Appendix 5.3), but the relative contribution of the dominant invertebrates did. Midges and caddisflies were the two dominant taxa that combined represented between 50-80% of the total invertebrate biomass. As predicted, the density of midges (wet stream 2070 ± 587 vs. dry 846 ± 392 ind./m^2) and caddisflies (wet stream 727 ± 91 vs. dry 51.0 ± 4.0 ind./m^2) were lower in the drier guppy-free streams compared to the wet stream (Fig. 5.3a-b). Caddisfly densities were significantly higher in streams with guppies ($p = 0.02$), but the number of midges

was lower ($p = 0.06$; Appendix 5.1). Guppies had the largest effect on caddisfly density (Hedges' g for wet stream 0.2 vs. dry 8.3) and midge density (Hedges' g for wet stream 0.5 vs. dry 1.0) in the driest stream (Appendix 5.1). The size distribution and average size of caddisfly and midge populations did not vary with the presence of guppies ($p = 0.69$; $p = 0.13$, respectively) or with streamflow (Fig. 5.3d, e). Guppy population densities were larger in the dry stream (9.50 ± 3.63 vs. wet stream 3.58 ± 0.97 ind./m^2; Fig. 5.3c), but streamflow did not noticeably affect the size distribution of guppies either (Fig. 5.3f).

5.4.2 Effects on stream function

Climate change and guppies had little effect on individual excretion and tissue chemistry. Per-capita and mass-specific nitrogen excretion rates and tissue chemistry did not vary in a consistent pattern across the streams (demonstrated by overlapping means and CIs, Fig. 5.4, Appendix 5.4). The same was true for per-capita caddisfly and guppy phosphorus excretion rates (Appendix 5.5 and 5.6). However, guppies lowered per-capita ($p = 0.04$) and mass-specific ($p = 0.03$) midge phosphorus excretion by 2-3 fold (Appendix 5.5). Nevertheless, the effect size of guppy presence did not vary with streamflow (e.g. Hedges' g for per-capita P excretion in wet stream 0.96 vs. dry 0.93; Appendix 5.7). Lastly, the C:N ratio of midge and caddisfly tissues were not related to guppy presence ($p = 0.97$, $p = 0.75$, respectively; Appendix 5.4). Midge, caddisfly, and guppy C:N ratios were also not affected by the different flow rates (overlapping means and CIs; Fig. 5.4). The lack of any pattern in the C:N ratios of tissues across streams indicates that these consumers were homeostatic (Sterner & Elser, 2002).

Population excretion rates of each taxon mimicked trends displayed by their densities (Fig. 5.5). Nitrogen and phosphorus population excretion rates for midges and caddisflies were up to 4-fold lower in the dry guppy-free stream (Fig. 5.5, Appendix 5.5). The presence of guppies further dropped midge population excretion rates ($p = 0.05$) and the guppy effect was larger for phosphorus population excretion compared to nitrogen (Hedges' g for P was up to 1.12 and for N up to 0.61; Appendix 5.4). However, guppies had the opposite effect on caddisfly population excretion rates. Caddisfly nitrogen and phosphorus excretion rates were up to 10-fold higher in the dry guppy-invaded stream (e.g. Hedges' g for N in wet stream 0.46 vs. dry 1.55; Appendix 5.4). Lastly, the guppy population excretion rates were also 4-fold higher in drier streams compared to the wet stream (Fig. 5.5c; Appendix 5.5i).

The effect of guppies on the relative nutrient contribution of excretion was enhanced by climate-driven changes in streamflow. In guppy-free streams phosphorus and nitrogen community excretion rates were 4-fold lower in the dry stream compared to the stream with current flow conditions (Fig. 5.6a; Appendix 5.6a for P). However, in the guppy-invaded streams the community excretion rates were 2-fold higher in the dry stream. Nitrogen uptake rates were 3-fold lower in guppy-invaded streams compared to guppy-free streams ($p = 0.006$; Fig. 5.6b), but the guppy effect did not vary substantially with streamflow (Hedges'g for wet stream 2.4 vs. dry 1.2; Appendix 5.4). The presence of guppies ($p = 0.35$) and changes in streamflow (i.e. overlapping CIs) also did not have an effect on phosphorus uptake rates (Appendix 5.6b). As a result, the percent nitrogen and phosphorus supplied by community excretion was 10-fold lower in the dry guppy-free stream compared to the wet guppy-free stream (Fig. 5.6c; Appendix 5.6c for P). This

is in contrast to the dry guppy-invaded stream, where percent of nutrients supplied by excretion was 10-fold higher compared to wet guppy-free stream. This guppy effect was significant for both nitrogen ($p = 0.02$) and phosphorus ($p = 0.06$). The effect size of guppies on percent nitrogen supplied was the largest in the driest stream at the ecosystem level (Hedges' g for dry stream 5.69 vs. wet 1.30), where community excretion supplied more nitrogen than the demand (up to 188% of the demand). For phosphorus, the guppy effect size was the largest at the community and ecosystem level in medium and low flow streams (Hedge's g up to 21.8). However, overall community excretion only supplied up to 8.32% of the phosphorus demand.

5.5 Discussion

Multiple threats, such as habitat destruction, overexploitation, climate change, and invasive species, can degrade ecosystem structure and function and diminish the capacity of natural systems to cope with the effects of these changes (Brook, Sodhi & Bradshaw, 2008). Yet over the past decade most studies have assessed the effects of these threats individually (Jackson *et al.*, 2016). Models predict that multiple anthropogenic stressors will have the greatest impact in freshwater systems (Jenkins, 2003), but verification of these models in natural systems is rare (Jackson *et al.*, 2016). We took a space-for-time substitution approach to explore the combined effects of invasive guppies and climate change on stream ecosystem structure and function. We show that climate-driven changes in streamflow can facilitate the effects of invasive guppies, but that the interaction between the effects depends on the response variable.

There appeared to be few interactions between guppies and climate on basal resources, except for a modest response in biofilm. In our guppy-free streams the declines in suspended resources and shifts from macrophytes to detritus with declining flow were comparable to our previous study (Frauendorf *et al.*, 2019). However, the overall benthic resource biomass was slightly higher in the dry stream, contrary to trends observed in our earlier study, which was conducted further upstream along the gradient (Frauendorf *et al.*, 2019). In Hawaii, riparian vegetation at lower elevation is often invaded by non-native species, while higher elevation streams are dominated by native taxa (Hughes *et al.*, 2017). As a result canopy cover at the downstream sites in this study were on average 20% higher compared to the upstream locations of our previous study (Table 5.1) (Frauendorf *et al.*, 2019). Higher canopy cover increases detrital input into the streams, leading to higher detrital basal resources. Guppies increased biofilm biomass and chlorophyll *a* by about 1.5-fold agreeing with previous studies on the effects of guppies in Hawaii (Holitzki *et al.*, 2013). However, these increases were not significant and did not vary with streamflow.

The effect of guppies on macroinvertebrate biomass was bigger with predicted changes in rainfall. Guppy density was higher in the drier streams, likely because guppies prefer low flow and pool habitats (Magurran, 2005), which are more common at the drier end of the rainfall gradient. As we had previously observed in the upstream reaches (Frauendorf *et al.*, 2019), invertebrate biomass decreases with declining streamflow in the absence of guppies. However, in guppy-invaded streams invertebrate biomass increased in the dry streams, which was largely driven by the response of the caddisflies. We expected guppies to lower midge density, because midges are known to be an important

food resource for guppies (Bassar *et al.*, 2010; Zandonà *et al.*, 2011). We did not expect guppies to change caddisfly abundance, because caddisflies are likely too large to be consumed by guppies (Holitzki *et al.*, 2013). Interestingly, guppies actually seem to facilitate the presence of caddisflies, a trend that has been suggested in previous studies in Hawaiian streams (Holitzki *et al.*, 2013). Caddisflies in Hawaii tend to graze on algae rather than filter-feed (Kondratieff, Bishop & Brasher, 1997), which could indicate that they may compete for food resources with grazing midges. Therefore, guppy presence might reduce the competition for caddisflies consuming algae. However, this is speculative and the exact mechanism needs to be tested. Lastly, it is important to note that these caddisflies are a non-native species that were introduced to the Hawaiian islands around 1965 (Denning & Beardsley, 1967). This result suggests that one invasive species (i.e. guppy) is potentially facilitating the existence of another non-native species (i.e. caddisfly), and this effect is strengthened with climate change.

Climate-driven changes in flow exacerbate the effect of guppies on nutrient recycling directly and indirectly. Individual excretion and population size structure of guppies, caddisflies, and midges did not vary consistently with declining flow or with the presence of guppies. This indicated that changes in density drove population excretion patterns, which supports what we have observed in previous chapters (Chapter 2, Chapter 4). Midge and caddisfly population excretion rates declined with lower flow in guppy-free streams, while guppy and caddisfly excretion rates increased in drier guppy-invaded streams. These changes in guppy and caddisfly population excretion drove the patterns in community excretion. As a result, community excretion rates were lower in the dry guppy-free stream and higher in the dry guppy-invaded stream compared to the guppy-

free stream with current flow conditions. However, it is important to note this 2-fold increase in the dry guppy-invaded stream is driven by caddisfly population excretion (up to 1000 μg N/hr/m^2) rather than guppy population excretion (up to 120 μg N/hr/m^2). This suggests that climate-driven changes in streamflow exacerbate the effects of guppies on nutrient recycling not only directly by increasing guppy population excretion rates, but also indirectly by increasing the excretion rates of another non-native species (Fig. 5.5). To our knowledge this mechanism (effects of an invasive species are exacerbated by climate change as a result of facilitating another non-native species) has not been shown in freshwater ecosystems.

The guppy effect on nutrient cycling is intensified with climate-driven changes in streamflow. Nutrient demand via uptake declined in the drier streams and guppy presence dropped the demand rates even further. This drop in demand rates is not surprising, given the significant contributions of guppy and caddisfly excretion to the nutrient supply. With high nutrient supply and low nutrient demand rates in the dry guppy-invaded stream, community excretion supplied up to 188% of the demand. Meanwhile in the wet guppy-free stream, community excretion supplied up to 20% of the demand. This suggests that in streams impacted by both low flow and guppies, the nutrient supply will exceed the nutrient demand. Increases in nitrogen and phosphorus availability can change animal communities in freshwater systems by altering stoichiometric imbalances between consumers and their food and by shifting whole community composition (Demi *et al.*, 2018). Therefore, these 10-fold increases in nutrient supply via community excretion can have some serious consequences within the stream reach as well as downstream areas.

Many of the combined guppies and climate change effects are synergistic, but this depends on the response variable. When examining the individual stressors, we know that climate driven changes in flow decreases midge and caddisfly biomass 10-fold (Frauendorf *et al.*, 2019). We also know that guppies increase caddisfly biomass 2-fold, while lowering midge biomass 2-fold (Holitzki *et al.*, 2013). In this study we show that midges decline by an additional 2-fold and caddisfly biomass increases by an additional 4-fold when streams experience both climate change and guppies. This suggests that the combined effects of the two stressors are additive in the case of the native midges, but synergistic when it comes to the non-native caddisflies. In the case of nutrient recycling we also show that the combined effect exceeds the sum of each individual stressor (e.g. relative contribution of excretion: individual climate change effect decreases 10-fold and guppy effect increases 3-fold (sum = 7-fold decline), but the combined stressor effect instead increases 10-fold), suggesting a synergistic effect. When compared to the overall effects of multiple stressors on freshwater systems, synergistic and additive effects are the second and third most common effect of multiple stressors (Jackson *et al.*, 2016). This study is the first one to empirically measure these combined effects in tropical freshwater island systems.

While this study is one of the first to empirically examine impacts of combined stressors, it comes with limited replicates and conclusions should be interpreted with caution. We only have two seasons of replication and we selected only three flow categories rather than the full continuum of changes in streamflow. However, many of these streams along the rainfall gradient are also invaded by other poeciliid species (Holitzki *et al.*, 2013), and we were interested in isolating the effect of just one invasive

species with changes in flow to ensure that there are no other underlying drivers in our results. Our study's limited scope is bolstered by extensive studies documenting the effects of climate change and invasive guppies in Hawaiian streams (Holitzki *et al.*, 2013; Frauendorf *et al.*, 2019, Chapter 4). When we examined the two stressors individually, our results are consistent with these studies, which gives us confidence in our results. In addition, we wanted to showcase with our study how useful a space-for-time substitution approach can be when testing effects of multiple stressors for freshwater systems. As with any space-for-time substitution approach, it is important to ensure that are no underlying confounding gradients in physicochemistry, biogeography or disturbance that can make it difficult to extrapolate the data (Johnson & Miyanishi, 2008; Woodward *et al.*, 2010b). Our rainfall gradient has the advantage that many space-for-time substitution limitations are addressed (Frauendorf *et al.*, 2019), and that several studies used this gradient, providing us with substantial background information to make strong predictions.

Although conducted with limited spatial and temporal replication, our findings have implications for conservation management of freshwater ecosystems (Jackson *et al.*, 2016). For stressor pairs that generate additive or synergistic effects, management that focuses on a single stressor should mitigate the effects significantly (Brown *et al.*, 2013). For local environmental managers it is more logistically plausible to manage a localized stressor rather than addressing stressors related to global changes (Denley *et al.*, 2019). Therefore, we suggest that working on policies eliminating guppies as a feasible immediate action for local environmental managers, while strategies to combat climate change need to be addressed at the state, national, and international level.

Table 5.1: Physical characteristics of guppy-free (GF) and guppy-invaded (GI) streams that have high, medium, and low streamflow. These values are averaged for the sampling period (July-September) across two years. Besides changes in streamflow, the resulting changes in canopy cover, and the presence of guppies, there are little differences in elevation, dissolved oxygen (DO), water temperature, pH, and background ammonium and phosphate concentrations between streams.

Stream	Wet GF Kolekole	Wet GI Umauma	Med GF Manoloa	Med GI Waikamalo	Dry GF Manowaiopae	Dry GI Kaiwilahilahi
Flow (L/s)	740.14	844.52	173.74	211.35	97.79	81.09
Elevation (m)	44	103	84	67	110	97
Canopy Cover (%)	52.1	59.4	83.7	86.6	91.3	93.8
DO (mg/L)	7.74	7.77	7.87	7.57	7.46	7.55
Temp. (°C)	24.27	24.27	23.98	24.33	23.47	23.54
pH	5.55	5.95	5.73	5.55	5.63	5.78
NH_4 (µg N/L)	0.58	0.88	0.42	1.58	1.88	0.94
PO_4 (µg P/L)	0.93	1.36	2.28	1.67	9.94	3.88

Table 5.2: Average (± 95% CI) resource availability in three guppy-free (GF) and guppy-invaded (GI) streams with high, medium, and low streamflow. Availability of total benthic detritus (g AFDM/m^2) increased in drier streams, while macrophyte (g AFDM/m^2) and suspended resource biomass (g AFDM/day) declined. There were little differences between GI and GF streams.

	Wet GF	Wet GI	Med GF	Med GI	Dry GF	Dry GI
Suspended (g/day)	1889 (250)	1603 (237)	549 (187)	539 (169)	367 (28)	229 (60)
Benthic (g/m^2)	55.1 (18)	35.9 (19)	57.5 (21)	44.4 (14)	62.6 (21)	69.1 (22)
Macrophyte	33.1 (11)	21.6 (12)	28.8 (11)	12.1 (4)	1.5 (0.5)	3.5 (1.1)
Detritus	20.5 (7)	13.7 (7)	27.8 (10)	29.7 (9)	60.3 (20)	53.6 (17)

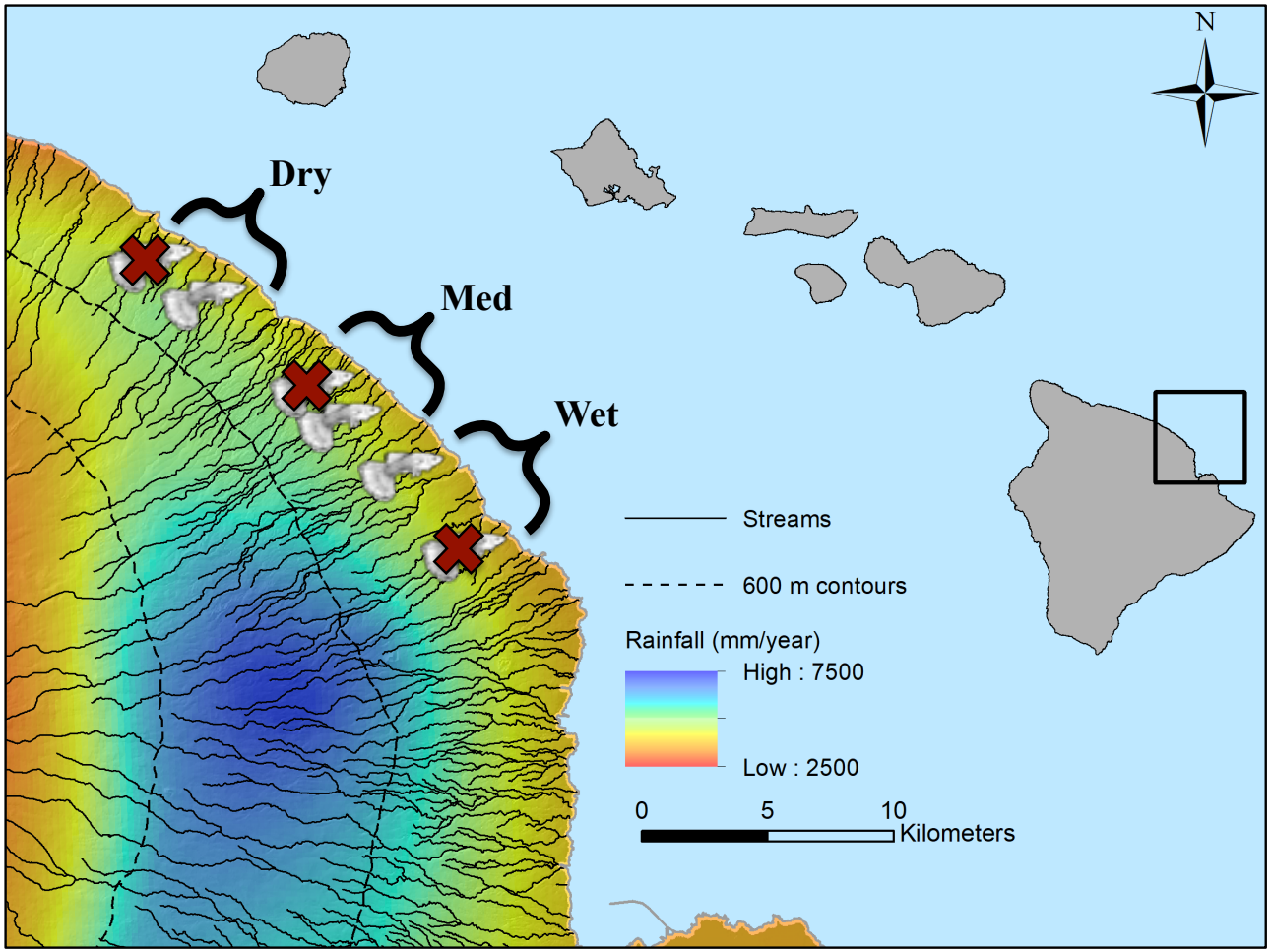

Figure 5.1: Six sampling sites along the North Hilo rainfall gradient on Hawaii Island. We grouped each of the six streams into wet, medium, and dry streamflow. Within each category, we had one stream that was invaded by guppies and one that remained guppy-free. This map was modified from Frauendorf *et al.* (2019).

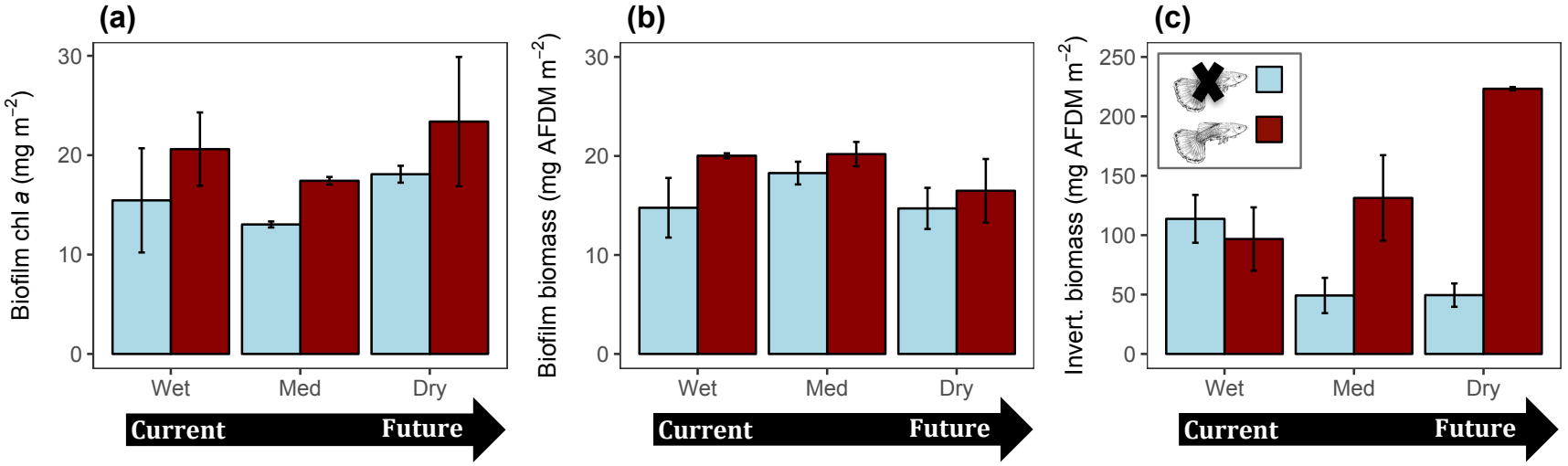

Figure 5.2: Average (± 95% CI) biofilm chlorophyll *a* concentration (a), biofilm biomass (b), and invertebrate biomass (c) in guppy-free (blue) and guppy-invaded (red) streams with high, medium, and low flow. Biofilm biomass and chlorophyll *a* concentrations were lower in guppy-free streams. Total invertebrate biomass declined in drier guppy-free streams, but increased in guppy-invaded streams. Block arrows indicate the direction of predicted declines in streamflow with climate change**.**

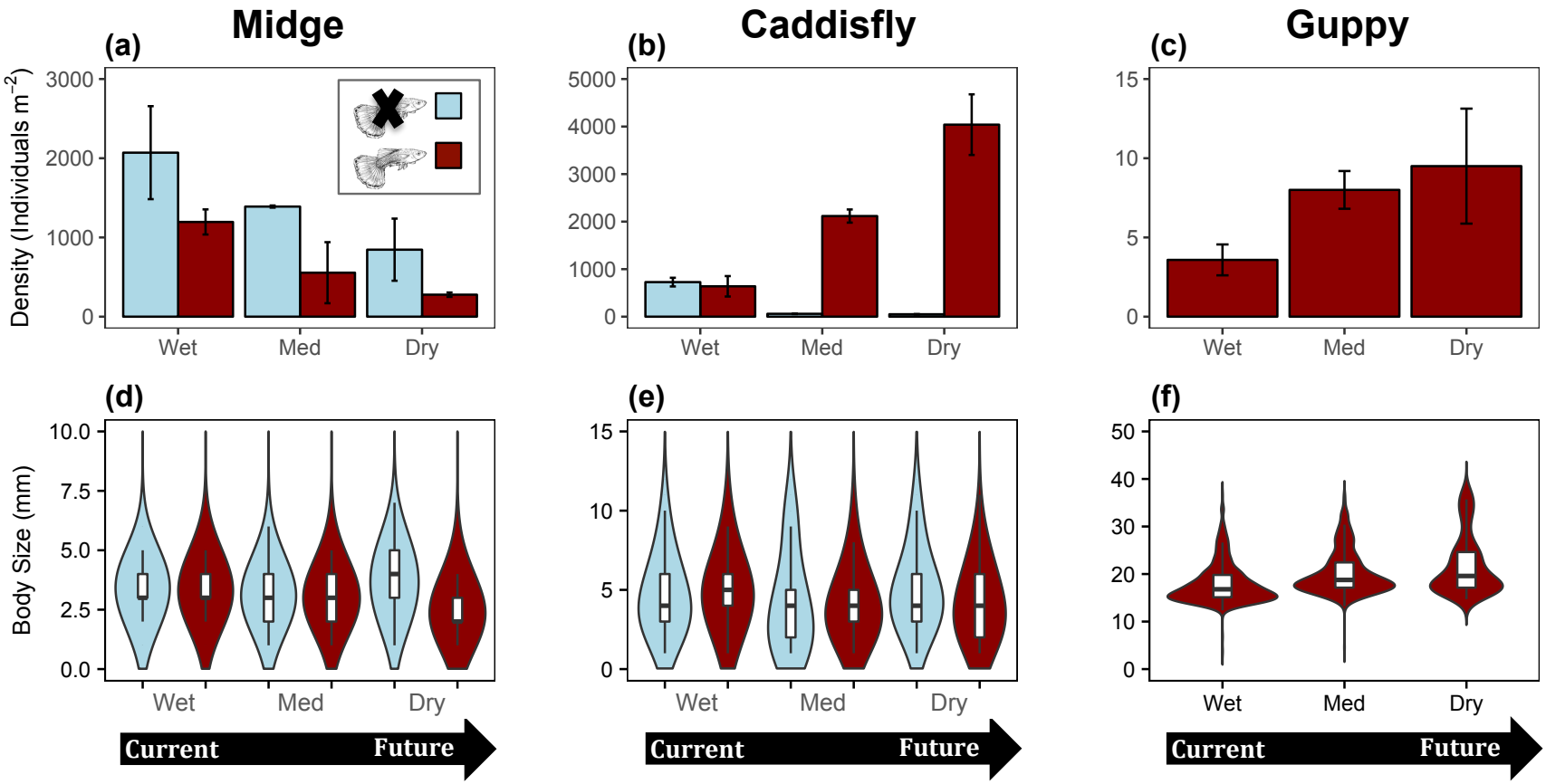

Figure 5.3: Average (± 95% CI) density (a-c) and size distribution (d-f) for midge, caddisfly, and guppy populations in guppy-free (blue) and guppy-invaded (red) streams with varying streamflow. Invertebrate densities declined in drier guppy-free streams, while in the dry guppy-invaded stream caddisfly and guppy densities increased. The violin plots suggest that there is little difference in the population size distribution between streams. Block arrows indicate the direction of predicted declines in streamflow with climate change.

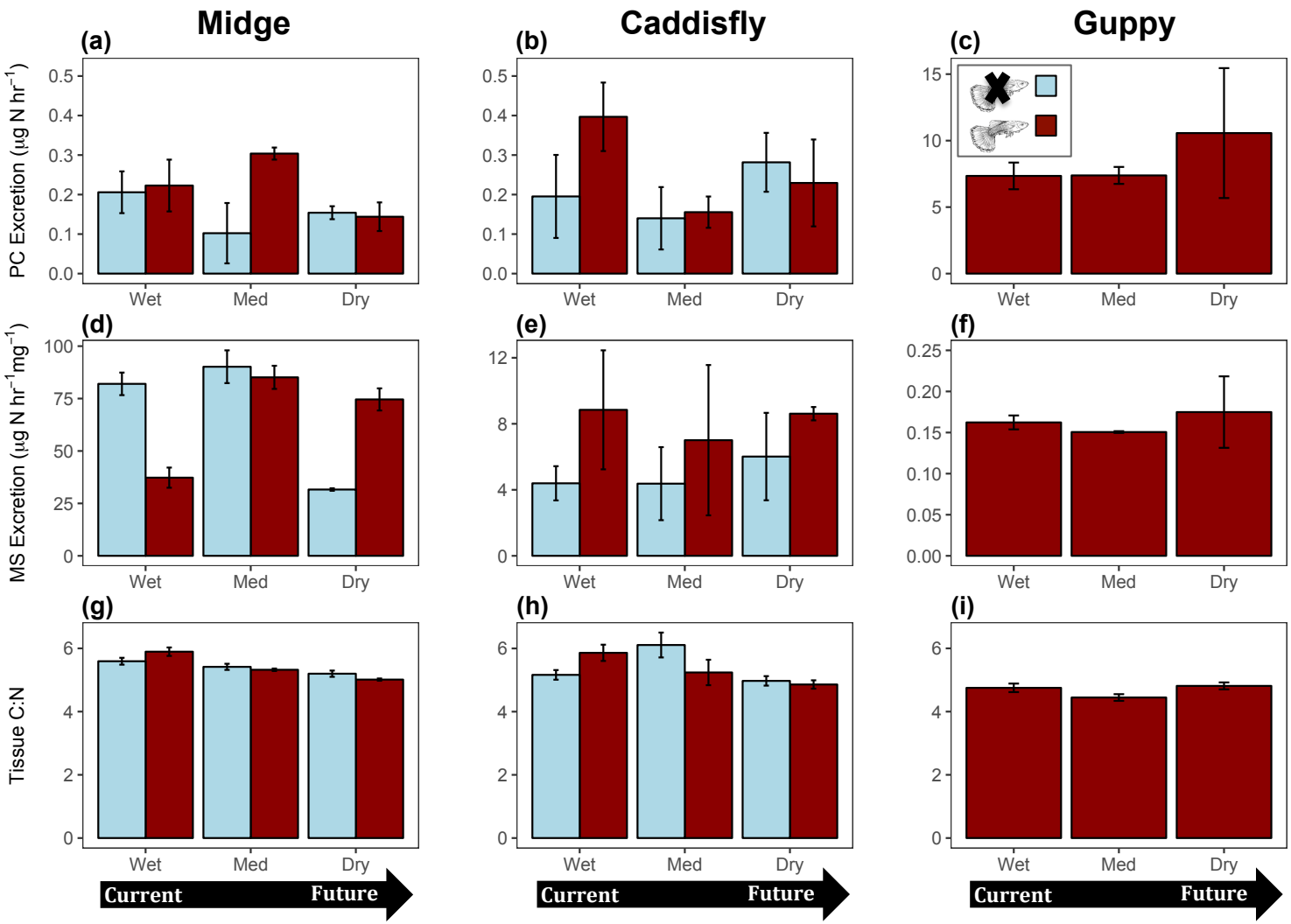
Midge
Caddisfly
Guppy
(a)
(b)
(c)
(d)
(e)
(f)
(g)
(h)
(i)
PC Excretion (μg N hr^{-1})
MS Excretion (μg N hr^{-1}mg^{-1})
Tissue C:N
Wet
Med
Dry
Current
Future

Figure 5.4: Average (± 95% CI) per-capita (PC, a-c) and mass-specific (MS, d-f) ammonium excretion of dominant consumers in guppy-free (blue) and guppy-invaded (red) streams that have high, medium, and low streamflow. All three taxa did not vary consistently across flow and with the introduction of guppies. The same holds true for C:N in tissues (g-i) across all taxa, indicating that each taxon maintained a homeostatic balance. Block arrows indicate the direction of predicted declines in streamflow with climate change.

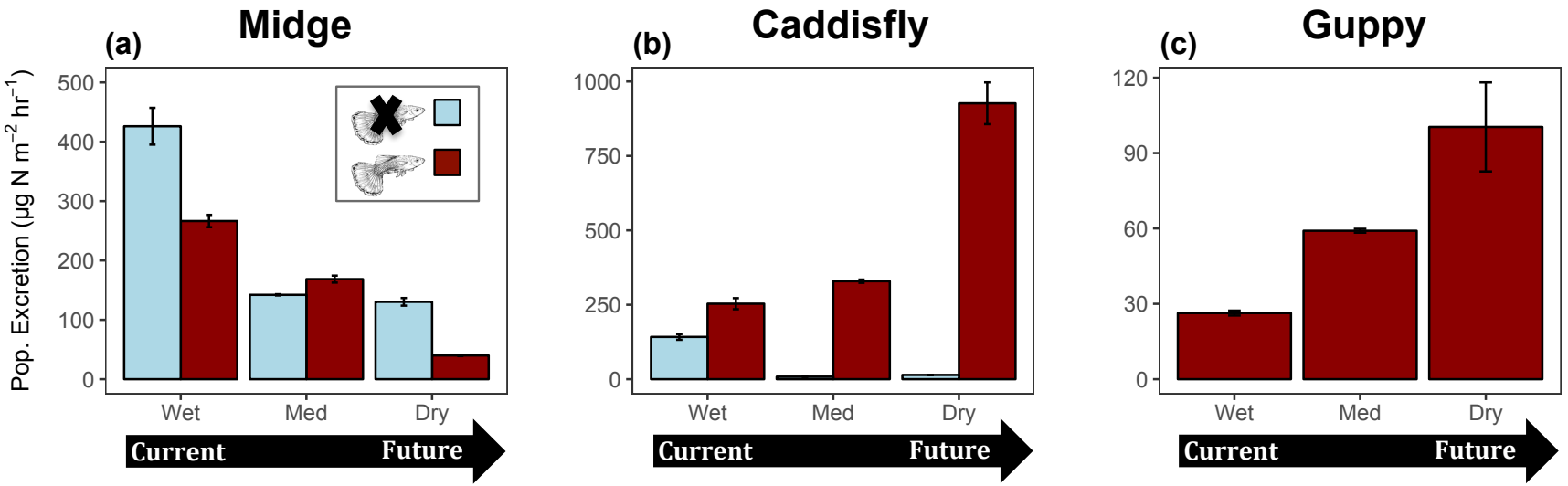

Figure 5.5: Average (± 95% CI) population nitrogen excretion for midges, caddisflies, and guppies in guppy-free (blue) and guppy-invaded (red) streams with varying streamflow. Population excretion declined in drier guppy-free streams, while in the dry guppy-invaded stream, caddisfly and guppy population excretion increased. Block arrows indicate the direction of predicted declines in streamflow with climate change.

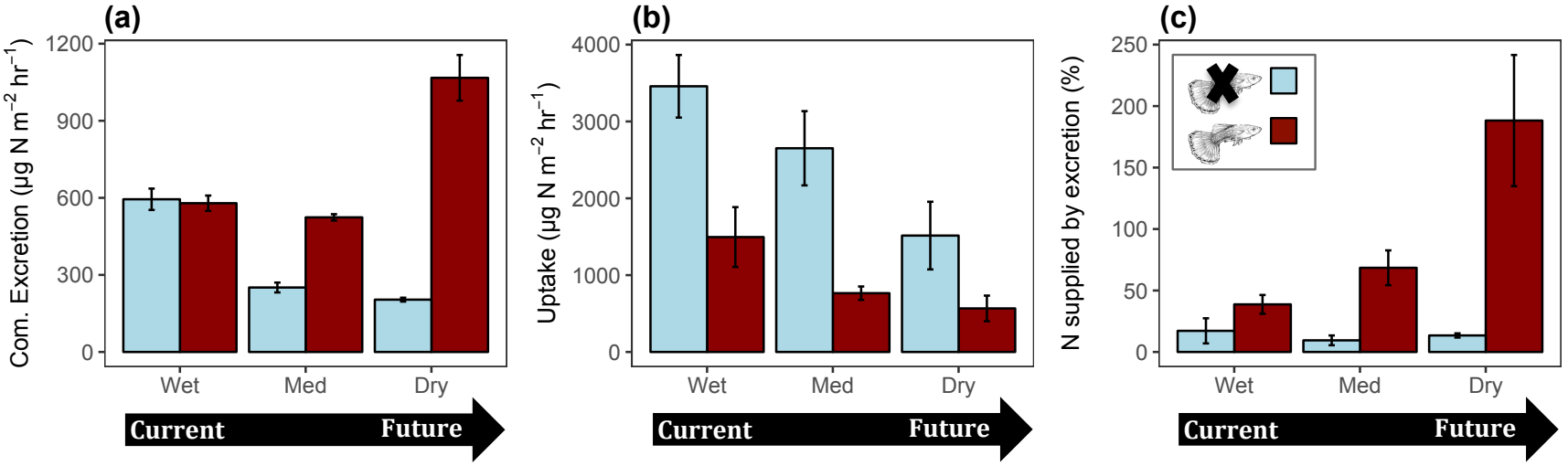

Figure 5.6: Average (± 95% CI) community nitrogen excretion rates (a) declined in drier guppy-free (blue) streams, while the opposite trend occurred in the dry guppy-invaded (red) stream. Average nitrogen demand via uptake (b) declined with guppy presence. Total nitrogen supplied by consumers (c) declined in guppy-free streams with lower flow. However, the trend reversed when guppies were present. Block arrows indicate the direction of predicted declines in streamflow with climate change.

Chapter 6: Discussion

Global climate change and species introductions are considered to be among the top five anthropogenic threats that streams and lakes face (Bellard *et al.*, 2015; IPBES, 2019). This dissertation specifically addressed the consequences of climate-driven changes in precipitation and guppy introduction as individual and combined stressors for tropical island streams, utilizing both a time series and a space-for-time substitution. We have demonstrated that when a new species establishes in an environment, ecosystem functions like nutrient recycling can vary substantially through time as a result of changes in individual traits and species density. Secondly, we have found that climate change can substantially decrease resource quantity and quality, as well as consumer biomass and the amount of nutrients supplied via excretion in tropical island streams. Lastly, we have shown that climate change appears to enhance effects of invasive guppies for some aspects of ecosystem structure and function, by affecting guppies directly and by indirectly facilitating the presence of another non-native species.

6.1 Implications for changes in stream structure and function

Introduced species and climate change have substantial effects on ecosystem structure, especially on macroinvertebrates. Invertebrates are diverse and productive members of most food webs and comprise the majority of metazoan diversity globally. They are a fundamental component of freshwater food webs because they affect communities at lower trophic levels (e.g. consumption, excretion, egestion) and at higher trophic levels by being an important food resource for organisms both inside and outside the stream

(Wallace & Webster, 1996). This is important to keep in mind as the changes in their community structure that we observed can have cascading effects in aquatic and adjacent terrestrial ecosystems. Therefore, a potential next step is to investigate the implications of both anthropogenic stressors for lower (e.g. microbial community) and higher (e.g. native fish, birds, bats) trophic levels. Secondly, the drivers behind our observed changes in macroinvertebrate communities (e.g. flow quantity, flow variability, resource quantity, resource quality) still need to be clarified in order to find potential ways to mitigate some of the effects of introduced species and climate change on these important organisms.

In streams without guppies under current rainfall conditions, invertebrate excretion supplied up to 70% of the stream nutrient demand, indicating that nutrient recycling is an important ecosystem process in these tropical island streams. This same level of invertebrate nutrient recycling (i.e. supplies 70% of the demand) has been shown in desert streams as well (Grimm, 1988). However, both climate change and invasive species altered these rates drastically. Streams are important sources of nutrients to estuary and coastal systems and can alter the productivity of near-shore habitats (e.g. Ringuet & Mackenzie, 2005; Hoover & Mackenzie, 2009). Therefore, changes in nutrient availability can affect the production of algae and microbes not only in the reaches where we measured these implications, but also downstream. A future direction for this research is to determine if the measured 10-fold declines (climate change) or 10-fold increases (climate change and guppy introduction) in nutrient excretion affect downstream and near-shore productivity. The effects of anthropogenic stressors on related ecosystem processes such as primary production and leaf litter decomposition need to be studied as well.

Recent research has shown that egested material can become an important food resource for some aquatic organisms and generate sites of enhanced microbial activity, but only 7% of all consumer-mediated nutrient recycling studies report egestion (Atkinson *et al.*, 2017). To fully understand and test ecological stoichiometric predictions we need to understand both the egestion and excretion components of nutrient recycling (Vanni & McIntyre, 2016). In addition, some studies have shown that egestion rates can be as high as excretion rates (Halvorson *et al.*, 2015), indicating that egested material can be an important component in a stream food web. In chapter 4 of this dissertation we show that anthropogenic stressors like climate change can alter these egestion rates because of changes in density and size of the dominant consumers. However, we were unable to determine the nutrient content of the egesta. This is because egestion can be hard to estimate by traditional incubation and analytical methods (Vanni & McIntyre, 2016). We therefore need to develop more sensitive, standardized protocols for measuring egestion rates and obtaining the elemental composition of the egesta. Once we have established these methods, we can more fully understand how anthropogenic stressors influence nutrient recycling, the relative contribution of excretion and egestion, and further develop ecological stoichiometric theory.

6.2 Anthropogenic stressors through time

Our research shows that the effects of anthropogenic stressors are not static across time and emphasizes the importance examining stressors through time. While a time-series approach from several sites is a preferred method when making inferences about ecological processes (Damgaard, 2019), it comes at a cost of time and money, neither of

which a graduate student tends to have. Space-for-time substitutions are a great approach that maintains realism, but shortens the time frame in which we can determine the influence of an ecological process. However, space-for-time substitutions have several limitations (i.e. site and species histories can vary or are unknown, biotic and abiotic factors vary along the spatial gradient, and the spatial variability may not represent the temporal variability) that need to be addressed to ensure they are an appropriate approach (Fukami & Wardle, 2005). Our space-for-time substitution in Hawaii addressed several of these limitations (i.e. same-aged lava flow leads to similar site and species history, collected biotic and abiotic factors to ensure there is no underlying gradient, using two sampling regimes (HTR vs. HSR) to determine that the spatial variability generally represented the temporal variability), giving us confidence in our results. However, many consider that variation in time is not accurately represented by what we see in space, and therefore suggest combining space-for-time substitutions with time-series to get the most accurate inference of an ecological processes (Thomaz *et al.*, 2012; Damgaard, 2019).

Unfortunately time is running out for many ecosystems impacted by humans, and in many cases we do not have enough time to wait for the results of a time-series data in order to craft mitigation or conservation strategies. For example, the impacts of climate change are projected to become more pronounced in the next two to three decades to the point where it may become difficult to reverse these impacts (IPCC, 2014). With imminent stressors like climate change, a space-for-time substitution approach is an expedient way to generate predictions about the effect of climate change through time that can help us to develop mitigation and conservation strategies. These hypotheses can then also be tested by targeted, cost-effective monitoring strategies to generate

appropriate time series data. While we want to emphasize the value of combining the time-series and space-for-time substitution approaches, space-for-time substitutions by themselves are a good way to start evaluating potential strategies to mitigate the effects of imminent anthropogenic stressors. However, we suggest drawing conclusions from space-for-time substitutions that have been sampled across multiple years to ensure that inter-annual variability does not skew the results from this approach. We also note that space-for-time substitutions are not only useful when estimating the effects of climate change, but also for measuring other anthropogenic stressors like urbanization and pollution by using spatial gradients that mimic those changes. In addition, in recent studies space-for-time substitutions have been suggested as a valuable approach to tackle empirical measurements of multiple stressors (Kelly, 2019).

6.3 Importance of measuring multiple stressors

Mounting evidence over the last two decades suggests that the net effects of multiple interacting stressors in freshwater ecosystems can differ from the effects of individual stressors (Jackson *et al.*, 2016; Nõges *et al.*, 2016). The majority of research, however, has focused on specific anthropogenic alterations (e.g. temperature, invasive species) rather than the combined effects (Jackson *et al.*, 2016). Part of the problem is that it can be difficult to empirically measure multiple stressors and determine the mechanisms behind what drives the changes. In chapter 5 we demonstrated that an appropriate space-for-time substitution can be a useful tool to empirically measure multiple stressors. Although this study was limited in replication and scope, we hope that it demonstrates the feasibility of the approach. Part of the reason we restricted the study was to limit our

examination of invasive species to a single species (guppies) whose effects were relatively well-characterized. However, examining the interaction of climate change and multiple invasive species in Hawaii is possible, and would allow for more replication. In the future, we also suggest combining this approach with the use of mesocosms to examine the drivers and mechanisms of the effects of multiple stressors in more detail.

Researchers have called for estimating effects of more than two or three combined stressors (Craig *et al.*, 2017), yet a study Bellard *et al*. (2015) show that at least within the U.S.A., biodiversity loss is most commonly due to 1-3 cumulative stressors and more than three cumulative stressors are actually rare. Because most watersheds are exposed to several threats that exert various types and levels of alteration on different spatial and temporal scales, new and actionable science is required to better inform management strategies (Craig *et al.*, 2017). Continuing to study and manage threats in isolation can be useful in a few circumstances, but since most systems face multiple challenges, management strategies that address only one stressor will fail to serve the future health of freshwater ecosystems. It is well recognized that an improved understanding of multiple threats can improve our ability to address management challenges (Allan *et al.*, 2013; Kuehne *et al.*, 2017). Acting immediately and simultaneously on multiple indirect and direct drivers, using a variety of approaches, has the potential to slow, halt and even reverse some aspects of biodiversity and ecosystem loss (IPBES, 2019).

Bibliography

Allan J.D. & Castillo M.M. (2007). *Stream Ecology: Structure and function of running waters*. Springer Science & Business Media.

Allan J.D., McIntyre P.B., Smith S.D.P., Halpern B.S., Boyer G.L., Buchsbaum A., *et al.* (2013). Joint analysis of stressors and ecosystem services to enhance restoration effectiveness. *Proceedings of the National Academy of Sciences* **110**, 372–377. https://doi.org/10.1073/pnas.1213841110

Allgeier J.E., Wenger S.J., Rosemond A.D., Schindler D.E. & Layman C.A. (2015). Metabolic theory and taxonomic identity predict nutrient recycling in a diverse food web. *Proceedings of the National Academy of Sciences* **112**, E2640–E2647. https://doi.org/10.1073/pnas.1420819112

Amrhein V., Greenland S. & McShane B. (2019). Scientists rise up against statistical significance. *Nature* **567**, 305. https://doi.org/10.1038/d41586-019-00857-9

Arar E.J. & Collins G.B. (1997). *Method 445.0: In vitro determination of chlorophyll a and pheophytin a in marine and freshwater algae by fluorescence*. United States Environmental Protection Agency, Office of Research and Development, National Exposure Research Laboratory.

Atkinson C.L., Capps K.A., Rugenski A.T. & Vanni M.J. (2017). Consumer-driven nutrient dynamics in freshwater ecosystems: from individuals to ecosystems. *Biological Reviews* **92**, 2003–2023. https://doi.org/10.1111/brv.12318

Atkinson C.L., Golladay S.W., Opsahl S.P. & Covich A.P. (2009). Stream discharge and floodplain connections affect seston quality and stable isotopic signatures in a coastal plain stream. *Journal of the North American Benthological Society* **28**, 360–370. https://doi.org/10.1899/08-102.1

Augustine D.J. & McNaughton S.J. (2006). Interactive effects of ungulate herbivores, soil fertility, and variable rainfall on ecosystem processes in a semi-arid savanna. *Ecosystems* **9**, 1242–1256. https://doi.org/10.1007/s10021-005-0020-y

Bador M., Donat M.G., Geoffroy O. & Alexander L.V. (2018). Assessing the robustness of future extreme precipitation intensification in the CMIP5 ensemble. *Journal of Climate* **31**, 6505–6525. https://doi.org/10.1175/JCLI-D-17-0683.1

Bale J.S., Masters G.J., Hodkinson I.D., Awmack C., Bezemer T.M., Brown V.K., *et al.* (2002). Herbivory in global climate change research: direct effects of rising temperature on insect herbivores. *Global Change Biology* **8**, 1–16. https://doi.org/10.1046/j.1365-2486.2002.00451.x

Bassar R.D., Ferriere R., López-Sepulcre A., Marshall M.C., Travis J., Pringle C.M., *et al.* (2012). Direct and Indirect Ecosystem Effects of Evolutionary Adaptation in the Trinidadian Guppy (*Poecilia reticulata*). *The American Naturalist* **180**, 167–185. https://doi.org/10.1086/666611

Bassar R.D., Marshall M.C., Lopez-Sepulcre A., Zandona E., Auer S.K., Travis J., *et al.* (2010). Local adaptation in Trinidadian guppies alters ecosystem processes. *Proceedings of the National Academy of Sciences* **107**, 3616–3621. https://doi.org/10.1073/pnas.0908023107

Bassiouni M. & Oki D.S. (2013). Trends and shifts in streamflow in Hawai‘i, 1913–2008. *Hydrological Processes* **27**, 1484–1500. https://doi.org/10.1002/hyp.9298

Bates D., Maechler M., Bolker B. & Walker S. (2015). Fitting linear mixed-effects models using lme4. *Journal of Statistical Software* **67**, 1–48

Bellard C., Leclerc C. & Courchamp F. (2015). Combined impacts of global changes on biodiversity across the USA. *Scientific Reports* **5**, 11828. https://doi.org/10.1038/srep11828

Benke A.C., Huryn A.D., Smock L.A. & Wallace J.B. (1999). Length-Mass Relationships for Freshwater Macroinvertebrates in North America with Particular Reference to the Southeastern United States. *Journal of the North American Benthological Society* **18**, 308–343. https://doi.org/10.2307/1468447

Benstead J.P., Cross W.F., March J.G., McDOWELL W.H., RamíRez A. & Covich A.P. (2010). Biotic and abiotic controls on the ecosystem significance of consumer excretion in two contrasting tropical streams: N and P excretion by stream consumers. *Freshwater Biology* **55**, 2047–2061. https://doi.org/10.1111/j.1365-2427.2010.02461.x

Blois J.L., Williams J.W., Fitzpatrick M.C., Jackson S.T. & Ferrier S. (2013). Space can substitute for time in predicting climate-change effects on biodiversity. *Proceedings of the National Academy of Sciences* **110**, 9374–9379

Boersma K.S., Bogan M.T., Henrichs B.A. & Lytle D.A. (2014). Invertebrate assemblages of pools in arid-land streams have high functional redundancy and are resistant to severe drying. *Freshwater Biology* **59**, 491–501. https://doi.org/10.1111/fwb.12280

Bolker B.M., Brooks M.E., Clark C.J., Geange S.W., Poulsen J.R., Stevens M.H.H., *et al.* (2009). Generalized linear mixed models: a practical guide for ecology and evolution. *Trends in Ecology & Evolution* **24**, 127–135. https://doi.org/10.1016/j.tree.2008.10.008

Brook B.W., Sodhi N.S. & Bradshaw C.J.A. (2008). Synergies among extinction drivers under global change. *Trends in Ecology & Evolution* **23**, 453–460. https://doi.org/10.1016/j.tree.2008.03.011

Brown C.J., Saunders M.I., Possingham H.P. & Richardson A.J. (2013). Managing for Interactions between Local and Global Stressors of Ecosystems. *PLOS ONE* **8**, e65765. https://doi.org/10.1371/journal.pone.0065765

Brown J.H., Gillooly J.F., Allen A.P., Savage V.M. & West G.B. (2004). Toward a metabolic theory of ecology. *Ecology* **85**, 1771–1789

Bunn S.E. & Arthington A.H. (2002). Basic Principles and Ecological Consequences of Altered Flow Regimes for Aquatic Biodiversity. *Environmental Management* **30**, 492–507. https://doi.org/10.1007/s00267-002-2737-0

Carle F.L. & Strub M.R. (1978). A new method for estimating population size from removal. *Biometrics* **34**, 621–630

Carlson B.E. & Langkilde T. (2017). Body size variation in aquatic consumers causes pervasive community effects, independent of mean body size. *Ecology and Evolution* **7**, 9978–9990. https://doi.org/10.1002/ece3.3511

Chadwick R., Boutle I. & Martin G. (2012). Spatial Patterns of Precipitation Change in CMIP5: Why the Rich Do Not Get Richer in the Tropics. *Journal of Climate* **26**, 3803–3822. https://doi.org/10.1175/JCLI-D-12-00543.1

Christensen M.R., Graham M.D., Vinebrooke R.D., Findlay D.L., Paterson M.J. & Turner M.A. (2006). Multiple anthropogenic stressors cause ecological surprises

in boreal lakes. *Global Change Biology* **12**, 2316–2322. https://doi.org/10.1111/j.1365-2486.2006.01257.x

Chu P.-S., Chen Y.R. & Schroeder T.A. (2010). Changes in precipitation extremes in the Hawaiian Islands in a warming climate. *Journal of Climate* **23**, 4881–4900. https://doi.org/10.1175/2010JCLI3484.1

Coetsee C., Stock W.D. & Craine J.M. (2011). Do grazers alter nitrogen dynamics on grazing lawns in a South African savannah? *African Journal of Ecology* **49**, 62–69. https://doi.org/10.1111/j.1365-2028.2010.01236.x

Cohen J. (1992). Quantitative methods in psychology. *Psychological Bulletin* **112**, 155–159

Collins S.M., Thomas S.A., Heatherly T., MacNeill K.L., Leduc A.O.H.C., López-Sepulcre A., *et al.* (2016). Fish introductions and light modulate food web fluxes in tropical streams: a whole-ecosystem experimental approach. *Ecology* **97**, 3154–3166. https://doi.org/10.1002/ecy.1530

Costello D.M. & Michel M.J. (2013). Predator-induced defenses in tadpoles confound body stoichiometry predictions of the general stress paradigm. *Ecology* **94**, 2229–2236

Covino T.P., Bernhardt E.S. & Heffernan J.B. (2018). Measuring and interpreting relationships between nutrient supply, demand, and limitation. *Freshwater Science* **37**, 448–455. https://doi.org/10.1086/699202

Covino T.P., McGlynn B.L. & McNamara R.A. (2010). Tracer additions for spiraling curve characterization (TASCC): Quantifying stream nutrient uptake kinetics from ambient to saturation. *Limnology and Oceanography: Methods* **8**, 484–498

Cox D.R. & Snell E.J. (1989). *The analysis of binary data*, 2nd edn. Chapman and Hall, London, UK.

Craig L.S., Olden J.D., Arthington A.H., Entrekin S., Hawkins C.P., Kelly J.J., *et al.* (2017). Meeting the challenge of interacting threats in freshwater ecosystems: A call to scientists and managers. *Elem Sci Anth* **5**. https://doi.org/10.1525/elementa.256

Cross W.F., Benstead J.P., Rosemond A.D. & Bruce Wallace J. (2003). Consumer-resource stoichiometry in detritus-based streams. *Ecology Letters* **6**, 721–732. https://doi.org/10.1046/j.1461-0248.2003.00481.x

Dalton C.M., El-Sabaawi R.W., Honeyfield D.C., Auer S.K., Reznick D.N. & Flecker A.S. (2017). The influence of dietary and whole-body nutrient content on the excretion of a vertebrate consumer. *PLOS ONE* **12**, e0187931. https://doi.org/10.1371/journal.pone.0187931

Damgaard C. (2019). A Critique of the Space-for-Time Substitution Practice in Community Ecology. *Trends in Ecology & Evolution* **34**, 416–421. https://doi.org/10.1016/j.tree.2019.01.013

De Laender F., Rohr J.R., Ashauer R., Baird D.J., Berger U., Eisenhauer N., *et al.* (2016). Reintroducing environmental change drivers in biodiversity–ecosystem functioning research. *Trends in Ecology & Evolution* **31**, 905–915. https://doi.org/10.1016/j.tree.2016.09.007

Deacon A.E., Ramnarine I.W. & Magurran A.E. (2011). How reproductive ecology contributes to the spread of a globally invasive fish. *PLoS ONE* **6**, e24416. https://doi.org/10.1371/journal.pone.0024416

Demi L.M., Benstead J.P., Rosemond A.D. & Maerz J.C. (2018). Litter P content drives consumer production in detritus-based streams spanning an experimental N:P gradient. *Ecology* **99**, 347–359. https://doi.org/10.1002/ecy.2118

Denley D., Metaxas A. & Fennel K. (2019). Community composition influences the population growth and ecological impact of invasive species in response to climate change. *Oecologia*. https://doi.org/10.1007/s00442-018-04334-4

Denning D.G. & Beardsley J.W. (1967). The collection of Cheumatopsyche analis in Hawaii (Trichoptera: Hydropsychidae). *Proceedings of the Entomological Society of Washington* **69**, 56–57

Diffenbaugh N.S. & Giorgi F. (2012). Climate change hotspots in the CMIP5 global climate model ensemble. *Climatic Change* **114**, 813–822. https://doi.org/10.1007/s10584-012-0570-x

Dodds W.K., Martí E., Tank J.L., Pontius J., Hamilton S.K., Grimm N.B., *et al.* (2004). Carbon and nitrogen stoichiometry and nitrogen cycling rates in streams. *Oecologia* **140**, 458–467. https://doi.org/10.1007/s00442-004-1599-y

Donat M.G., Lowry A.L., Alexander L.V., O'Gorman P.A. & Maher N. (2017). Addendum: More extreme precipitation in the world's dry and wet regions. *Nature Climate Change* **7**, 154–158. https://doi.org/10.1038/nclimate3160

Donat M.G., Lowry A.L., Alexander L.V., O'Gorman P.A. & Maher N. (2016). More extreme precipitation in the world's dry and wet regions. *Nature Climate Change* **6**, 508–513. https://doi.org/10.1038/nclimate2941

Downing J.A., Mcclain M., Twilley R., Melack J.M., Elser J., Rabalais N.N., *et al.* (1999). The impact of accelerating land-use change on the N-Cycle of tropical aquatic ecosystems: Current conditions and projected changes. *Biogeochemistry* **46**, 109–148. https://doi.org/10.1007/BF01007576

Dudgeon D. (2014). Threats to freshwater biodiversity in a changing world. In: *Global Environmental Change*. (Ed. B. Freedman), pp. 243–253. Springer Netherlands, Dordrecht.

Dudgeon D. (2011). *Tropical stream ecology*. Elsevier.

Dudgeon D., Arthington A.H., Gessner M.O., Kawabata Z.-I., Knowler D.J., Lévêque C., *et al.* (2006). Freshwater biodiversity: importance, threats, status and conservation challenges. *Biological Reviews* **81**, 163. https://doi.org/10.1017/S1464793105006950

Durlak J.A. (2009). How to Select, Calculate, and Interpret Effect Sizes. *Journal of Pediatric Psychology* **34**, 917–928. https://doi.org/10.1093/jpepsy/jsp004

Eady B.R., Hill T.R. & Rivers-Moore N.A. (2014). Shifts in aquatic macroinvertebrate community structure in response to perenniality, southern Cape, South Africa. *Journal of Freshwater Ecology* **29**, 475–490. https://doi.org/10.1080/02705060.2014.910146

Elison-Timm O., Giambelluca T.W. & Diaz H.F. (2015). Statistical downscaling of rainfall changes in Hawai'i based on the CMIP5 global model projections: Downscaled Rainfall Changes in Hawai'i. *Journal of Geophysical Research: Atmospheres* **120**, 92–112. https://doi.org/10.1002/2014JD022059

Ellner S.P., Geber M.A. & Hairston N.G. (2011). Does rapid evolution matter? Measuring the rate of contemporary evolution and its impacts on ecological

dynamics. *Ecology Letters* **14**, 603–614. https://doi.org/10.1111/j.1461-0248.2011.01616.x

El-Sabaawi R.W. (2017). How fishes can help us answer important questions about the ecological consequences of evolution. *Copeia* **105**, 558–568. https://doi.org/10.1643/OT-16-530

El-Sabaawi R.W., Frauendorf T.C., Marques P.S., Mackenzie R.A., Manna L.R., Mazzoni R., *et al.* (2016). Biodiversity and ecosystem risks arising from using guppies to control mosquitoes. *Biology Letters* **12**, 20160590. https://doi.org/10.1098/rsbl.2016.0590

El-Sabaawi R.W., Kohler T.J., Zandoná E., Travis J., Marshall M.C., Thomas S.A., *et al.* (2012a). Environmental and organismal predictors of intraspecific variation in the stoichiometry of a neotropical freshwater fish. *PLoS ONE* **7**, e32713. https://doi.org/10.1371/journal.pone.0032713

El-Sabaawi R.W., Marshall M.C., Bassar R.D., López-Sepulcre A., Palkovacs E.P. & Dalton C. (2015). Assessing the effects of guppy life history evolution on nutrient recycling: from experiments to the field. *Freshwater Biology* **60**, 590–601. https://doi.org/10.1111/fwb.12507

El-Sabaawi R.W., Zandonà E., Kohler T.J., Marshall M.C., Moslemi J.M., Travis J., *et al.* (2012b). Widespread intraspecific organismal stoichiometry among populations of the Trinidadian guppy: evolutionary ecology of organismal stoichiometry. *Functional Ecology* **26**, 666–676. https://doi.org/10.1111/j.1365-2435.2012.01974.x

Elser J.J., Dobberfuhl D.R., MacKay N.A. & Schampel J.H. (1996). Organism size, life history, and N:P stoichiometry. *BioScience* **46**, 674–684. https://doi.org/10.2307/1312897

Feld C.K. & Hering D. (2007). Community structure or function: effects of environmental stress on benthic macroinvertebrates at different spatial scales. *Freshwater Biology* **52**, 1380–1399. https://doi.org/10.1111/j.1365-2427.2007.01749.x

Fox J.W. (2006). Using the Price equation to partition the effects of biodiversity loss on ecosystem function. *Ecology* **87**, 2687–2696

Fox J.W. & Harpole W.S. (2008). Revealing how species loss affects ecosystem function: The trait-based Price equation partition. *Ecology* **89**, 269–279. https://doi.org/10.1890/07-0288.1

Fox J.W. & Kerr B. (2012). Analyzing the effects of species gain and loss on ecosystem function using the extended Price equation partition. *Oikos* **121**, 290–298. https://doi.org/10.1111/j.1600-0706.2011.19656.x

Frauendorf T.C., MacKenzie R.A., Tingley R.W., Frazier A.G., Riney M.H. & El-Sabaawi R.W. (2019). Evaluating ecosystem effects of climate change on tropical island streams using high spatial and temporal resolution sampling regimes. *Global Change Biology* **25**, 1344–1357. https://doi.org/10.1111/gcb.14584

Frazier A.G. & Giambelluca T.W. (2017). Spatial trend analysis of Hawaiian rainfall from 1920 to 2012. *International Journal of Climatology* **37**, 2522–2531. https://doi.org/10.1002/joc.4862

Frazier A.G., Giambelluca T.W., Diaz H.F. & Needham H.L. (2016). Comparison of geostatistical approaches to spatially interpolate month-year rainfall for the

Hawaiian Islands. *International Journal of Climatology* **36**, 1459–1470. https://doi.org/10.1002/joc.4437

Fritschie K.J. & Olden J.D. (2016). Disentangling the influences of mean body size and size structure on ecosystem functioning: an example of nutrient recycling by a non-native crayfish. *Ecology and Evolution* **6**, 159–169. https://doi.org/10.1002/ece3.1852

Fritschie K.J. & Olden J.D. (2018). Estimating the effects of non-native species on nutrient recycling using species-specific and general allometric models. *Freshwater Biology* **63**, 539–552. https://doi.org/10.1111/fwb.13092

Fukami T. & Wardle D.A. (2005). Long-term ecological dynamics: reciprocal insights from natural and anthropogenic gradients. *Proceedings of the Royal Society of London B: Biological Sciences* **272**, 2105–2115. https://doi.org/10.1098/rspb.2005.3277

Gallardo B., Clavero M., Sánchez M.I. & Vilà M. (2016). Global ecological impacts of invasive species in aquatic ecosystems. *Global Change Biology* **22**, 151–163. https://doi.org/10.1111/gcb.13004

Ghalambor C.K., Hoke K.L., Ruell E.W., Fischer E.K., Reznick D.N. & Hughes K.A. (2015). Non-adaptive plasticity potentiates rapid adaptive evolution of gene expression in nature. *Nature* **525**, 372–375. https://doi.org/10.1038/nature15256

Giambelluca T.W., Chen Q., Frazier A.G., Price J.P., Chen Y.-L., Chu P.-S., *et al.* (2013). Online Rainfall Atlas of Hawai'i. *Bulletin of the American Meteorological Society* **94**, 313–316. https://doi.org/10.1175/BAMS-D-11-00228.1

Glazier D.S. (2005). Beyond the "3/4 power law": variation in the intra- and interspecific scaling of metabolic rate in animals. *Biological Reviews* **80**, 611–662. https://doi.org/10.1017/S1464793105006834

Gonzalez A., Cardinale B.J., Allington G.R.H., Byrnes J., Endsley K.A., Brown D.G., *et al.* (2016). Estimating local biodiversity change: a critique of papers claiming no net loss of local diversity. *Ecology* **97**, 1949–1960. https://doi.org/10.1890/15-1759.1

Gorbach K.R., Shoda M.E., Burky A.J. & Benbow M.E. (2014). Benthic community responses to water removal in tropical mountain streams. *River Research and Applications* **30**, 791–803. https://doi.org/10.1002/rra.2679

Griffiths N.A. & Hill W.R. (2014). Temporal variation in the importance of a dominant consumer to stream nutrient cycling. *Ecosystems* **17**, 1169–1185. https://doi.org/10.1007/s10021-014-9785-1

Grimm N.B. (1988). Role of macroinvertebrates in nitrogen dynamics of a desert stream. *Ecology* **69**, 1884–1893. https://doi.org/10.2307/1941165

Grömping U. (2006). Relative importance for linear regression in R: The package relaimpo. *Journal of Statistical Software* **17**, 1–27

Grossiord C., Granier A., Gessler A., Scherer-Lorenzen M., Pollastrini M. & Bonal D. (2013). Application of Loreau & Hector's (2001) partitioning method to complex functional traits. *Methods in Ecology and Evolution* **4**, 954–960. https://doi.org/10.1111/2041-210X.12090

Gutiérrez-Fonseca P.E., Ramírez A. & Pringle C.M. (2018). Large-scale climatic phenomena drive fluctuations in macroinvertebrate assemblages in lowland tropical streams, Costa Rica: The importance of ENSO events in determining

long-term (15y) patterns. *PLOS ONE* **13**, e0191781. https://doi.org/10.1371/journal.pone.0191781

Haase P., Pilotto F., Li F., Sundermann A., Lorenz A.W., Tonkin J.D., *et al.* (2019). Moderate warming over the past 25 years has already reorganized stream invertebrate communities. *Science of The Total Environment* **658**, 1531–1538. https://doi.org/10.1016/j.scitotenv.2018.12.234

Halvorson H.M., Fuller C., Entrekin S.A. & Evans-White M.A. (2015). Dietary influences on production, stoichiometry and decomposition of particulate wastes from shredders. *Freshwater Biology* **60**, 466–478. https://doi.org/10.1111/fwb.12462

Hamby D.M. (1994). A review of techniques for parameter sensitivity analysis of environmental models. *Environmental Monitoring and Assessment* **32**, 135–154. https://doi.org/10.1007/BF00547132

Handelsman C.A., Broder E.D., Dalton C.M., Ruell E.W., Myrick C.A., Reznick D.N., *et al.* (2013). Predator-induced phenotypic plasticity in metabolism and rate of growth: rapid adaptation to a novel environment. *Integrative and Comparative Biology* **53**, 975–988. https://doi.org/10.1093/icb/ict057

Hauer F.R. & Lamberti G.A. (2011). *Methods in Stream Ecology*. Academic Press.

Hedges L.V. & Olkin I. (2014). *Statistical Methods for Meta-Analysis*. Academic Press.

Heino J., Virkkala R. & Toivonen H. (2009). Climate change and freshwater biodiversity: detected patterns, future trends and adaptations in northern regions. *Biological Reviews* **84**, 39–54. https://doi.org/10.1111/j.1469-185X.2008.00060.x

Hendry A.P. (2016). *Eco-evolutionary Dynamics*. Princeton University Press, Princeton.

Holitzki T.M., MacKenzie R.A., Wiegner T.N. & McDermid K.J. (2013). Differences in ecological structure, function, and native species abundance between native and invaded Hawaiian streams. *Ecological Applications* **23**, 1367–1383

Holmes R.M., Aminot A., Kérouel R., Hooker B.A. & Peterson B.J. (1999). A simple and precise method for measuring ammonium in marine and freshwater ecosystems. *Canadian Journal of Fisheries and Aquatic Sciences* **56**, 1801–1808. https://doi.org/10.1139/f99-128

Hooper D.U., Adair E.C., Cardinale B.J., Byrnes J.E.K., Hungate B.A., Matulich K.L., *et al.* (2012). A global synthesis reveals biodiversity loss as a major driver of ecosystem change. *Nature* **486**, 105–108. https://doi.org/10.1038/nature11118

Hoover D.J. & Mackenzie F.T. (2009). Fluvial fluxes of water, suspended particulate matter, and nutrients and potential impacts on tropical coastal water biogeochemistry: Oahu, Hawai'i. *Aquatic Geochemistry* **15**, 547–570. https://doi.org/10.1007/s10498-009-9067-2

Hughes F., Asner G.P., Litton C.M., Selmants P.C., Hawbaker T.J., Jacobi J.D., *et al.* (2017). Influence of invasive species on carbon storage in Hawai 'i's ecosystems. In: *Influence of invasive species on carbon storage in Hawai 'i's ecosystems Baseline and projected future carbon storage and carbon fluxes in ecosystems of Hawai'i*. (Eds P.C. Selmants, C.P. Giardina, J.D. Jacobi & Z. Zhu), pp. 43–55. US Department of the Interior, US Geological Survey Professional Paper 1834, Reston, VA.

IPBES (2019). *Global Assessment Summary for Policymakers*. (Eds S. Díaz, J. Settele, E. Brondízio, H.T. Ngo & M. Guéze),.

IPCC (2013). *Climate Change 2013: The Physical Science Basis: Working Group I Contribution to the Fifth Assessment Report of the Intergovernmental Panel on Climate Change*. (Eds T.F. Stocker, D. Qin, G.K. Plattner, M. Tignor, S.K. Allen, J. Boschung, et al.), Cambridge University Press.

IPCC (2014). *IPCC, 2014: Climate Change 2014: Synthesis Report. Contribution of Working Groups I, II and III to the Fifth Assessment Report of the Intergovernmental Panel on Climate Change*. (Eds Core Writing Team, R.K. Pachauri & L.A. Meyer), Cambridge University Press, IPCC, Geneva, Switzerland.

IPCC (2012). *Managing the Risks of Extreme Events and Disasters to Advance Climate Change Adaptation: Special Report of the Intergovernmental Panel on Climate Change*. (Eds C.B. Field, V. Barros, T.F. Stocker, D. Qin, D.J. Dokken, K.L. Ebi, et al.), Cambridge University Press.

Isbell F., Gonzalez A., Loreau M., Cowles J., Díaz S., Hector A., *et al.* (2017). Linking the influence and dependence of people on biodiversity across scales. *Nature* **546**, 65–72. https://doi.org/10.1038/nature22899

Jackman S. (2017). *pscl: Classes and methods for R developed in the political science computational laboratory*.

Jackson M.C., Evangelista C., Zhao T., Lecerf A., Britton J.R. & Cucherousset J. (2017). Between-lake variation in the trophic ecology of an invasive crayfish. *Freshwater Biology* **62**, 1501–1510. https://doi.org/10.1111/fwb.12957

Jackson M.C., Loewen C.J.G., Vinebrooke R.D. & Chimimba C.T. (2016). Net effects of multiple stressors in freshwater ecosystems: a meta-analysis. *Global Change Biology* **22**, 180–189. https://doi.org/10.1111/gcb.13028

Jansson R., Nilsson C. & Malmqvist B. (2007). Restoring freshwater ecosystems in riverine landscapes: the roles of connectivity and recovery processes. *Freshwater Biology* **52**, 589–596. https://doi.org/10.1111/j.1365-2427.2007.01737.x

Jardine T.D., Bond N.R., Burford M.A., Kennard M.J., Ward D.P., Bayliss P., *et al.* (2015). Does flood rhythm drive ecosystem responses in tropical riverscapes? *Ecology* **96**, 684–692. https://doi.org/10.1890/14-0991.1

Jenkins M. (2003). Prospects for Biodiversity. *Science* **302**, 1175–1177. https://doi.org/10.1126/science.1088666

Jochum M., Barnes A.D., Ott D., Lang B., Klarner B., Farajallah A., *et al.* (2017). Decreasing Stoichiometric Resource Quality Drives Compensatory Feeding across Trophic Levels in Tropical Litter Invertebrate Communities. *The American Naturalist* **190**, 131–143. https://doi.org/10.1086/691790

Johnson E.A. & Miyanishi K. (2008). Testing the assumptions of chronosequences in succession. *Ecology Letters* **11**, 419–431. https://doi.org/10.1111/j.1461-0248.2008.01173.x

Jones J.B. (1997). Benthic organic matter storage in streams: influence of detrital import and export, retention mechanisms, and climate. *Journal of the North American Benthological Society* **16**, 109–119

Joyce P., Warren L.L. & Wotton R.S. (2007). Faecal pellets in streams: their binding, breakdown and utilization. *Freshwater Biology* **52**, 1868–1880. https://doi.org/10.1111/j.1365-2427.2007.01828.x

Kakouei K., Kiesel J., Domisch S., Irving K.S., Jähnig S.C. & Kail J. (2018). Projected effects of Climate-change-induced flow alterations on stream macroinvertebrate abundances. *Ecology and Evolution* **8**, 3393–3409. https://doi.org/10.1002/ece3.3907

Kelly M. (2019). Adaptation to climate change through genetic accommodation and assimilation of plastic phenotypes. *Philosophical Transactions of the Royal Society B: Biological Sciences* **374**, 20180176. https://doi.org/10.1098/rstb.2018.0176

Kent C., Chadwick R. & Rowell D.P. (2015). Understanding Uncertainties in Future Projections of Seasonal Tropical Precipitation. *Journal of Climate* **28**, 4390–4413. https://doi.org/10.1175/JCLI-D-14-00613.1

Khalyani A.H., Gould W.A., Harmsen E., Terando A., Quinones M. & Collazo J.A. (2015). Climate Change implications for tropical islands: Interpolating and interpreting statistically downscaled GCM projections for management and planning. *Journal of Applied Meteorology and Climatology* **55**, 265–282. https://doi.org/10.1175/JAMC-D-15-0182.1

Kohler T.J., Heatherly T.N., El-Sabaawi R.W., Zandonà E., Marshall M.C., Flecker A.S., *et al.* (2012). Flow, nutrients, and light availability influence Neotropical epilithon biomass and stoichiometry. *Freshwater Science* **31**, 1019–1034. https://doi.org/10.1899/11-141.1

Kondratieff B.C., Bishop R.J. & Brasher A.M. (1997). The life cycle of an introduced caddisfly, Cheumatopsyche pettiti (Banks) (Trichoptera: Hydropsychidae) in Waikolu Stream, Molokai, Hawaii. *Hydrobiologia* **350**, 81–85. https://doi.org/10.1023/A:1003023529064

Kuehne L.M., Olden J.D., Strecker A.L., Lawler J.J. & Theobald D.M. (2017). Past, present, and future of ecological integrity assessment for fresh waters. *Frontiers in Ecology and the Environment* **15**, 197–205. https://doi.org/10.1002/fee.1483

Kusumawathie P.H.D., Wickremasinghe A.R., Karunaweera N.D. & Wijeyaratne M.J.S. (2008). Costs and effectiveness of application of Poecilia reticulata (guppy) and temephos in anopheline mosquito control in river basins below the major dams of Sri Lanka. *Transactions of the Royal Society of Tropical Medicine and Hygiene* **102**, 705–711. https://doi.org/10.1016/j.trstmh.2008.03.013

Larson E.I., Poff N.L., Atkinson C.L. & Flecker A.S. (2018). Extreme flooding decreases stream consumer autochthony by increasing detrital resource availability. *Freshwater Biology* **63**, 1483–1497. https://doi.org/10.1111/fwb.13177

Lauer A., Zhang C., Elison-Timm O., Wang Y. & Hamilton K. (2013). Downscaling of climate change in the Hawaii region using CMIP5 results: on the choice of the forcing fields. *Journal of Climate* **26**, 10006–10030. https://doi.org/10.1175/JCLI-D-13-00126.1

Lefcheck J.S., Byrnes J.E.K., Isbell F., Gamfeldt L., Griffin J.N., Eisenhauer N., *et al.* (2015). Biodiversity enhances ecosystem multifunctionality across trophic levels and habitats. *Nature Communications* **6**, 6936. https://doi.org/10.1038/ncomms7936

Lehmann J., Coumou D. & Frieler K. (2015). Increased record-breaking precipitation events under global warming. *Climatic Change* **132**, 501–515. https://doi.org/10.1007/s10584-015-1434-y

Lester R.E., Close P.G., Barton J.L., Pope A.J. & Brown S.C. (2014). Predicting the likely response of data-poor ecosystems to climate change using space-for-time substitution across domains. *Global Change Biology* **20**, 3471–3481. https://doi.org/10.1111/gcb.12634

Liu H. & Stiling P. (2006). Testing the enemy release hypothesis: a review and meta-analysis. *Biological Invasions* **8**, 1535–1545. https://doi.org/10.1007/s10530-005-5845-y

Loeb C. (1981). An in situ method for measuring the primary productivity and standing crop of the epilithic periphyton community in lentic systems. *Limnology and Oceanography* **26**, 394–399

Longman R.J., Frazier A.G., Newman A.J., Giambelluca T.W., Schanzenbach D., Kagawa-Viviani A., *et al.* (2019). High-Resolution Gridded Daily Rainfall and Temperature for the Hawaiian Islands (1990–2014). *Journal of Hydrometeorology* **20**, 489–508. https://doi.org/10.1175/JHM-D-18-0112.1

Loreau M. & Hector A. (2001). Partitioning selection and complementarity in biodiversity experiments. *Nature* **412**, 72–76. https://doi.org/10.1038/35083573

Lytle D.A. & Poff N.L. (2004). Adaptation to natural flow regimes. *Trends in Ecology & Evolution* **19**, 94–100. https://doi.org/10.1016/j.tree.2003.10.002

MacKenzie R.A., Wiegner T.N., Kinslow F., Cormier N. & Strauch A.M. (2013). Leaf-litter inputs from an invasive nitrogen-fixing tree influence organic-matter dynamics and nitrogen inputs in a Hawaiian river. *Freshwater Science* **32**, 1036–1052. https://doi.org/10.1899/12-152.1

Magurran A.E. (2005). *Evolutionary Ecology: The Trinidadian Guppy*. Oxford University Press.

Magurran A.E. (2009). Threats to Freshwater Fish. *Science* **325**, 1215–1216. https://doi.org/10.1126/science.1177215

Manly B.F.J. (2006). *Randomization, Bootstrap and Monte Carlo Methods in Biology*, Third. Chapman and Hall/CRC.

McGlinn D.J., Xiao X., May F., Gotelli N.J., Engel T., Blowes S.A., *et al.* (2019). Measurement of Biodiversity (MoB): A method to separate the scale-dependent effects of species abundance distribution, density, and aggregation on diversity change. *Methods in Ecology and Evolution* **10**, 258–269. https://doi.org/10.1111/2041-210X.13102

McIntosh M.D., Schmitz J.A., Benbow M.E. & Burky A.J. (2008). Structural and functional changes of tropical riffle macroinvertebrate communities associated with stream flow withdrawal. *River Research and Applications* **24**, 1045–1055. https://doi.org/10.1002/rra.1104

McIntyre P.B., Flecker A.S., Vanni M.J., Hood J.M., Taylor B.W. & Thomas S.A. (2008). Fish distributions and nutrient cycling in streams: can fish create biogeochemical hotspots? *Ecology* **89**, 2335–2346

Moore J.W. & Olden J.D. (2017). Response diversity, nonnative species, and disassembly rules buffer freshwater ecosystem processes from anthropogenic change. *Global Change Biology* **23**, 1871–1880. https://doi.org/10.1111/gcb.13536

Mora C., Frazier A.G., Longman R.J., Dacks R.S., Walton M.M., Tong E.J., *et al.* (2013). The projected timing of climate departure from recent variability. *Nature* **502**, 183–187. https://doi.org/10.1038/nature12540

Moser D., Lenzner B., Weigelt P., Dawson W., Kreft H., Pergl J., *et al.* (2018). Remoteness promotes biological invasions on islands worldwide. *Proceedings of the National Academy of Sciences* **115**, 9270–9275. https://doi.org/10.1073/pnas.1804179115

Neres-Lima V., Brito E.F., Krsulović F.A.M., Detweiler A.M., Hershey A.E. & Moulton T.P. (2016). High importance of autochthonous basal food source for the food web of a Brazilian tropical stream regardless of shading. *International Review of Hydrobiology* **101**, 132–142. https://doi.org/10.1002/iroh.201601851

NOAA (2017). *Media Advisory: Wet Season Rainfall Outlook for the State of Hawaii*. National Oceanic and Atmospheric Administration, Honolulu, USA.

Nõges P., Argillier C., Borja Á., Garmendia J.M., Hanganu J., Kodeš V., *et al.* (2016). Quantified biotic and abiotic responses to multiple stress in freshwater, marine and ground waters. *Science of The Total Environment* **540**, 43–52. https://doi.org/10.1016/j.scitotenv.2015.06.045

Northington R.M. & Webster J.R. (2017). Experimental reductions in stream flow alter litter processing and consumer subsidies in headwater streams. *Freshwater Biology* **62**, 737–750. https://doi.org/10.1111/fwb.12898

Ogle D.H., Wheeler P. & Dinno A. (2018). *FSA: Fisheries Stock Analysis*.

Ohlberger J., Buehrens T.W., Brenkman S.J., Crain P., Quinn T.P. & Hilborn R. (2018). Effects of past and projected river discharge variability on freshwater production in an anadromous fish. *Freshwater Biology* **63**, 331–340. https://doi.org/10.1111/fwb.13070

Oksanen J., Blanchet F.G., Friendly M., Kindt R., Legendre P., McGlinn D., *et al.* (2017). *vegan: Community Ecology Package*.

Parsons T.R., Maita Y. & Lalli C.M. (1984). *A Manual of chemical and biological methods for seawater analysis*, First. Pergamon Press Ltd., Great Britain.

Patrick C.J., McGarvey D.J., Larson J.H., Cross W.F., Allen D.C., Benke A.C., *et al.* (2019). Precipitation and temperature drive continental-scale patterns in stream invertebrate production. *Science Advances* **5**, eaav2348. https://doi.org/10.1126/sciadv.aav2348

Piggott J.J., Townsend C.R. & Matthaei C.D. (2015). Reconceptualizing synergism and antagonism among multiple stressors. *Ecology and Evolution* **5**, 1538–1547. https://doi.org/10.1002/ece3.1465

Poff N.L., Allan J.D., Bain M.B., Karr J.R., Prestegaard K.L., Richter B.D., *et al.* (1997). The natural flow regime. *BioScience* **47**, 769–784

Poff N.L., Larson E.I., Salerno P.E., Morton S.G., Kondratieff B.C., Flecker A.S., *et al.* (2018). Extreme streams: species persistence and genomic change in montane insect populations across a flooding gradient. *Ecology Letters* **21**, 525–535. https://doi.org/10.1111/ele.12918

Poff N.L. & Ward J.V. (1989). Implications of streamflow variability and predictability for lotic community structure: a regional analysis of streamflow patterns. *Canadian Journal of Fisheries and Aquatic Sciences* **46**, 1805–1818. https://doi.org/10.1139/f89-228

Polato N.R., Gill B.A., Shah A.A., Gray M.M., Casner K.L., Barthelet A., *et al.* (2018). Narrow thermal tolerance and low dispersal drive higher speciation in tropical

mountains. *Proceedings of the National Academy of Sciences* **115**, 12471-12476. https://doi.org/10.1073/pnas.1809326115

Povak N.A., Hessburg P.F., Giardina C.P., Reynolds K.M., Heider C., Salminen E., *et al.* (2017). A watershed decision support tool for managing invasive species on Hawai‘i Island, USA. *Forest Ecology and Management* **400**, 300–320. https://doi.org/10.1016/j.foreco.2017.05.046

Price G.R. (1972). Extension of covariance selection mathematics. *Annals of Human Genetics* **35**, 485–490. https://doi.org/10.1111/j.1469-1809.1957.tb01874.x

Price G.R. (1970). Selection and covariance. *Nature* **227**, 520–521

Pyne M.I. & Poff N.L. (2017). Vulnerability of stream community composition and function to projected thermal warming and hydrologic change across ecoregions in the western United States. *Global Change Biology* **23**, 77–93. https://doi.org/10.1111/gcb.13437

Pyrce R. (2004). *Hydrological low flow indices and their uses*. Watershed Science Centre.

Rahel F.J. & Olden J.D. (2008). Assessing the Effects of Climate Change on Aquatic Invasive Species. *Conservation Biology* **22**, 521–533. https://doi.org/10.1111/j.1523-1739.2008.00950.x

Rauscher S.A., Kucharski F. & Enfield D.B. (2010). The role of regional SST warming variations in the drying of Meso-America in future climate projections. *Journal of Climate* **24**, 2003–2016. https://doi.org/10.1175/2010JCLI3536.1

Rempel L.L., Richardson J.S. & Healey M.C. (2000). Macroinvertebrate community structure along gradients of hydraulic and sedimentary conditions in a large gravel-bed river. *Freshwater Biology* **45**, 57–73. https://doi.org/10.1046/j.1365-2427.2000.00617.x

Reznick D., Butler IV M.J. & Rodd H. (2001). Life-history evolution in guppies. VII. The comparative ecology of high-and low-predation environments. *The American Naturalist* **157**, 126–140

Reznick D.N., Bassar R.D., Travis J. & Helen Rodd F. (2012). Life-history evolution in guppies viii: the demographics of density regulation in guppies (*Poecilia reticulata*). *Evolution* **66**, 2903–2915. https://doi.org/10.1111/j.1558-5646.2012.01650.x

Reznick D.N., Shaw F.H., Rodd F.H. & Shaw R.G. (1997). Evaluation of the rate of evolution in natural populations of guppies (*Poecilia reticulata*). *Science* **275**, 1934–1937. https://doi.org/10.1126/science.275.5308.1934

Ricciardi A. (2007). Are modern biological invasions an unprecedented form of global change? *Conservation Biology* **21**, 329–336. https://doi.org/10.1111/j.1523-1739.2006.00615.x

Ricciardi A., Hoopes M.F., Marchetti M.P. & Lockwood J.L. (2013). Progress toward understanding the ecological impacts of nonnative species. *Ecological Monographs* **83**, 263–282

Riney M. (2015). *The impacts of stream flow rates on food resource quality and diets of native endemic atyid shrimps (Atyoida bisulcata) in Hawaiian streams*. University of Hawaii at Hilo, Hilo, Hawaii, USA.

Ringuet S. & Mackenzie F.T. (2005). Controls on nutrient and phytoplankton dynamics during normal flow and storm runoff conditions, southern Kaneohe Bay, Hawaii. *Estuaries* **28**, 327–337

Rolls R.J., Hayden B. & Kahilainen K.K. (2017). Conceptualising the interactive effects of climate change and biological invasions on subarctic freshwater fish. *Ecology and Evolution* **7**, 4109–4128. https://doi.org/10.1002/ece3.2982

Rosenblatt A.E. & Schmitz O.J. (2014). Interactive effects of multiple climate change variables on trophic interactions: a meta-analysis. *Climate Change Responses* **1**, 8. https://doi.org/10.1186/s40665-014-0008-y

Rudolf V.H.W. & Rasmussen N.L. (2013). Population structure determines functional differences among species and ecosystem processes. *Nature Communications* **4**, 2318. https://doi.org/10.1038/ncomms3318

Salas M. & Dudgeon D. (2003). Life histories, production dynamics and resource utilization of mayflies (Ephemeroptera) in two tropical Asian forest streams. *Freshwater Biology* **48**, 485–499

Sarremejane R., Mykrä H., Huttunen K.-L., Mustonen K.-R., Marttila H., Paavola R., *et al.* (2018). Climate-driven hydrological variability determines inter-annual changes in stream invertebrate community assembly. *Oikos* **127**, 1586–1595. https://doi.org/10.1111/oik.05329

Scholl E.A., Rantala H.M., Whiles M.R. & Wilkerson G.V. (2016). Influence of Flow on Community Structure and Production of Snag-Dwelling Macroinvertebrates in an Impaired Low-Gradient River. *River Research and Applications* **32**, 677–688. https://doi.org/10.1002/rra.2882

Seddon A.W.R., Macias-Fauria M., Long P.R., Benz D. & Willis K.J. (2016). Sensitivity of global terrestrial ecosystems to climate variability. *Nature* **531**, 229. https://doi.org/10.1038/nature16986

Small G.E. & Pringle C.M. (2009). Deviation from strict homeostasis across multiple trophic levels in an invertebrate consumer assemblage exposed to high chronic phosphorus enrichment in a Neotropical stream. *Oecologia* **162**, 581–590. https://doi.org/10.1007/s00442-009-1489-4

Sterner R.W. & Elser J.J. (2002). *Ecological Stoichiometry: The Biology of Elements from Molecules to the Biosphere*. Princeton University Press.

Stoks R., Geerts A.N. & Meester L.D. (2014). Evolutionary and plastic responses of freshwater invertebrates to climate change: realized patterns and future potential. *Evolutionary Applications* **7**, 42–55. https://doi.org/10.1111/eva.12108

Strauch A.M., Giardina C.P., MacKenzie R.A., Heider C., Giambelluca T.W., Salminen E., *et al.* (2017). Modeled Effects of Climate Change and Plant Invasion on Watershed Function Across a Steep Tropical Rainfall Gradient. *Ecosystems* **20**, 583–600. https://doi.org/10.1007/s10021-016-0038-3

Strauch A.M., Mackenzie R.A., Bruland G.L., Tingley R. & Giardina C.P. (2014). Climate change and land use drivers of fecal bacteria in tropical Hawaiian rivers. *Journal of Environment Quality* **43**, 1475. https://doi.org/10.2134/jeq2014.01.0025

Strauch A.M., MacKenzie R.A., Giardina C.P. & Bruland G.L. (2015). Climate driven changes to rainfall and streamflow patterns in a model tropical island hydrological

system. *Journal of Hydrology* **523**, 160–169. https://doi.org/10.1016/j.jhydrol.2015.01.045

Strauch A.M., MacKenzie R.A., Giardina C.P. & Bruland G.L. (2018). Influence of declining mean annual rainfall on the behavior and yield of sediment and particulate organic carbon from tropical watersheds. *Geomorphology* **306**, 28–39. https://doi.org/10.1016/j.geomorph.2017.12.030

Strayer D.L. (2012). Eight questions about invasions and ecosystem functioning. *Ecology Letters* **15**, 1199–1210. https://doi.org/10.1111/j.1461-0248.2012.01817.x

Strayer D.L. & Dudgeon D. (2010). Freshwater biodiversity conservation: recent progress and future challenges. *Journal of the North American Benthological Society* **29**, 344–358. https://doi.org/10.1899/08-171.1

Strickland J.D.H. & Parsons T.R. (1972). *A practical handbook of seawater analysis*, Second. Fisheries Research Board of Canada, Ottawa.

Taylor B.W., Keep C.F., Hall R.O., Koch B.J., Tronstad L.M., Flecker A.S., *et al.* (2007). Improving the fluorometric ammonium method: matrix effects, background fluorescence, and standard additions. *Journal of the North American Benthological Society* **26**, 167–177. https://doi.org/10.1899/0887-3593(2007)26[167:ITFAMM]2.0.CO;2

Thomaz S.M., Agostinho A.A., Gomes L.C., Silveira M.J., Rejmánek M., Aslan C.E., *et al.* (2012). Using space-for-time substitution and time sequence approaches in invasion ecology. *Freshwater Biology* **57**, 2401–2410. https://doi.org/10.1111/fwb.12005

Thomsen M.S., Olden J.D., Wernberg T., Griffin J.N. & Silliman B.R. (2011). A broad framework to organize and compare ecological invasion impacts. *Environmental Research* **111**, 899–908. https://doi.org/10.1016/j.envres.2011.05.024

Tingley III R.W. (2017). *Conserving streams with changing climate: a multi-scaled research framework to consider current and future condition of Hawaiian stream habitats*. Michigan State University, East Lansing, MI.

Torchiano M. (2018). *effsize: Efficient Effect Size*.

Travis J., Reznick D., Bassar R.D., López-Sepulcre A., Ferriere R. & Coulson T. (2014). Chapter One - Do eco-evo feedbacks help us understand nature? Answers from studies of the Trinidadian guppy. In: *Advances in Ecological Research*. Eco-Evolutionary Dynamics, (Eds J. Moya-Laraño, J. Rowntree & G. Woodward), pp. 1–40. Academic Press.

Trenberth K.E., Fasullo J.T. & Shepherd T.G. (2015). Attribution of climate extreme events. *Nature Climate Change* **5**, 725–730. https://doi.org/10.1038/nclimate2657

Tsang Y.-P., Wieferich D., Fung K., Infante D.M. & Cooper A.R. (2014). An approach for aggregating upstream catchment information to support research and management of fluvial systems across large landscapes. *SpringerPlus* **3**, 589. https://doi.org/10.1186/2193-1801-3-589

Tuckett Q.M., Simon K.S., Saros J.E., Coghlan S.M. & Kinnison M.T. (2014). Biomass versus biodiversity: the relative contribution of population attributes to consumer nutrient loading in aquatic systems. *Evolutionary Ecology Research* **16**, 705–723

Vanni M.J. (2002). Nutrient cycling by animals in freshwater ecosystems. *Annual Review of Ecology and Systematics* **33**, 341–370. https://doi.org/10.1146/annurev.ecolsys.33.010802.150519

Vanni M.J., Flecker A.S., Hood J.M. & Headworth J.L. (2002). Stoichiometry of nutrient recycling by vertebrates in a tropical stream: linking species identity and ecosystem processes. *Ecology Letters* **5**, 285–293

Vanni M.J. & McIntyre P.B. (2016). Predicting nutrient excretion of aquatic animals with metabolic ecology and ecological stoichiometry: a global synthesis. *Ecology* **97**, 3460–3471

Vilà M., Espinar J.L., Hejda M., Hulme P.E., Jarošík V., Maron J.L., *et al.* (2011). Ecological impacts of invasive alien plants: a meta-analysis of their effects on species, communities and ecosystems: Ecological impacts of invasive alien plants. *Ecology Letters* **14**, 702–708. https://doi.org/10.1111/j.1461-0248.2011.01628.x

Violle C., Navas M.-L., Vile D., Kazakou E., Fortunel C., Hummel I., *et al.* (2007). Let the concept of trait be functional! *Oikos* **116**, 882–892. https://doi.org/10.1111/j.2007.0030-1299.15559.x

Vitousek P.M. (1995). The Hawaiian Islands as a model system for ecosystem studies. *Pacific Science* **49**, 2–16

Wallace J.B. & Webster J.R. (1996). The Role of Macroinvertebrates in Stream Ecosystem Function. *Annual Review of Entomology* **41**, 115–139. https://doi.org/10.1146/annurev.en.41.010196.000555

Walther G.-R., Roques A., Hulme P.E., Sykes M.T., Pyšek P., Kühn I., *et al.* (2009). Alien species in a warmer world: risks and opportunities. *Trends in Ecology & Evolution* **24**, 686–693. https://doi.org/10.1016/j.tree.2009.06.008

Weiss L.C., Pötter L., Steiger A., Kruppert S., Frost U. & Tollrian R. (2018). Rising pCO2 in Freshwater Ecosystems Has the Potential to Negatively Affect Predator-Induced Defenses in Daphnia. *Current Biology* **28**, 327-332.e3. https://doi.org/10.1016/j.cub.2017.12.022

Wenger S.J., Isaak D.J., Luce C.H., Neville H.M., Fausch K.D., Dunham J.B., *et al.* (2011). Flow regime, temperature, and biotic interactions drive differential declines of trout species under climate change. *Proceedings of the National Academy of Sciences* **108**, 14175–14180. https://doi.org/10.1073/pnas.1103097108

Whiles M.R., Huryn A.D., Taylor B.W. & Reeve J.D. (2009). Influence of handling stress and fasting on estimates of ammonium excretion by tadpoles and fish: recommendations for designing excretion experiments. *Limnology and Oceanography: Methods* **7**, 1–7

Whitaker D. & Christman M. (2014). *clustsig: Significant Cluster Analysis*.

Wickham H. (2017). *tidyverse: Easily Install and Load the "Tidyverse."*

Woodward G., Dybkjær J.B., Ólafsson J.S., Gíslason G.M., Hannesdóttir E.R. & Friberg N. (2010a). Sentinel systems on the razor's edge: effects of warming on Arctic geothermal stream ecosystems. *Global Change Biology* **16**, 1979–1991. https://doi.org/10.1111/j.1365-2486.2009.02052.x

Woodward G., Perkins D.M. & Brown L.E. (2010b). Climate change and freshwater ecosystems: impacts across multiple levels of organization. *Philosophical Transactions of the Royal Society B: Biological Sciences* **365**, 2093–2106. https://doi.org/10.1098/rstb.2010.0055

Wu Z., Dijkstra P., Koch G.W., Peñuelas J. & Hungate B.A. (2011). Responses of terrestrial ecosystems to temperature and precipitation change: a meta-analysis of

experimental manipulation. *Global Change Biology* **17**, 927–942. https://doi.org/10.1111/j.1365-2486.2010.02302.x

Yvon-Durocher G., Montoya J.M., Trimmer M. & Woodward G. (2011). Warming alters the size spectrum and shifts the distribution of biomass in freshwater ecosystems. *Global Change Biology* **17**, 1681–1694. https://doi.org/10.1111/j.1365-2486.2010.02321.x

Zandonà E., Auer S.K., Kilham S.S., Howard J.L., López-Sepulcre A., O'Connor M.P., *et al.* (2011). Diet quality and prey selectivity correlate with life histories and predation regime in Trinidadian guppies: diet correlates with life histories in guppy. *Functional Ecology* **25**, 964–973. https://doi.org/10.1111/j.1365-2435.2011.01865.x

Zhang C., Wang Y., Hamilton K. & Lauer A. (2016). Dynamical Downscaling of the Climate for the Hawaiian Islands. Part II: Projection for the Late Twenty-First Century. *Journal of Climate* **29**, 8333–8354. https://doi.org/10.1175/JCLI-D-16-0038.1

Zimmer K.D., Herwig B.R. & Laurich L.M. (2006). Nutrient excretion by fish in wetland ecosystems and its potential to support algal production. *Limnology and Oceanography* **51**, 197–207. https://doi.org/10.4319/lo.2006.51.1.0197

Zwiers F.W., Schnorbus M.A. & Maruszeczka G.D. (2011). *Hydrologic impacts of climate change on BC water resources: Summary report for Campbell, Columbia and Peace River watersheds*. Pacific Climate Impacts Consortium, University of Victoria, Victoria, BC.

Appendix

Appendix A: Supplementary information for Chapter 2

Appendix 2.1: Five functions to help facilitate running the partitioning method in R.

Function 1: **Characterize relationship between body size and effect trait**

We establish an allometric relationship between the logarithm of the individual body mass and logarithm of the response variable (individual traits like excretion, respiration). We created the function '**allo_fit**' in R to calculate the allometric coefficients (*a* and *b* based on equation (1) in chapter 2) and the variance-covariance matrix for each allometric relationship as the output.

```
allo_fit <- function(data, response, size){
  response <- data[[deparse(substitute(response))]]
  size <- data[[deparse(substitute(size))]]
  positives <- which(response > 0 & size > 0)
  response <- response[positives]
  size <- size[positives]
  model <- lm(log(response) ~ log(size))
  return(list(coef = coef(model),
              vcov = vcov(model),
              fit = model))
}
```

Input parameters:
#response: Name of the response variable (e.g. excretion, respiration)
#size: Name of the size variable (e.g. length, mass)
#data: Name of dataset storing the above variables

Output parameters:
(1) Vector with the estimated intercept and slope
(2) Variance-covariance matrix of the estimate
(3) Model fit for any further manipulation or reporting

Note: The function deletes values smaller or equal to zero, to avoid undefined logarithms.

Appendix 2.1: Continued

Function 2: **Create 95% confidence intervals around allometric coefficients**

A Monte Carlo simulation was run to propagate the error associated with the response variable. This function results in a table with a 1000 simulated slopes and intercepts for each allometric relationships between size and the individual trait (e.g. per capita excretion). We applied this function to obtain an average of the allometric coefficients with 95% confidence intervals for each sampling event and stream combination.

```
allo_mc <- function(x, n = 1000, predict = FALSE, xpred = seq(0,2, 0.01)){
  coefs <- MASS::mvrnorm(n, mu = x[[1]], Sigma = x[[2]])
  temp <- list(coefs = coefs)
  if (predict == TRUE){
    preds <- matrix(NA, nrow = n, ncol = length(xpred))
    for (i in 1:n){
      preds[i,] <- coefs[i,1] * xpred^coefs[i,2]
    }
    temp <- list(coefs = coefs,
                 xpred = xpred,
                 pred_ci = apply(preds, 2, quantile, c(0.025, 0.5, 0.975)))
  }
  return(temp)
}
```

Input parameters:
#x: The output of allo_fit
#n: Number of parameter combinations to be simulated. Default is set to 1000.
#predict: Default is FALSE, in which case the predicted size range will be the default 'xpred'. To customize the size range for the 'xpred' parameter, set 'predict' parameter to TRUE.
#xpred: Default is the predicted size range between 0 and 2 at 0.01 increments. Once 'pred' is set to TRUE, customize the size range and increments to use as predictor.

Output parameter:
A table with two columns for the intercepts and slopes of each Monte Carlo simulation.

Appendix 2.1: Continued

Function 3: **Combine steps 1 and 2, size structure, and density into a single file**
This function wraps the previous two functions parameters into a single list of parameters for a given time and location, which can be used as the input for the function change_decomp. Blue colored text indicates that this function needs to be customized to the specific data frame used.

```
pop_bundle <- function(loc, time, nsims){

  e.data <- subset(individual_trait_data, stream == loc & month_intro == time)
  d.data <- subset(demography_data, stream == loc & month_intro == time)

  if (nrow(edata) > 0 & nrow(pdata) > 0){

    fit <- allo_fit(response = N_rate, size = size, data = e.data)
    coefs <- allo_mc(fit, n = nsims)$coefs

    size_str <- cbind(d.data$size, d.data$frequency)

    pop_dens <- d.data$pop_dens[1]

    return(list(coefs = coefs, size_str = size_str, pop_dens = pop_dens))

  } else { # If the sampling is not found, return empty list
    return(list(coefs = NA, size_str = NA, pop_dens = NA))
  }
}
```

Input parameters:
#loc: Location/sampling site (e.g. the name of the stream)
#time: time point (e.g. month since species introduction)
#nsims: The number of MC simulations
#Specify e.data and d.data file names and 'loc' and 'time' parameter names specific to your data file

Output parameters:
(1) coef: A table of MC coefficients resulting from fitting an allometric model (from function allo_mc)
(2) size_str: Size structure of the population. Since this is the probability of each size class, the sum must equal to 1.
(3) pop_dens: Population size or density (# per unit area)

Appendix 2.1: Continued

Function 4: **Calculate population level effect on ecosystem function**

This function applies the parameters from the 'pop_bundle' function to equations (1) and (2) of chapter 2. With this function we are able to estimate total population effect (e.g. population excretion) on ecosystem function, with the associated 95% confidence intervals.

```
ind2pop <- function(params){

  pop_rate <- rep(NA, nrow(params$coefs))

  for (it in 1:nrow(params$coefs)){

    temp <- rep(NA, nrow(params$size_str))
    for (sz in 1:nrow(params$size_str)){
      temp[sz] <- (exp(params$coefs[it, 1]) * params$size_str[sz, 'size'] ^ params$coefs[it,
2]) * params$size_str[sz, 'prop']
    }

    pop_rate[it] <- sum(temp) * params$pop_dens
  }

  return(pop_rate)
}
```

Input parameter:
#params: Population parameters created by 'pop_bundle'

Output parameter:
Calculated population effect of each Monte Carlo simulation.

Note: Use mean() and quantile((), c(0.025, 0.975)) commands to obtain the average population effect with 95% CI

Appendix 2.1: Continued

Function 5: **Decompose population level effect into trait and demographic**

This function incorporates equations (3-8) of chapter 2 and the parameters from the 'pop_bundle' function to calculate the proportional contribution of the individual trait (A), size distribution (S), population density (D), and the interaction of S and A with their associate 95% confidence intervals to the change of the population effect between any two points in time or space.

```
change_decomp <- function(pop1, pop2){
 if (all(!is.na(pop2))){
   R1 = ind2pop(params = list(coefs = pop1$coefs,
                              size_str = pop1$size_str,
                              pop_dens = pop1$pop_dens))
   R2 = ind2pop(params = list(coefs = pop2$coefs,
                              size_str = pop2$size_str,
                              pop_dens = pop2$pop_dens))

   change <- R2/R1

   A = R2 / ind2pop(params = list(coefs = pop1$coefs,
                                  size_str = pop2$size_str,
                                  pop_dens = pop2$pop_dens))
   S = R2 / ind2pop(params = list(coefs = pop2$coefs,
                                  size_str = pop1$size_str,
                                  pop_dens = pop2$pop_dens))
   D = R2 / ind2pop(params = list(coefs = pop2$coefs,
                                  size_str = pop2$size_str,
                                  pop_dens = pop1$pop_dens))
   I = change / (A * S * D)

   return(cbind(change, A, S, D, I))
 } else {
  return(NA)
 }}
```

Input parameters:
pop1: Reference population parameters from 'pop_bundle' function (time 1)
pop2: Changed population parameters from 'pop_bundle' function (time 2)

Output parameter:
A matrix with four columns (one per contributor) and as many rows as number of Monte Carlo simulations.

Note: Use apply((), 2, quantile, c(0.025, 0.5, 0.975)) command to obtain the averages and 95% confidence intervals of all contributors.

Appendix 2.2: Derivation of the density and the functional trait interaction ($I_{A,D}$), following the same principles as in equation (8) of chapter 2. $E_{(z)}$ describes the trait at a given size z, $P_{(z)}$ depicts the proportion of individuals in the population with the size z, and N is the population density.

$$I_{A,D} = \frac{\int E_{(z,t2)} P_{(z,t2)} N_{(t2)} dz}{\int E_{(z,t1)} P_{(z,t2)} N_{(t1)}\, dz} \cdot \frac{\int E_{(z,t1)} P_{(z,t2)} dz}{\int E_{(z,t2)} P_{(z,t2)}\, dz} \cdot \frac{N_{(t1)}}{N_{(t2)}} = 1$$

Appendix 2.3: Application of the Appendix 2.1 functions in an example in R. This example is for estimating population excretion in the CAI stream during the first (month 14) and second (month 25) year post guppy introduction. The "allo_fit", "allo_mc", "ind2pop", and "change_decomp" functions need to be run first. Function "pop_bundle" needs to be modified specifically to the data set (see step 3).

```
library(tidyverse)

e.data<-read.csv(file.choose(),as.is = TRUE) #select individual trait file
d.data<-read.csv(file.choose(),as.is = TRUE) #select demography file


Step 1: Characterize relationship between body size and effect trait
Fits log-log model of per-capita excretion as a function of size:
ca.14 <- subset(e.data, stream == 'CA' & month_intro == 14)
fit.ca.14 <- allo_fit(response = N_rate, size = size, data = ca.14)
fit.ca.14 # Returns coefficients (intercept and slope) and a variance-covariance matrix


Step 2: Create 95% confidence intervals around allometric coefficients
Simulates coefficients from "allo_fit" function for 1000 combinations:
mc.ca.14 <- allo_mc(fit.CA.14, n = 1000)
head(mc.ca.14$coefs) # Returns a table with 1000 simulations of slopes and intercepts
```

Appendix 2.3: Continued

Step 3: **Combine steps 1 and 2, size structure, and density into a single file**

Wraps parameters into a single list for a given time and location. Specify e.data and d.data file names and 'loc' and 'time' parameter names specific to your data file.

```
pop_bundle <- function(loc, time, nsims){
  e.data <- subset(individual_trait_data, stream == loc & month_intro == time)
  d.data <- subset(demography_data, stream == loc & month_intro == time)
if (nrow(edata) > 0 & nrow(pdata) > 0){
    fit <- allo_fit(response = N_rate, size = size, data = e.data)
    coefs <- allo_mc(fit, n = nsims)$coefs
    size_str <- cbind(d.data$size, d.data$frequency)
    pop_dens <- d.data$pop_dens[1]
    return(list(coefs = coefs, size_str = size_str, pop_dens = pop_dens)) }
 else { return(list(coefs = NA, size_str = NA, pop_dens = NA))
  }}

#Run specified pop_pundle for your two populations
CA.14 <- pop_bundle(loc = 'CA', month_int = 14, nsims = 1000) # for year 1
CA.25<- pop_bundle(loc = 'CA', month_int = 25, nsims = 1000) # for year 2
```

Note: Since this function includes steps 1 and 2, one can start with this function if there is no interest in the individual trait relationships. "Pop_bundle" function needs to be specified for the appropriate individual and demography data frame names.

Step 4: **Calculate population level effect on ecosystem function**

```
Estimates population excretion:
Rt <- ind2pop(params = CA.14)
mean(Rt) # average population excretion
quantile(Rt, c(0.025, 0.975)) # 95% CI
```

Step 5: **Decompose population level effect into trait and demographic**

```
Calculates the contribution to change of each component between two time points
decomp <- change_decomp(CA.14, CA.25)
apply(decomp, 2, quantile, c(0.025, 0.5, 0.975)) # returns a table with mean and 95% CI
for each component

Double check if all the components equal 1
product <- apply(decomp[,c('A','S','D','I')], 1, prod)
plot(decomp[,'change'] ~ product,
ylab = 'Proportional Change',
xlab = 'Product of Components',
pch = 16, cex = 0.8)
abline(0, 1, lty = 2)
```

Appendix 2.4: Allometric log-log relationships of body size and per-capita guppy excretion (E) in four streams for each sampling year. CAI and LOL streams were under low light conditions, while TAY and UPL had higher light conditions. Stars indicate the significance of the relationships (* p < 0.1; ** p < 0.05; *** p < 0.01), while the numbers in brackets are standard error.

	$\log(E) = a + b \log(size)$													
	CAI				LOL				TAY			UPL		
	2009	2010	2011	2014	2009	2010	2011	2014	2009	2010	2011	2009	2010	2011
a	0.547***	0.620*	0.494***	0.762**	1.003***	0.552***	0.874***	0.710***	0.541***	0.619***	0.780	0.620***	0.550***	0.182
	(0.066)	(0.358)	(0.087)	(0.298)	(0.170)	(0.115)	(0.185)	(0.104)	(0.091)	(0.142)	(0.534)	(0.054)	(0.057)	(0.129)
b	2.946***	0.673	3.173***	3.203***	3.557***	3.026***	2.479***	3.017***	3.011***	2.701***	1.169	3.225***	3.292***	2.294***
	(0.174)	(0.957)	(0.212)	(0.696)	(0.385)	(0.313)	(0.497)	(0.210)	(0.223)	(0.328)	(0.954)	(0.126)	(0.172)	(0.338)
Observations	23	22	31	15	31	29	29	15	19	32	14	39	33	32
R^2	0.764	0.131	0.525	0.335	0.546	0.459	0.453	0.782	0.675	0.388	0.151	0.779	0.748	0.062
Residual Std. Error	0.300	1.966	0.517	0.559	0.731	0.589	1.066	0.260	0.460	0.910	1.205	0.357	0.371	0.782
F Statistic	67.917***	3.010*	32.020***	6.561**	34.872***	22.872***	22.372***	46.510***	35.342***	19.019***	2.137	130.261***	91.821***	1.981

Appendix 2.5: Kruskall-Wallis results for comparing the size structure of each of the four streams.

Stream	chi-squared	df	p-value
CAI	187.10	3	< 0.0001
TAY	69.34	2	< 0.0001
UPL	296.53	2	< 0.0001
LOL	106.03	3	< 0.0001

Appendix 2.6: The following equations derive the scenario, where body size does not scale with the individual the effect trait (i.e. no allometric relationship). The same principals are applied as in equations (2 – 6) of chapter 2. In this case, the population effect on an ecosystem function (R) is the product of the effect trait (E) and population density (N):

$$R = E\,N\,.$$

Therefore, the proportional change ($\frac{R_{t2}}{R_{t1}}$) from a given time ($t1$) to the next sampling time ($t2$) is equal to:

$$\frac{E_{(t2)}N_{(t2)}}{E_{(t1)}N_{(t1)}} = \frac{R_{t2}}{R_{t1}} = A\,D,$$

which is also the product of the proportional contribution of the effect trait (A)

$$A = \frac{E_{(t2)}N_{(t2)}}{E_{(t1)}N_{(t2)}} = \frac{E_{(t2)}}{E_{(t1)}}$$

and the proportional contribution of density (D)

$$D = \frac{E_{(t2)}N_{(t2)}}{E_{(t1)}N_{(t2)}} = \frac{N_{(t2)}}{N_{(t1)}}.$$

Appendix B: Supplementary information for Chapter 3

Appendix 3.1: Length-mass relationships (mass (mg) = a * length (mm) ^ b) for Hawaiian stream macroinvertebrates that represented > 1% of invertebrate abundance. If the size spectrum of the invertebrate taxa was > 1 mm, length and ash-free dry mass (AFDM) or dry mass (DM) were measured according to Benke et al. (1999); otherwise invertebrate's AFDM was averaged (± standard error). We required a minimum sample size (n) of 10 and a regression with an $R^2 \geq 0.6$.

Order	Family	Genus	Measure	a	b	R^2	Size Range (mm)	n
Odonata	Coenagrionidae	*Megalagrion*	AFDM	0.0002	3.3378	0.93	1.9 - 29.4	22
	Libellulidae	*Pantala*	DM	0.0029	2.5275	0.82	1.3 - 3.9	14
Collembola	Isotomidae		AFDM	0.0147 ± 0.0022			1.2-2.2	31
Trichoptera	Hydropsychidae	*Cheumatopsyche*	AFDM	0.0002	3.4602	0.87	2.1 - 11.0	38
	Hydroptilidae	*Oxyethira*	AFDM	0.0015	3.6697	0.73	1.0 - 2.9	24
		Hydroptila	AFDM	0.0009	3.2907	0.64	1.1 - 3.2	30
Diptera	Chironomidae		AFDM	0.0002	3.3013	0.70	1.7 - 11.1	72
	Culicidae	*Aedes*	AFDM	0.0031	1.7878	0.69	4.2 - 7.6	21
	Canacidae	*Procanace*	AFDM	0.0002	5.7159	0.60	1.9 - 3.6	19
	Ephydridae	*Scatella*	AFDM	0.0089	1.7905	0.73	1.9 - 3.1	22
Hemiptera	Mesoveliidae	*Mesovelia*	DM	0.0190	1.975	0.85	0.8 - 2.2	24
Cyclopoida	Cyclopidae		AFDM	0.0051 ± 0.0001			1.5 - 2.0	130
Trombidiformes	Hydrachnoidea		AFDM	0.0041 ± 0.0005			0.5	50
Pulmonata	Lymnaeidae	*Erinna*	AFDM	0.0126	2.1417	0.84	1.0 - 12.5	22
	Planorbidae	*Chlanospira*	DM	0.0326	2.8268	0.75	0.8 - 2.6	43
Hirudinea	Erpobdellidae	*Barbronia*	AFDM	0.0006	2.8172	0.82	5.6 - 14.9	26
Oligochaetae			AFDM	0.0054	1.7166	0.90	4.9 - 185	29

Appendix 3.2: Generalized linear model (glm) and generalized mixed effect model (glmm) output of mean annual rainfall (MAR) or baseflow (Q_{90}) in relation to a given response variable for both high temporal resolution (HTR) and high spatial resolution (HSR) sampling regimes. We used the "lme4" and "pscl" packages from the statistical program R (Bates *et al.*, 2015; Jackman, 2017).

Type	Year	Response variable	Fixed effect	Model	Family	N	R^2	Estimate	Standard Error	t-value	p-value
	2012	Seasonal rain	MAR	glm	Gaussian	8	0.9456	0.2457	0.0241	10.215	<0.0001
	2015	Seasonal rain	MAR	glm	Gaussian	8					0.5911
	2016	Seasonal rain	MAR	glm	Gaussian	8	0.7895	0.1041	0.0220	4.7440	0.0032
	2012	Q_{90}	MAR	glm	Gaussian	8	0.7224	0.0094	0.0024	3.9460	0.0076
	2015	Q_{90}	MAR	glm	Gaussian	8	0.7561	0.0081	0.0019	4.3040	0.0051
	2016	Q_{90}	MAR	glm	Gaussian	8	0.7628	0.0126	0.0029	4.3880	0.0046
	2012	Flow variability	MAR	glm	Gamma	8	0.7790	<0.0001	0.0000	4.3280	0.0049
	2015	Flow variability	MAR	glm	Gamma (log link)	8	0.9925	-0.0038	0.0008	-5.0340	0.0024
	2016	Flow variability	MAR	glm	Gamma (log link)	8	0.8056	-0.0012	0.0002	-5.2370	0.0019
	2012	Flood intensity	MAR	glm	Gamma	8	0.9582	<0.0001	0.0000	3.0680	0.0220
	2015	Flood intensity	MAR	glm	Gamma	8	0.9782	<0.0001	0.0000	3.1730	0.0192
	2016	Flood intensity	MAR	glm	Gamma (log link)	8	0.9059	-0.0023	0.0003	-6.5360	0.0006
	2015/ 2016	Canopy Cover	Q_{90}	glm	Gaussian	16	0.6953	-1.6426	0.4441	-3.6990	0.0101
HSR	2012	Benthic biomass	Q_{90}	glm	Gamma	4					0.3350
HSR	2015	Benthic biomass	Q_{90}	glm	Gaussian	7	0.9044	2.3097	0.3361	6.8710	0.0010
HSR	2016	Benthic biomass	Q_{90}	glm	Gaussian	8	0.7683	2.1215	0.4757	4.4600	0.0043
HTR	2012	Benthic biomass	Q_{90}	glmm	Gamma	48					0.0676
HSR	2012	Suspended biomass	Q_{90}	glm	Gamma (log link)	4	0.6188	0.2371	0.0950	2.4950	0.0520
HSR	2015	Suspended biomass	Q_{90}	glm	Gamma (log link)	7	0.6149	0.1121	0.0378	2.9640	0.0314
HSR	2016	Suspended biomass	Q_{90}	glm	Gaussian	8	0.7863	11.620	2.4730	4.6990	0.0033
HTR	2012	Suspended biomass	Q_{90}	glmm	Gamma (log link)	35	0.2881	0.0600	0.0210	2.8600	0.0042

Appendix 3.2: Continued

Type	Year	Response variable	Fixed Effect	Model	Family	N	R^2	Estimate	Standard Error	t-value	p-value
HSR	2012	Macrophyte presence	Q_{90}	glm	Gaussian	4	0.9690	3.6737	0.4655	7.8910	0.0157
HSR	2015	Macrophyte presence	Q_{90}	glm	Gaussian	7	0.8773	4.8153	0.8054	5.9790	0.0019
HTR	2012	Macrophyte presence	Q_{90}	glmm	Gamma (log link)	47	0.3386	0.0945	0.0295	3.2050	0.0014
HSR	2012	Detritus presence	Q_{90}	glm	Gamma (log link)	4	0.9800	-0.1341	0.0132	-10.180	0.0095
HSR	2015	Detritus presence	Q_{90}	glm	Gamma (log link)	7	0.9931	-0.3717	0.0426	-8.7330	0.0003
HTR	2012	Detritus presence	Q_{90}	glmm	Gamma (log link)	47	0.2150	-0.0394	0.0147	-2.6890	0.0072
HSR	2012	Periphyton Chl *a*	Q_{90}	glm	Gaussian	4					0.5301
HSR	2015	Periphyton Chl *a*	Q_{90}	glm	Gamma	7					0.3900
HSR	2016	Periphyton Chl *a*	Q_{90}	glm	Gaussian	8					0.2744
HTR	2012	Periphyton Chl *a*	Q_{90}	glmm	Gamma (log link)	48					0.8340
HSR	2012	Periphyton biomass	Q_{90}	glm	Gaussian	4					0.2620
HSR	2015	Periphyton biomass	Q_{90}	glm	Gamma (log link)	7					0.2270
HSR	2016	Periphyton biomass	Q_{90}	glm	Gaussian	8					0.1900
HTR	2012	Periphyton biomass	Q_{90}	glmm	Gamma	44					0.4660
	2012	Primary production	Q_{90}	glm	Gaussian	4	0.9934	4.3480	0.2511	17.315	0.0033
HSR	2012	Invertebrate biomass	Q_{90}	glm	Gamma (log link)	4	0.7367	0.1345	0.0534	2.5180	0.0281
HSR	2015	Invertebrate biomass	Q_{90}	glm	Gamma (log link)	7	0.7372	0.1564	0.0425	3.6830	0.0143
HSR	2016	Invertebrate biomass	Q_{90}	glm	Gamma (log link)	8	0.6045	0.0648	0.0215	3.0120	0.0236
HTR	2012	Invertebrate biomass	Q_{90}	glmm	Gamma (log link)	48	0.7326	0.1013	0.0204	4.9720	<0.0001

Appendix 3.3: Benthic resource availability (mg of ash-free dry mass (AFDM) m^{-2}) at 8 streams across a rainfall gradient in 2015. Mean annual rainfall (MAR) and baseflow (Q_{90}) drive changes in the availability of the two dominant resources, leaf litter, and macrophytes.

	WET →							**DRY**
Stream	HON	KAP	KOL	UMA	LOA	MAK	PAH	KAA
MAR (mm)	5764	5868	6520	5178	5168	4748	4527	3703
Q_{90} (L $s^{-1}km^{-2}$)	26.43	18.87	20.92	11.27	5.19	3.67	0.32	0.06
Resource type (mg AFDM m^{-2}):								
Leaf litter			0.084	2.974	1.578	1.812	0.934	9.477
Grass			0.005	0.17		0.073		0.084
Macrophytes	48.123	27.201	49.169	4.509	5.806	0.248	0.121	0.001
Miscellaneous	0.826	1.331	2.931	2.432	3.327	0.726	0.391	0.136
Seeds					0.09		0.015	0.058
Wood	0.006		0.014	2.582	0.538			0.005
Total (mg AFDM m^{-2})	48.955	28.533	52.203	12.666	11.339	2.859	1.46	9.762

Appendix 3.4: Average macroinvertebrate biomass (mg AFDM/m^2) during the sampling periods (May-September) across 3 years in eight streams along the rainfall gradient.

			WET →							**DRY**
Order	Family	Genus	HON	KAP	KOL	UMA	LOA	MAK	PAH	KAA
Odonata	Coenagrionidae	*Megalagrion*	8.632	1.928		0.977				
	Libellulidae	*Pantala*							0.580	
Colembolla	Isotomidae							0.439		0.648
Trichoptera	Hydropsychidae	*Cheumatopsyche*	5.142	31.526	414.587	52.184	61.032	16.041	0.787	
	Hydroptilidae	*Oxyethira*				0.225				0.419
		Hydroptila		2.144	1.927	0.107	5.113	0.517		
Diptera	Chironomidae		10.319	50.860	17.256	7.014	7.984	1.013	3.550	10.865
	Culicidae	*Aedes*								1.493
	Canacidae	*Procanace*	1.058	18.393		1.637				
	Ephidridae	*Scatella*	4.222	4.459	4.539	2.775		0.396	5.048	
Hemiptera	Mesoveliidae	*Mesovelia*								3.800
Cyclopoida	Cyclopidae					0.034		0.078	0.281	1.026
Trombidiformes	Hydrachnoidea		1.214	0.542	3.779	0.091	0.395	0.797	2.541	0.507
Pulmonata	Lymnaeidae	*Erinna*				0.936		4.245		4.820
	Planorbidae	*Chlanospira*					3.191			6.271
Hirudinea	Erpobdellidae	*Barbronia*				1.520		10.832		
Oligochaetae			5.252	1.368	17.584	9.605	50.720	0.887	8.520	0.205
		Total	35.840	111.220	459.671	77.104	128.435	35.246	21.308	30.053
		MAR (mm)	5764	5868	6520	5178	5168	4748	4527	3703
		Q_{90} (L $s^{-1}km^{-2}$)	26.43	18.87	20.92	11.27	5.19	3.67	0.32	0.06

Appendix 3.5: Percent dissimilarity in macroinvertebrate composition (high temporal resolution sampling regime only) between streams based on SIMPER analysis.

	DRY → WET					
	Streams	% dis	Streams	% dis	Streams	% dis
DRY	KAA_MAK	23.3	MAK_UMA	35.9	UMA_KOL	25.02
↓	KAA_UMA	31.7	MAK_KOL	37.9		
WET	KAA_KOL	37.7				

Appendix C: Supplementary information for Chapter 4

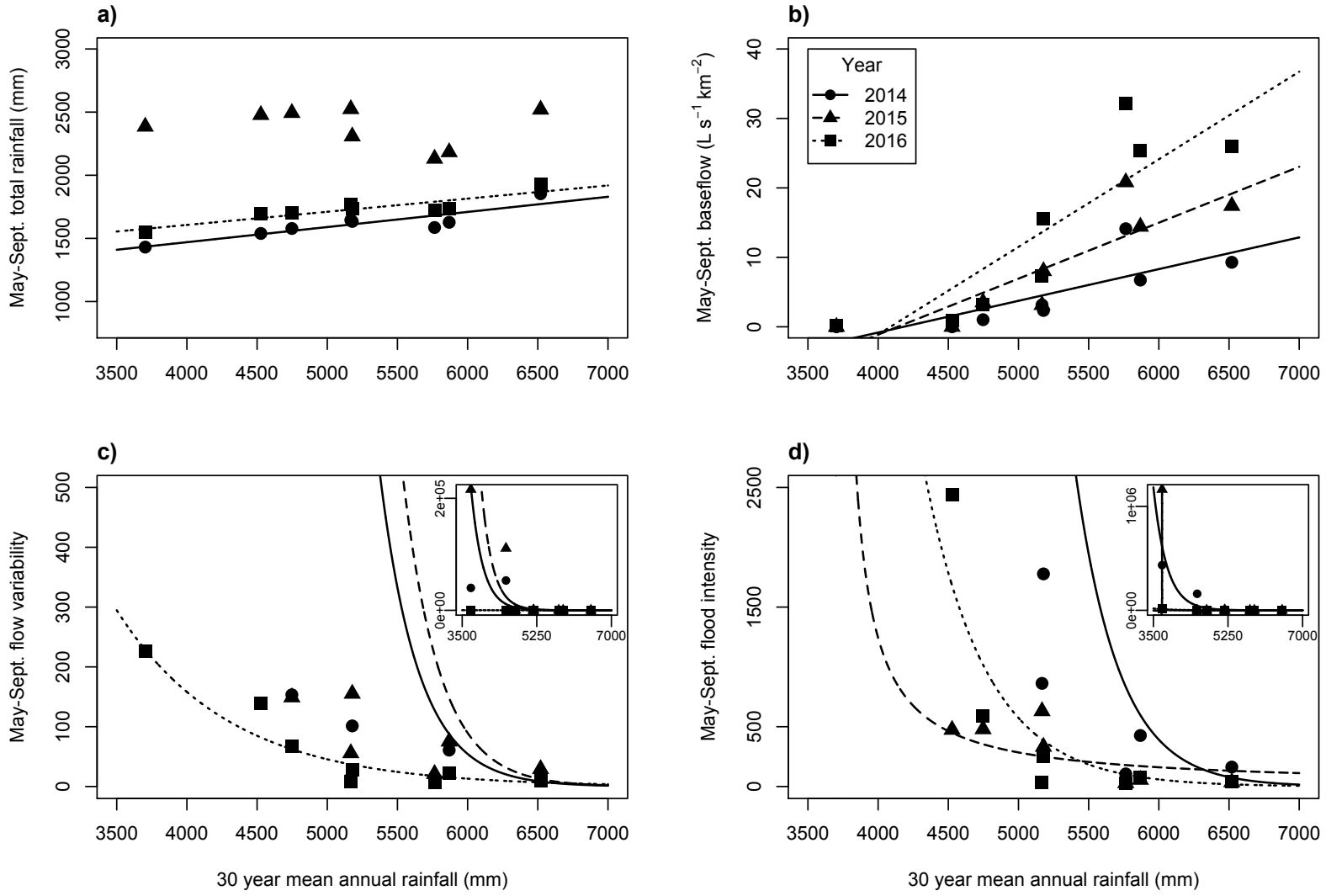

Appendix 4.1: Rainfall and streamflow variables of eight sites (one point per stream) across the three sampling years. The 30-year mean annual rainfall average related to the total rainfall during the sampling period in years 2014 and 2016 (a). Baseflow (b; Q_{90}) increased with rainfall; while streamflow variability (c; Q_{10}/Q_{90}) and flood intensity (d; peak flow/Q_{50}) exponentially declined with rainfall. Lines indicate the significant model output of each relationship ($p \leq 0.05$). Note: (c) and (d) y-axes have been cut short to display the relationships better. The inset graphs represent the full data set.

Appendix 4.2: Generalized linear model output of mean annual rainfall (MAR) in relation to a seasonal rainfall (May-Sept.), baseflow (Q_{90}), flow variability (Q_{10}/Q_{90}), and flood intensity (peak flow/Q_{50}). We used the "lme4" and "pscl" packages from the statistical program R (Bates *et al.*, 2015; Jackman, 2017). R^2 values are maximum likelihood pseudo r-squared values (Cox & Snell, 1989). Significant relationships are in bold.

Year	Response Variable	Fixed Effect	Family	N	R^2	Estimate	Standard Error	t-value	p-value
2014	**Seasonal rain**	**MAR**	Gaussian	8	0.7771	0.1198	0.0262	4.5730	**0.0038**
2015	Seasonal rain	MAR	Gaussian	8					0.5911
2016	**Seasonal rain**	**MAR**	Gaussian	8	0.7895	0.1041	0.0220	4.7440	**0.0032**
2014	**Q_{90}**	**MAR**	Gaussian	8	0.6295	0.0046	0.0014	3.1820	**0.0190**
2015	**Q_{90}**	**MAR**	Gaussian	8	0.7561	0.0081	0.0019	4.3040	**0.0051**
2016	**Q_{90}**	**MAR**	Gaussian	8	0.7628	0.0126	0.0029	4.3880	**0.0046**
2014	**Flow variability**	**MAR**	Gamma (log link)	8	0.9914	-0.0036	0.0008	-4.6510	**0.0035**
2015	**Flow variability**	**MAR**	Gamma (log link)	8	0.9925	-0.0038	0.0008	-5.0340	**0.0024**
2016	**Flow variability**	**MAR**	Gamma (log link)	8	0.8056	-0.0012	0.0002	-5.2370	**0.0019**
2014	**Flood intensity**	**MAR**	Gamma (log link)	8	0.8995	-0.0032	0.0006	-5.4770	**0.0015**
2015	**Flood intensity**	**MAR**	Gamma	8	0.9782	<0.0001	<0.0001	3.1730	**0.0192**
2016	**Flood intensity**	**MAR**	Gamma (log link)	8	0.9059	-0.0023	0.0003	-6.5360	**0.0006**

Appendix 4.3: Generalized linear model output of per capita (PC) and mass-specific (MS) excretion and tissue carbon to nitrogen ratios in relation to baseflow (Q_{90}) and sample year. We used the "lme4" and "pscl" packages from the statistical program R (Bates *et al.*, 2015; Jackman, 2017). R^2 values are maximum likelihood pseudo r-squared values (Cox & Snell, 1989). Significant relationships are in bold.

Organism	Nutrient	Response Variable	Fixed Effect	Family	N	R^2	Estimate	Standard Error	t-value	p-value
Shrimp	NH_4	**PC excretion**	**Q_{90}**	Gaussian	18	0.7349	0.2660	0.0446	5.9700	**<0.0001**
			Year							0.9640
Caddisfly	NH_4	PC excretion	Q_{90}	Gaussian	15					0.4860
			Year							0.2820
Midge	NH_4	PC excretion	Q_{90}	Gamma (log link)	18					0.4190
			Year							0.8370
Shrimp	PO_4	**PC excretion**	**Q_{90}**	Gamma (log link)	10	0.6772	0.1629	0.0358	4.5550	**0.0026**
			Year							0.9538
Caddisfly	PO_4	PC excretion	Q_{90}	Gaussian	8					0.6120
			Year							0.5020
Midge	PO_4	**PC excretion**	**Q_{90}**	Gamma (log link)	10	0.6585	-0.0893	0.0220	-4.0650	**0.0048**
			Year							0.0597
Shrimp	NO_3	PC excretion	Q_{90}	Gaussian	10					0.8470
			Year							0.5310
Shrimp	NH_4	**MS excretion**	**Q_{90}**	Gamma	18	0.3223	-0.4732	0.1924	-2.4600	**0.0265**
			Year							0.1940
Caddisfly	NH_4	MS excretion	Q_{90}	Gamma (log link)	15					0.8373
			Year							0.0566
Midge	NH_4	**MS excretion**	Q_{90}	Gamma (log link)	18					0.8404
			Year			0.1958	-0.9430	0.3273	-2.8810	**0.0114**

Appendix 4.3: Continued

Organism	Nutrient	Response Variable	Fixed Effect	Family	N	R^2	Estimate	Standard Error	t-value	p-value
Shrimp	PO_4	MS excretion	Q_{90}	Gaussian	10					0.1990
			Year							0.4400
Caddisfly	PO_4	MS excretion	Q_{90}	Gamma (log link)	8					0.3800
			Year							0.4610
Midge	PO_4	**MS excretion**	**Q_{90}**	Gamma (log link)	10	0.5132	-0.1466	0.0615	-2.3860	**0.0485**
			Year							0.1989
Shrimp	NO_3	**MS excretion**	**Q_{90}**	Gamma (log link)	10	0.5507	-0.1128	0.0341	-3.3130	**0.0129**
			Year							0.2948
Shrimp	C:N	**Tissue C:N**	Q_{90}	Gaussian	18					0.5588
			Year			0.4360	0.3573	0.1071	3.3350	**0.0045**
Caddisfly	C:N	Tissue C:N	Q_{90}	Gaussian	15					0.6860
			Year							0.9720
Midge	C:N	**Tissue C:N**	**Q_{90}**	Gamma	18	0.4885	-0.0006	0.0003	-2.3260	**0.0345**
			Year							0.0876

Appendix 4.4: Generalized linear model (glm) output of population density, size frequency and excretion in relation to baseflow (Q_{90}) and sample year. We used the "lme4" and "pscl" packages from the statistical program R (Bates *et al.*, 2015; Jackman, 2017). R^2 values are maximum likelihood pseudo r-squared values (Cox & Snell, 1989). Significant relationships are in bold.

Organism	Nutrient	Response variable	Fixed effect	Family	N	R^2	Estimate	Standard Error	t-value	p-value
Shrimp		**Average Size**	**Q_{90}**	Gaussian	8	0.6385	3.7690	1.1580	3.2550	**0.0173**
Caddisfly		Average Size	Q_{90}	Gaussian	15					0.1530
			Year							0.2110
Midge		Average Size	Q_{90}	Gaussian	18					0.7330
			Year							0.9370
Shrimp		**Density**	**Q_{90}**	Gamma (log link)	8	0.7315	0.0564	0.0093	6.0540	**<0.0001**
Caddisfly		**Density**	**Q_{90}**	Gamma (log link)	15	0.2946	0.0883	0.0316	2.7980	**0.0161**
			Year							0.1877
Midge		**Density**	**Q_{90}**	Gamma (log link)	18	0.5827	0.0722	0.0159	4.5530	**0.0004**
			Year							0.6363
Shrimp	NH_4	**Pop. excretion**	**Q_{90}**	Gamma (log link)	18	0.8601	0.1409	0.0138	10.210	**<0.0001**
			Year							0.2380
Caddisfly	NH_4	**Pop. excretion**	**Q_{90}**	Gamma (log link)	15	0.4528	0.1300	0.0298	4.3580	**0.0009**
			Year							0.0732
Midge	NH_4	**Pop. excretion**	**Q_{90}**	Gamma (log link)	18	0.5406	0.0879	0.0219	4.0180	**0.0011**
			Year							0.9588
Shrimp	PO_4	**Pop. excretion**	**Q_{90}**	Gamma (log link)	10	0.8947	0.3025	0.0450	6.7280	**0.0003**
			Year							0.8369
Caddisfly	PO_4	Pop. excretion	Q_{90}	Gamma	8					0.3240
			Year							0.2080
Midge	PO_4	Pop. excretion	Q_{90}	Gamma	10					0.6030
			Year							0.5960

Appendix 4.4: Continued

Organism	Nutrient	Response variable	Fixed effect	Family	N	R^2	Estimate	Standard Error	t-value	p-value
Shrimp	NO_3	**Pop. excretion**	**Q_{90}**	Gamma (log link)	10	0.9476	0.4420	0.0633	6.9820	**0.0002**
			Year							0.1450

Appendix 4.5: Generalized linear model (glm) output of community excretion, nutrient uptake, and percent nutrients contributed via excretion in relation to baseflow (Q_{90}) and sample year. We used the "lme4" and "pscl" packages from the statistical program R (Bates *et al.*, 2015; Jackman, 2017). R^2 values are maximum likelihood pseudo r-squared values (Cox & Snell, 1989). Significant relationships are in bold.

Nutrient	Response Variable	Fixed Effect	Family	N	R^2	Estimate	Standard Error	t-value	p-value
NH_4	**Com. excretion**	**Q_{90}**	Gamma (log link)	18	0.6731	0.1145	0.0194	5.8960	**<0.0001**
		Year							0.2360
PO_4	Com. excretion	Q_{90}	Gamma (log link)	10					0.0645
		Year							0.3420
NO_3	**Com. excretion**	**Q_{90}**	Gamma (log link)	10	0.9476	0.4420	0.0633	6.9820	**0.0002**
		Year							0.1450
NH_4	Uptake	Q_{90}	Gamma (log link)	18					0.7645
		Year							0.0563
PO_4	Uptake	Q_{90}	Gamma	10					0.0601
		Year							0.5219
NO_3	Uptake	Q_{90}	Gamma	10					0.0733
		Year							0.5012
NH_4	**Contribution**	**Q_{90}**	Gamma (log link)	18	0.5019	0.0823	0.0252	3.2710	**0.0052**
		Year							0.1248
PO_4	Contribution	Q_{90}	Gamma (log link)	10					0.6600
		Year							0.6040
NO_3	**Contribution**	**Q_{90}**	Gamma (log link)	10	0.7989	0.3429	0.0621	5.5270	**0.0009**
		Year							0.1980

Appendix 4.6: Generalized linear model (glm) output of per capita (PC), mass-specific (MS), population, and community egestion in relation to baseflow (Q_{90}) and sample year. We used the "lme4" and "pscl" packages from the statistical program R (Bates *et al.*, 2015; Jackman, 2017). R^2 values are maximum likelihood pseudo r-squared values (Cox & Snell, 1989). Significant relationships are in bold.

Organism	Response Variable	Fixed Effect	Family	N	R^2	Estimate	Standard Error	t-value	p-value
Shrimp	PC egestion	Q_{90}	Gaussian	9					0.6460
		Year							0.4130
Caddisfly	**PC egestion**	Q_{90}	Gaussian	7					0.4345
		Year			0.8997	-0.0643	0.0108	-5.9700	**0.0040**
Shrimp	MS egestion	Q_{90}	Gaussian	9					0.9840
		Year							0.3320
Caddisfly	**MS egestion**	Q_{90}	Gamma (log link)	7					0.7576
		Year			0.8949	-2.7326	0.5526	-4.9450	**0.0078**
Shrimp	**Pop. egestion**	**Q_{90}**	Gamma (log link)	9	0.7371	0.1030	0.0299	3.4420	**0.0138**
		Year							0.2619
Caddisfly	**Pop. egestion**	**Q_{90}**	Gamma (log link)	7	0.7921	0.2726	0.0395	6.9030	**0.0023**
		Year				-3.6734	0.6696	-5.4860	**0.0054**
	Com. egestion	**Q_{90}**	Gamma (log link)	9	0.7896	0.2989	0.0390	7.6710	**0.0003**
		Year				-3.3358	0.6207	-5.3740	**0.0017**

Appendix D: Supplementary information for Chapter 5

Appendix 5.1: Results of the t-test that compared resources and invertebrate consumers between guppy-invaded and guppy-free streams, independent of flow. If the p-value was significant, the effect size (using Hedge's g) of guppy presence was calculated separately for low, medium, and high flow streams. The effect size was classified as large (LG), medium (MD), small (SM) or negligible (NG). Positive effect sizes indicate that guppies decreased the response variable, while a negative effect size indicates that guppies increased the response variable.

Response Variable	t-value	DF	p-value	Hedge's g		
				Wet	Med	Dry
Suspended biomass	0.341	9.83	0.7405			
Tot. benthic biomass	1.242	15.825	0.2322			
Macrophyte biomass	0.361	15.812	0.7228			
Detritus biomass	1.501	12.624	0.1578			
Biofilm Chl *a*	-1.788	9.248	0.1065			
Biofilm biomass	-1.722	9.968	0.1158			
Tot. Invert. biomass	2.589	7.977	**0.0322**	0.283 (SM)	-1.174 (LG)	-9.744 (LG)
Midge body size	1.647	9.932	0.1308			
Midge density	1.510	9.861	**0.0623**	0.498 (SM)	1.113 (LG)	1.034 (LG)
Caddis body size	0.433	6.729	0.6786			
Caddis density	-2.989	5.489	**0.0272**	0.210 (SM)	-3.484 (LG)	-8.277 (LG)

Appendix 5.2: Substrate composition (%) in each stream with high, medium, or low flow that had either guppies present (GI) or absent (GF). There was no consistent patter across the streams.

Stream	Wet GF Kolekole	Wet GI Umauma	Med GF Manoloa	Med GI Waikamalo	Dry GF Manowaiopae	Dry GI Kaiwilahilahi
Bedrock	0	80	28	0	27	33
Boulder	70	10	0	33	0	7
Cobble	20	10	55	0	47	20
Gravel	10	0	17	67	17	33
Sand	0	0	0	0	10	7

Appendix 5.3: Average biomass (mg AFDM/m^2) of dominant macroinvertebrate taxa during the sampling periods (June-September) across 2 years in six streams with high, medium, and low streamflow. Within each flow category, one stream is guppy free (GF), while the other is invaded by guppies (GI).

Order	Family	Genus	Wet GF Kolekole	Wet GI Umauma	Med GF Manoloa	Med GI Waikamalo	Dry GF Manowaiopae	Dry GI Kaiwilahilahi
Odonata	Coenagrionidae	*Megalagrion*	0.0056					
Colembolla	Isotomidae		0.0202	0.1012	0.2835		0.1215	0.0202
Trichoptera	Hydropsychidae	*Cheumatopsyche*	69.7944	63.0672	6.2094	118.0697	15.6711	208.5595
	Hydroptilidae	*Oxyethria*			5.7370			
		Hydroptila	1.2446	4.7586	13.5593	3.1169	9.6521	2.5971
Diptera	Chironomidae		30.5475	18.8701	15.9257	6.4782	8.8032	2.0352
	Ephidridae	*Scatella*	0.3930	0.0490			0.3220	0.0876
	Ceratopogonidae	*Dasyhelea*	0.0735	0.0162	0.0537	0.0632	0.1007	0.0184
Cyclopoida	Cyclopidae		0.0070			0.0070	0.0070	
Trombidiformes	Hydrachnoidea		0.1807	0.0452	0.0508	0.0169	0.0169	0.0113
Pulmonata	Lymnaeidae	*Erinna*				0.2471	1.1411	
	Planorbidae	*Chlanospira*	0.2867			0.2829	0.6543	0.3676
		Ancylini				0.3186	9.0923	0.0898
Podocopida			0.0824	0.0680	0.0752	0.0036	0.3044	0.0501
Hirudinea	Erpobdellidae	*Barbronia*	5.6096		4.9857	2.4353	1.7134	1.7002
Oligochaetae			5.4727	9.7757	2.0281	0.5892	3.3948	7.7154
		Total	113.718	96.751	48.909	131.629	50.995	223.253

Appendix 5.4: Results of the t-test that compared per-capita (PC), mass-specific (MS), population (pop.), and community nitrogen excretion rates between guppy-invaded and guppy-free streams, independent of flow. In addition, tissue C:N, nitrogen demand (via uptake), and percent nitrogen supplied by community excretion was compared. If the p-value was significant, the effect size (using Hedge's g) of guppy presence was calculated for low, medium, and high flow streams. The effect size was classified as large (LG), medium (MD), small (SM) or negligible (NG). Positive effect sizes indicate that guppies decreased the response variable, while a negative effect size indicates that guppies increased the response variable.

Response Variable	t-value	DF	p-value	Hedge's g		
				Wet	Med	Dry
Midge PC excretion	-1.045	9.862	0.3211			
Midge MS excretion	0.147	9.693	0.8859			
Midge C:N	-0.042	6.875	0.9675			
Midge Pop. excretion	0.646	9.281	**0.0534**	0.335 (SM)	-0.075 (NG)	0.609 (MD)
Caddis PC excretion	-0.721	9.562	0.4882			
Caddis MS excretion	-1.715	8.508	0.1223			
Caddis C:N	0.329	9.680	0.7490			
Caddis Pop. excretion	-2.716	5.699	**0.0367**	-0.461 (SM)	-2.813 (LG)	-1.568 (LG)
Community excretion	-2.447	9.377	**0.0359**	-0.040 (NG)	-1.921 (LG)	-1.300 (LG)
Uptake	3.701	8.242	**0.0057**	2.414 (LG)	2.111 (LG)	1.150 (LG)
% N supplied	-3.100	5.213	**0.0254**	-1.298 (LG)	-2.510 (LG)	-5.688 (LG)

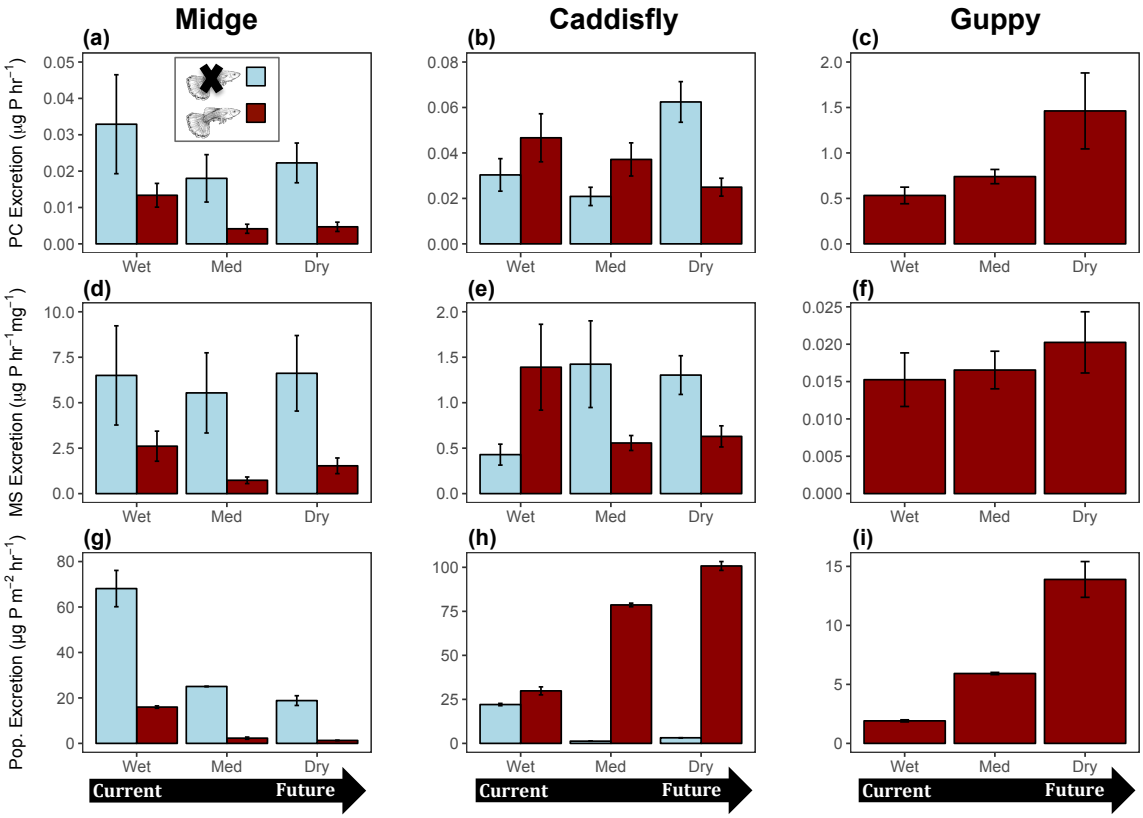

Appendix 5.5: Average (± 95% CI) per-capita (PC, a-c), mass-specific (MS, d-f), and population (g-i) phosphate excretion of dominant consumers and the introduced guppy in guppy-free (blue) and guppy-invaded (red) streams that have high, medium, and low streamflow. Flow did not have an effect on PC and MS excretion rates, but guppies declined individual midge excretion rates across the three streamflow categories. Population excretion rates declined in drier guppy-free streams, but increased for caddisflies and guppies in drier guppy-invaded streams. Block arrows indicate the direction of predicted declines in streamflow with climate change.

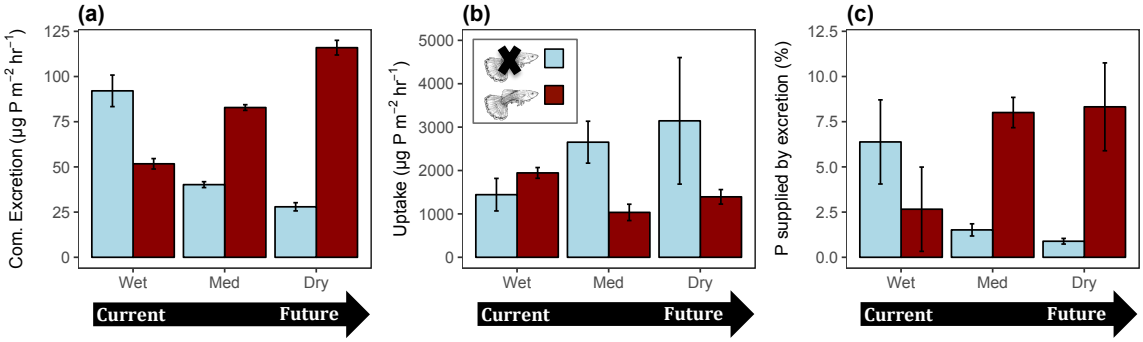

Appendix 5.6: Phosphate supply rates via community excretion (a), phosphate demand rates via uptake (b), and percent phosphate supplied by community excretion (c) in guppy-free (blue) and guppy-invaded (red) streams with high, medium, and low streamflow. There was little difference in uptake rates, but community excretion rates and percent of phosphorus supplied by community excretion declined in drier guppy-free streams. On the other hand, community excretion rates and percent phosphorus supplied increased in drier guppy-invaded streams. Block arrows indicate the direction of predicted declines in streamflow with climate change.

Appendix 5.7: Results of the t-test that compared per-capita (PC), mass-specific (MS), population (pop.), and community phosphorus excretion rates between guppy-invaded and guppy free streams, independent of flow. In addition, phosphorus demand rates (via uptake), and percent phosphorus supplied by community excretion was compared. If the p-value was significant, the effect size (using Hedge's g) of guppy presence was calculated for low, medium, and high flow streams. The effect size was classified as large (LG), medium (MD), small (SM) or negligible (NG). Positive effect sizes indicate that guppies decreased the response variable, while a negative effect size indicates that guppies increased the response variable.

	t-value	DF	p-value	Hedge's g		
				Wet	Med	Dry
Midge PC excretion	2.122	78.70	**0.0370**	-0.958 (LG)	0.733 (MD)	0.926 (LG)
Midge MS excretion	2.154	61.96	**0.0351**	-0.752 (MD)	0.585 (MD)	0.715 (MD)
Midge Pop. excretion	1.345	24.69	**0.0141**	-0.726 (MD)	0.839 (LG)	1.124 (LG)
Caddis PC excretion	0.520,	106.55	0.6040			
Caddis MS excretion	0.499	105.56	0.6188			
Caddis Pop. excretion	-3.923	24.84	**0.0269**	-0.275 (SM)	-1.704 (LG)	-1.857 (LG)
Community excretion	-1.659	9.891	**0.0284**	5.383 (LG)	-21.52 (LG)	-21.85 (LG)
Uptake	0.986	8.102	0.3527			
% P supplied	-2.143	9.847	**0.0582**	1.291 (LG)	-8.536 (LG)	-4.023 (LG)